# DEVELOPMENT A STRUCTURAL FINITE ELEMENT MODEL OF TRABECULAR BONE

[1] Saif Alrafeek and [1]Peter A. Gustafson
[1] Western Michigan University , Kalamazoo, MI, USA

email: saifghazyfais.alrafeek@wmich.edu, peter.gustafson@wmich.edu
web: www.wmich.edu

## INTRODUCTION

Most studies used to create models of trabecular bone tissue, which is essentially porous, incorporate the use of continuum of non-porous structures [1]. Others studies using these non-porous structures have been dependent on CT/MRI scan data [2]. Both of these methodological approaches may lack efficacy which may limit their utility to the orthopedic surgical community. Implementation of a structural FE model developed upon a stochastic approach, one that is less dependent on detailed CT and MRI scans, may prove to be a viable alternative. The mechanical characteristics of the trabecular tissue network were investigated by analyzing a structure composed of randomly oriented beam elements. Beam properties (such as length, orientation, cross section and connectivity) were set stochastically. The beam elements may capture the behavior of the trabecular tissue more efficiently when compared with continuum methods.

## METHODS

Trabecular bone consists of a three-dimensional network structure mainly composed of rod-shaped and plate-shaped fundamental units named "trabeculae". In this work, the trabeculae were modeled as beam elements. Two methods were employed to develop the modeling process: First: repetition of beams in terms of unit-cells over a 19mm X 12mm X 12mm cubic trabecular bone specimen. Second: creating randomly oriented beams over a 4 mm X 4mm X 4mm cubic specimen. For the first method, the unit-cell was designed as a hexagonal shape. Each side of the hexagonal unit cell was created by a strut, a line-based shape geometry. The cross section of the beams was defined as a circular shape of 0.125 mm radius. For the second method, beams were created algorithmically so that beam properties were stochastically determined [Figure(1)].

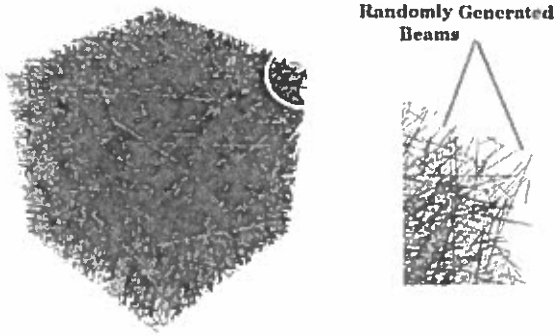


**Figure 1**: Trabecular bone specimen (highly structured from randomly generated beams).

The cross section of beams in the second method was defined as a circular shape of 0.025 mm radius. For both methods, the beam element type that was utilized is a 2 – node linear beam element (B31). ABAQUS was used as an FE solver in the current procedure.

## RESULTS AND DISCUSSION

The Individual FE models created in this study exhibited the mechanical properties listed in Table (1). The models demonstrated acceptable ranges of Young modulus and within the limits of trabecular bone properties as in [3]. The individual FE models exhibited properties of transverse isotropy material. For the FE model created from unit-cells, E1 is approximate to E3. Also, E1 is approximate to E2 in the FE model constructed from random beams. Consecutively, E1 and E2 are approximately the same [3]. However, trabecular bone material properties have been demonstrated as orthotropic material in [4]. Thus, the current model may provide a foundation for future parametric study and

research to reach orthrotropy. Parametric study may be conducted employing trabecular bone appearant density and trabeculae radii (beam radii and shape). Other parameters may be included. In this study, appearant density and trabeculae radii were within the published ranges.

## CONCLUSIONS

One of the advantages of utilizing beam elements in creating trabecular bone FE models is that porosity is a critical variable that is preserved through this study. Changing the FE model parameters, appearant density and beam cross section radii, led to variability in the estimates of the gross mechanical properties of the trabecular bone tissue. However, the FE simulation results may be improved if more parameter are taken into account. The results of this study quantify the variation in trabecular tissue material properties estimates, which may be useful for analyzing modeling results for the complete bony tissue. Continued research will enhance opportunities to expand upon this work.

## REFERENCES


1. Evans, S.P., et al., J Biomech **45**, 2702 -2705, 2012.
2. Depalle, B., et al. J Mechanical behavior of Biomedical Materials **18**, 200 – 212, 2013.
3. Bartel, D.L. *Orthopedic Biomechanics, P*earson Education, Inc., 2006.
4. Dalstra, M., et al., J Biomech **26**, 523 – 535, 1993.


## ACKNOWLEDGEMENTS


This work was supported by MoHESR (Iraqi Ministry of Higher Education and Scientific Research). Additional support was provided by: Western Michigan University (WMU) [College of Engineering and Applied Sciences (CEAS) and Homer Stryker M.D School of Medicine (WMed)]. And Borgess Orthopedics.


**Table 1:** Predicted Independent Elastic Constants, Appearant Density and beams circular section radius

| | | FE Models | | Literature | |
|---|---|---|---|---|---|
| | | **FE Model (unit-cells)** | **FE Model (random beams)** | **Bartel, D.L. [3]** | **Dalstra, M. [4]** |
| **Elastic Constants** | **E1 ( MPa)** | 1107.967 | 40.98 | 237 | 96.4 |
| | **E2 ( MPa)** | 273.568 | 43.7 | 309 | 49.1 |
| | **E3 ( MPa)** | 1172.313 | 67.22 | 823 | 25.2 |
| **Parameters Considered** | **Appearant Density (g/cm3)** | 1.783 | 1.18 | 0.09 ~ 1 | 0.1 ~ 0.959 |
| | **Beams circular section radius (mm)** | 0.125 | 0.025 | - | - |

# A COMPARATIVE ANALYSIS OF THE CENTER OF MASS AND CENTER OF PRESSURE RELATIONSHIP IN A PIROUETTE PERFORMED BY AN AMATEUR AND PROFESSIONAL DANCER

Mackenzie Blust and Gordon Alderink

Biomechanics and Motor Performance Laboratory
Grand Valley State University, Grand Rapids, MI
Email: blustm@mail.gvsu.edu

## INTRODUCTION

In both ballet and jazz, the pirouette requires a dancer to have good postural control and dynamic stability. Maintenance of balance in a single-leg stance position during an en dehors rotation proves difficult for many dancers. Dynamic stability of a pirouette can be analyzed by determining the relationship between the center of mass (COM) and center of pressure (COP) throughout the turn. A multitude of factors contribute to the position of COM relative to COP during a pirouette including, but not limited to: trunk inclination, preparation position and push force, inclination angle of the rotation axis, movement of contributing joints, and the use of visual spotting [1].

Previously, bipedal balance has been investigated during quiet standing using an inverted pendulum model [2]. Winter, et al. [2] noted that during postural sway, the COP consistently oscillated outside the COM, indicating that it upheld a central position of the COM between the two feet. This model implies that the ankle joint is primarily responsible for the control of the COM and that the difference between COM and COP is proportional to the horizontal acceleration of the COM [3]. Analysis of the movement of COM relative to the COP of single-leg stance has further been studied among dancers on retiré position [4].

Comparing the biomechanical execution of a pirouette between dancers of different skill has the potential to increase understanding of the importance of balance during a pirouette and the mechanisms by which stability is maintained. The purpose of this study was to compare the center of mass, center of pressure, and their relationship during a pirouette executed by a professional and an amateur dancer.

## METHODS

Participants of the study included a female amateur dancer (height: 158.6 cm, weight: 49.4 kg) with 18 years of experience and a male professional dancer (height: 163 cm, weight: 59.9 kg) with 30 years of experience. The amateur dancer was a university dance minor and instructor. The professional formerly trained at a national ballet school, danced for nationally recognized companies, and held leadership roles for teaching dance. Participants were free of significant medical history. Marker (Plug-in Gait/Oxford Foot Model) trajectories were recorded by eight Vicon MX-T40 (120 Hz) cameras (Oxford Metrics, Oxford, UK). Position data were synchronized with ground reaction forces (Advanced Mechanical Technology, Inc,. Watertown, MA) collected at 1200 Hz. Vicon BodyLanguage software was used to smooth trajectory (Woltring, MSE 15) and raw force data ($4^{th}$-order, zero-lag Butterworth, 10 Hz), and determine joint motion, net internal joint moments, and net power, normalized to percent turn cycle. Twelve trials for each style of pirouette—ballet and jazz—were collected. A complete turn cycle included preparation, toe-off of gesture foot into the turn, and ended with touch-down of the gesture leg. Toe-off was defined as the release of the right foot from the force plate to start the rotation. Both dancers executed the turn on their dominant left leg (stance leg) with right leg in passé. Participants chose the best trial from each set of three and the best perceived pirouette from all performed. A custom MatLab program (MathWorks, Natick, MA) was used to determine COM relative to COP.

## RESULTS and DISCUSSION

The pattern of movement, in the global coordinate system, of the COM relative to the COP in percent turn cycle appear to be similar (Fig. 1a and 1b) between the professional and amateur dancers.

The displacement of COM relative to COP during the turn, without the effects of toe-off displacement, were analyzed from 50% cycle for ballet and 55% of the cycle for jazz. In the ballet pirouette (Fig. 1a) the professional dancer exhibited slightly less sway of the COM than the amateur dancer throughout the turn. The mean displacement for the professional in x-direction was 21.24 mm and in y-direction was 40.47 mm. The mean displacement for the amateur in x-direction was 21.22 mm and y-direction was 47.93 mm. In the jazz pirouette (Fig. 1b) the data indicate a greater difference of COM sway between the two dancers. The mean displacement for the professional in x-direction was 17.21 mm and in y-direction was 39.78 mm. The mean displacement for the amateur in x-direction was 27.72 mm and y-direction was 49.31 mm. This indicates that the professional dancer had more control of COM in the jazz pirouette than the amateur.

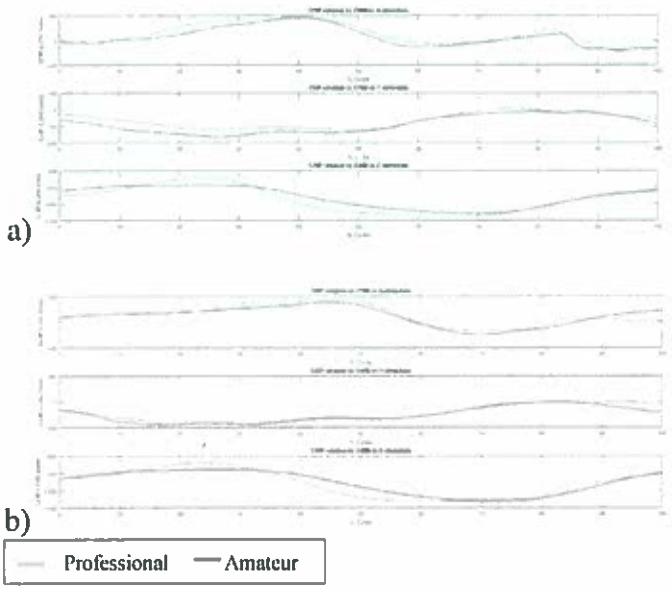


**Figure 1.** COP relative to COM (vertical axis) in percent turn cycle. The vertical line indicates the toe-off into turn. a) ballet pirouette b) jazz pirouette

Peak displacement of the COM relative to the COP of the supporting limb occurred for both dancers near toe-off. The professional dancer had greater displacement along the global x-axis compared to the amateur dancer who had greater initial toe-off displacement along the global y-axis.

The COM and COP data suggest that the professional dancer displayed greater dynamic control than the amateur dancer, especially during the jazz pirouette. Chia-Wei Lin, et al. [4] found that in single-leg stance on retire position, superior experienced dancers were able to maintain balance on demi-pointe longer than novice or experienced dancers. They attributed this stability to the dancer's increased ability to control COM and COP, likely gained from training [4]. The findings of the current study appear to corroborate the conclusions reached by Chia-Wei Lin, et al. For example, decreased displacement of COM for the professional dancer may be related to his increased ability to control the COM. While the average COM displacement difference, in a single turn, between the dancers was relatively small, the balance control exhibited by the professional shows a result of training and experience that could have a larger impact during multiple turns. Greater COM displacement after toe-off for both dancers can potentially be explained, i.e. by the distance between the support and gesture foot in preparatory phase. Training focused on control of COM may improve technique by minimizing abnormal joint moments and reducing muscular co-actions that make a turn aesthetically and technically unappealing. Results are limited to the comparative purposes of the study.

## REFERENCES

1. Lin CW, et al. Differences of Ballet Turns Performance Between Experienced and Novice Ballet Dancers. *Res Q Exerc Sport* **85,** 330–40, 2014.
2. Winter DA, et al. Stiffness Control of Balance in Quiet Standing. *J Neurophysiol* **80,** 1211–1221, 1998.
3. Gage, W. H., Winter, D. A., Frank, J. S. & Adkin, A. L. Kinematic and kinetic validity of the inverted pendulum model in quiet standing. *Gait Posture* **19,** 124–132 (2004).
4. Lin CW, et al. A Comparison of Ballet Dancers with Different Level of Experience in Performing Single-Leg Stance on Retiré Position. *Motor Control* **18,** 199–212, 2014.

## ACKNOWLEDGMENTS

Lauren Hickox, M.S.E. for technical assistance.

# CROSS SECTIONAL ANALYSIS OF SENIOR FITNESS TESTING

Alyssa Braun, Alexandra Colacino, Megan Salvatore, DPT, Nathan W. Saunders, PhD

University of Mount Union, Alliance, OH, USA
email: saundenw@mountunion.edu, web: www.mountunion.edu

## INTRODUCTION

A cross-sectional analysis will be conducted based on the data collected from a number of different senior fitness tests. Data will be collected using an APDM Opal sensor system. This is the first portable gait and balance lab designed for clinical researchers, and will make it easier to collect, store, analyze, and interpret data. [1] These sensors are able to accurately measure movements and turns, as well as gait speed, arm swing and lean angle to help make predictions about a participant's fitness. [2]

Previous studies have raised questions about body worn sensors, due to the fact that the short routine tests take place in controlled settings where participants are given specific directions. This means the tests may not reveal one's true mobility in everyday life. A study done by Wang et al. revealed that the data collected from the APDM monitors in free-living activities only varies slightly from the data collected in controlled situations. [3] The APDM Opal sensor system should be able to accurately facilitate the information needed to make comparisons and draw conclusions about the results of senior fitness testing.

## METHODS

A total of 30-40 participants, both male and female, will be recruited for this study. Participants must be age 65 and older, have no known cognitive or balance disorders, and be able to walk without the help of an assistive device. The participants will be recruited from locations within the Alliance area. These locations include churches, community centers, independent living facilities and the YMCA. Testing will be conducted in a hallway with a minimum length of 25 meters.

Participants will complete two trials of three tests, which are part of the Senior Fitness Test (SFT). The protocols used in this study are adapted from those created by Rikli and Jones [4]. The tests include a Chair Stand, 8 Foot Up-and-Go and 6-Minute Walk Test. Each participant will be wearing APDM opal sensors (positioned at the wrists, tops of the feet, lumbar spine and sternum) in order to collect data. Each opal sensor consists of a tri-axial accelerometer, tri-axial gyroscope and tri-axial magnetometer [5]. The data collected by the opal sensors includes, gait speed, stride rate, turn duration, 8 foot up-and-go time, number of chair stands, sit-to-stand and stand-to-sit durations, and lean angle.

Both the Chair Stand and 8 Foot Up-and-Go tests will use a chair with a 17-inch height. The chair stand test evaluates how many times the participant can go from the seated to standing position in 30 seconds. The 8 Foot Up-and-Go Test requires the participant to stand from the seated position, walk 8 feet around a cone and return to the seated position as fast as possible without running. During the 6-Minute Walk Test, participants will walk back and forth down the hallway, at a self-selected pace, until time ends or until the participant can no longer continue. A chair will be placed at the halfway mark in case a participant feels the need to rest. This test evaluates the total distance a participant can walk in 6 minutes.

A cross-sectional analysis will be conducted based on the data collected from these three tests. The average of the two trials will be used for further analyses. Multiple linear regression will be used to test for gender and age differences in various performance outcomes, such as gait speed, stride rate, and lean angle.

## RESULTS AND DISCUSSION

Research and data collection is set to begin on February 1st, 2017.

## CONCLUSIONS

Research and data collection is set to begin on February 1st, 2017.

## REFERENCES


1. King, MML. Mobility Lab to Assess Balance and Gait with Synchronized Body-Worn Sensors." *J Bioeng Biomed Sci.*, 2013.
2. Mancini, M., et al. "Continuous Monitoring of Turning Mobility and it's Association to Falls and Cognitive Function: A Pilot Study." J Gerontol A Biol Sci Med Sci. **71.8**, 1102-108, 2016.
3. Wang, K, et al. "Inertial Measurement of Free-Living Activities: Assessing Mobility to Predict Falls.", 2014.
4. Rikli RE, et al. "Functional Fitness Normative Scores for Community-Residing Older Adults, Ages 60-94." *J Aging Phys Act* **7.2,** 162-181, 1999.
5. "The Opal." *APDM.* APDM Wearable Technologies, 2015. Web. 15 Jan. 2017.

# NONLINEAR DYNAMICS OF CANE-ASSISTED UPRIGHT BALANCE FOR INDIVIDUALS WITH NEUROLOGICAL IMPARIMENT

[1]James Chagdes, and [1]Amit Shukla

[1]Miami University, Oxford, OH, USA
email: James.Chagdes@MiamiOH.edu web: http://users.miamioh.edu/chagdejr/

## INTRODUCTION

The single-degree-of-freedom (1-DOF) inverted pendulum has been widely accepted as a valid model for investigating upright human balance [1]. The simplicity of such a model allows the capture of nonlinear dynamical behavior while describing the motion using a simple equation for postural sway. Recently the 1-DOF inverted pendulum has been used to better understand the space of control parameters that result in stable upright balance [2, 3]. These models have demonstrated that there are two types of instabilities – a leaning instability and an instability leading to excessive oscillation.

While these models provide insight into the stability of upright bipedal stance, they are not sufficient for individuals that require the aid of assistive technologies, such as a passive-cane. Without a valid model one is unable to understand the control parameters required for maintain upright posture or if similar instabilities even exist when assistive technologies are used. Therefore in this study, we developed a mathematical model of human posture while using a passive-cane to examine the nonlinear dynamics of stance.

## METHODS

We model cane-assisted human balance using a two-degree-of-freedom (2-DOF) five-bar mechanism to represent the human body, upper arm, forearm, cane, and ground (Fig. 1). The mathematical model was derived in the anterior-posterior direction by adapting the simple inverted pendulum of Chagdes et al. [2, 3] coupled to a three-bar linkage to incorporate the upper arm, forearm, and cane dynamics. The human body has a mass $m_{body}$ and moment of inertia $I_{body}$ about its center of mass (CoM) which is a distance of $h_{body}$ from the ankle joint. Likewise, the upper arm and forearm have masses of $m_{arm}$ and $m_{forearm}$ with moment of inertias of $I_{arm}$ and $I_{forearm}$ about each member's CoM which is a distance of $h_{arm}$ and $h_{forearm}$ from the shoulder and elbow joint, respectively.

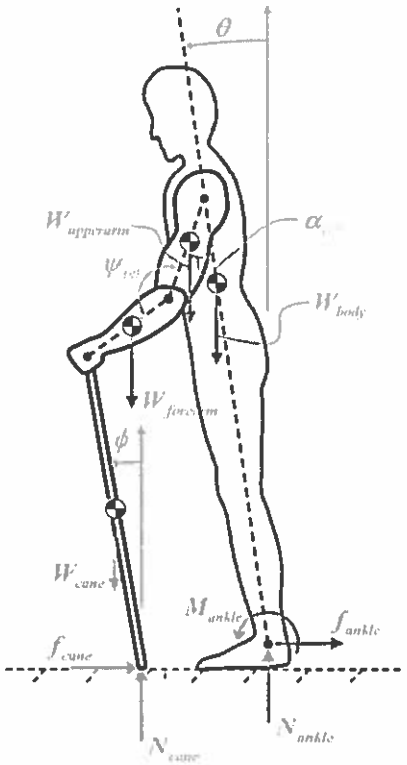


**Figure 1**: Schematic of cane-assisted balance: a five-bar mechanism model.

Rotation of the body $\theta$, upper arm $\alpha$, forearm $\psi$, and cane $\phi$ are restricted to the anterior-posterior (AP) direction. To represent such a system only two independent generalized coordinates are required; we have chosen $\mathbf{q} = \{\theta, \phi\}^T$, the angular position of the body $\theta$ and the cane $\phi$. Utilizing the loop closure equations and the Freudenstein equation the two

dependent coordinates, $\alpha(\theta,\phi)$ and $\psi(\theta,\phi)$, could be solved as functions of $\theta$ and $\phi$. Control of the model can be achieved through passive and active corrective muscle torque $\mathbf{M}$, which apply at the different joints with and without time-delay, $\tau$.

$$\mathbf{I}(\underline{q})\ddot{\underline{q}} + \mathbf{C}(\dot{\underline{q}},\underline{q}) + \mathbf{G}(\underline{q}) = \mathbf{M}(\dot{\underline{q}},\underline{q}) \qquad (1)$$

Details of the resulting equations of motion seen in Eq. (1) are available from the author upon request.

A parametric study was completed to understand how changes in the model control parameters associated with the onset of aging or neurological impairments affect the stability of cane-assisted upright human stance. We specifically varied passive ankle stiffness to mimic the effects of muscle loss/gain and neuromuscular time-delay to mimic the effects of impairment to the neuromuscular system. Additionally a parametric study was completed to understand how changes to the cane affect the stability of balance. The parameters of the cane that were varied were mass, length, and positioning.

## RESULTS AND DISCUSSION

Neuromuscular time-delay is commonly increased due to aging or neurological impairment, such as Parkinson's, multiple sclerosis, and concussion. In our model this effect is captured by an increased delay, $\tau$. The result, presented in Fig. 2 show a stable upright equilibrium when $\tau < 300$ ms but a dynamic instability of upright balance and the emergence of limit cycle oscillations (LCOs) when $\tau \geq 300$ ms. The amplitude of the limit cycle oscillations grows as the time delay increases. This behavior is identical to the predicted delay induced instability of bipedal stance [2, 3]. The presents of LCOs in our model suggests that cane-assistance is not suitable for stability of neurologically impaired upright balance

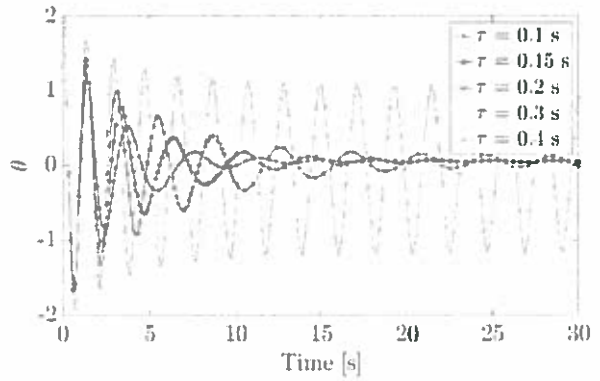


**Figure 2:** Time series realizations of postural sway for various levels of neuromuscular time-delays

The length of the cane, $L_{cane}$, significantly impact postural response and this is shown in Fig. 3. This model predicts that when the cane length is reduced for an individual with an increased neuromuscular delay of 300 ms, length of cane can dramatically destabilize the postural response by creating large LCOs of increasing magnitude. It was found that when the cane length was increased for an individual with increased neuromuscular time-delay of 300 ms, the cane improved the postural response by decreasing the magnitude of LCOs. These results highlight the impact of cane dimensions and require detailed design studies using the model presented in this work.

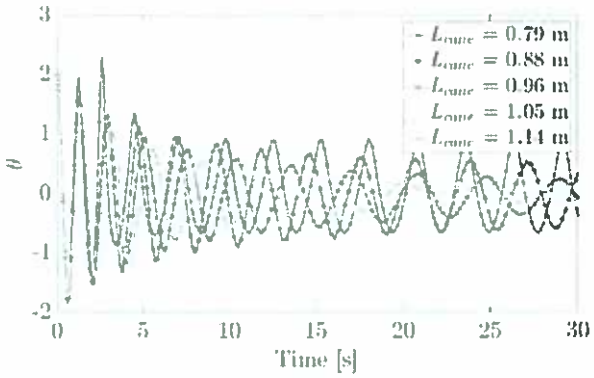


**Figure 3:** Time series realizations of postural sway for various lengths of the cane with $\tau = 0.3$ ms representing impaired, unstable, unassisted balance

## CONCLUSIONS

A simple nonlinear mathematical model of cane-assisted human balance along with a combination passive and active feedback controller was to investigate the dynamical behavior about the upright equilibrium. This model and the study presented in this paper is a first step in investigating the role of cane as an assistive device for people with balance disorders. Such a model can aid in the design of customized passive or active assistive technology for people of difference physical properties and impairments which is part of the future work related to this research

## REFERENCES


1. Peterka RJ *J. Neurophysiol.* **88**(3), 1097–1118, 2002.
2. Chagdes JR, et al. *J. Biomech.* **49**(7), 1170–1179, Mar. 2016.
3. Chagdes JR, et al. *J. Sport Heal. Sci.* **5**(1), 14–24, Mar. 2016.

# Effect of Storage Condition, Orientation, Location and Gender on Rat Back Skin Mechanical Properties

[1] Sheng Chen and [1] Sara Roccabianca

[1] Michigan State University, East Lansing, MI, USA
Email: roccabis@egr.msu.edu

## INTRODUCTION

The determination of biomechanical properties of soft tissues like skin involves mechanical tensile test. In practice, skin samples cannot always be tested right after removal from the subjects. Hence, a storage protocol that can preserve most of the mechanical properties of skin tissue plays an important role in studies that involve mechanical tensile test. The purpose of this work is to study the effect of different storage conditions on rat skin by evaluating mechanical characteristics on certain parameters, and to determine the storage protocol that preserve skin mechanical properties the most. Also, the differences due to orientation, location and gender are studied in this work.

## METHODS

Sixteen Sprague Dawley rats, eight males and eight females, aged between 10 to 12 weeks were used in the study. The dorsal skin was shaved and the whole piece of back skin flap was excised. A custom made dog bone shape die was used to punch specimens from the flap. Four specimens were collected from each animal, two from the cranial location, on each side of the spine, and two from the caudal location, on each side of the spine. The animals were divided into two groups of eight animals, four males and four females: in Group I, the samples were cut along the spine direction (axial); in Group II, specimens were cut in the direction perpendicular to the spine (transverse).

Specimens from Group I were used for storage effect study. They were separated into four storage protocols randomly. Protocol I: specimens were tested right after they were cut from back skin flap. Protocol II: specimens were stored in 4°C for 24 hours before testing. In Protocol III: specimens were flash frozen in isopentane that submerged in dry ice (-78.5°C), then stored at -80°C, and thawed at 4°C for 6h before testing. Protocol IV: flash-freezing and storing process were the same as Protocol III, then specimens were thawed at 4°C for 24h before testing. Specimens from Group II were stored using the best storage protocol (Protocol III) determined by Group I specimens before testing.

Quasi-static uniaxial tensile test was performed on skin specimens to estimate mechanical properties. 4 markers were placed on the central part of the sample to track the length changing by Digital Image Correlation method using a CCD camera (i.e., Hitachi model KP-M2AN). The whole tensile test had three parts. Part I: 10 cycles of preconditioning at 20% strain; Part II: strain-incremental cyclic loading aiming for ideal stress level; Part III: rupture loading. Before each part of the test, 10g of preload was applied to the specimen and dimensions of the specimen were recorded to serve as reference configurations for corresponding stress-stretch curve. Testing speed was 0.83mm/s.

## RESULTS AND DISCUSSION

Mechanical properties of rat back skin are evaluated by using five parameters, as shown in Table 1. **Initial slope,** is to describe the beginning 2% deformation of the rupture stress-stretch curve, we hypothesize that this response is dominated by the elastin content and approximately linear. **Maximum slope,** is to describe the almost linear part of the rupture stress-stretch curve at high stress level, which we hypothesize is dominated by the mechanical behavior of collagen fibers. **Rupture strain and ultimate tensile strength (UTS),** are the strain and stress value when skin specimen breaks. **Toughness,** is the area under rupture stress-stretch loading curve, representing the work input done per unit volume of a specimen during rupture loading.

ANOVA results in Table 1 shows that there are no statistically significant (5%) differences between four storage protocols on five evaluated parameters. Figure 1 shows that Protocol III is the one that reserves the stress-stretch curve characteristics the most in both cyclic loading and rupture loading curves, compare to the fresh ones in Protocol I.

Since no significant effects from different storage protocols were found, data from Group I specimens, along with data from Group II, are used to analyze the effects of orientation, location and gender on rat back skin. By running Student's t-test, no statistically significant differences were found between male & female, left & right back. Caudal location has significant higher mean values than cranial location on all parameters, except for rupture strain, on which caudal location is also higher, just not significant.

As to the differences between axial and transverse directions, axial specimens show significantly higher mean values on rupture strain and toughness at both cranial and caudal locations; moreover, axial specimens have significantly higher initial slope and lower maximum slope than transverse specimens at caudal location, which is the same trend at cranial location too, just not significant.

The effect of storage conditions on rat skin has been studied by previous researchers, but not extensively. T. L. Foutz et al., 1992 reported that tissue freezing significantly increased fracture strength [1], but didn't affect yield strength, ultimate strength. However, their study didn't give clear definitions of evaluated parameters. R. D. Marangoni et al., 1966 reported that flash freezing plus -92.8°C storage condition preserved guinea pig skin mechanical properties the most, compared to 1.6°C and 37.8°C storage conditions [2], which supports the results in current study. When it comes to orientation differences, A. Karimi et al., 2015 [3] reported bigger maximum slope values of transverse specimens than axial specimens on mice back skin, as reported in current study.

## CONCLUSIONS

The study shows that there are no statistically significant differences between our 4 storage protocols. The study also reports no differences between male and female animals, but statistically significant differences on orientation and location.

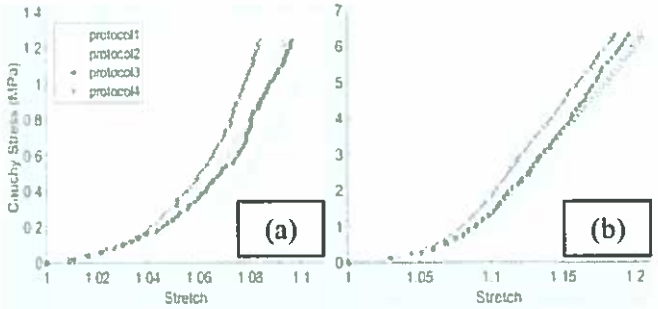


**Figure 1**: (a) Averaged cyclic loading curves based on different storage protocols using the last cycle from tensile test Part II. (b) Averaged rupture loading curves based on different storage protocols.

## REFERENCES & ACKNOWLEDGEMENTS


1. Foutz, TI et al., *American Journal of Veterinary Research* **53**, 788-792, 1992.
2. Marangoni, RD et al., *Annal of the New York Academy of Sciences* **136,** 441-453, 1966.
3. Karimi, A et al., *Computer Methods in Biomechanics and Biomedical Engineering* **18,** 1768-1774, 2015.



We gratefully acknowledge Christina Chan, PhD and Ryan Thompson for the technical assistance.


**Table 1:** Means, standard deviation and ANOVA p-value of evaluated parameters based on storage protocols

| | Protocol I | Protocol II | Protocol III | Protocol IV | P value of ANOVA |
|---|---|---|---|---|---|
| **Initial Slope** | 5.33 ± 3.40 | 3.17 ± 1.34 | 5.49 ± 4.76 | 5.95 ± 4.48 | 0.46 |
| **Maximum Slope** | 59.74 ± 20.32 | 76.44 ± 25.46 | 91.33 ± 51.29 | 64.36 ± 17.94 | 0.21 |
| **Rupture Strain** | 0.31 ± 0.05 | 0.30 ± 0.06 | 0.31 ± 0.04 | 0.28 ± 0.06 | 0.68 |
| **UTS** | 10.83 ± 4.40 | 13.01 ± 4.01 | 14.63 ± 3.51 | 12.12 ± 3.39 | 0.27 |
| **Toughness** | 1.34 ± 0.68 | 1.37 ± 0.63 | 1.64 ± 0.35 | 1.34 ± 0.53 | 0.67 |

# Gait Asymmetry during Uphill, Downhill and Level Walking while Outdoors

[1]HyeYoung Cho, [1]Nathaniel Romine, [2]Junyoung Kim, [1]Michel Heijnen, [2]Babak Ziaie, [1]Shirley Rietdyk

[1]Health and Kinesiology, Purdue University, West Lafayette, IN, USA
[2]Electrical and Computer Engineering, Purdue University, West Lafayette, IN, USA
email: cho273@purdue.edu

## INTRODUCTION

In recent research of gait assessment, symmetricity of gait has been regarded as a fundamental assumption for comprehensive data analysis. However, this assumption overlooks the anatomical and kinematic differences of lower limbs, and it could be related to the different contributions of the lower limbs in implementing propulsion and control tasks [1]. Since challenge is associated with gait asymmetry [2], more challenging tasks, such as uphill and downhill walking, may demonstrate more asymmetric gait patterns. A new device, SmartGait, has made possible the assessments of step length and step time during unrestrained outdoor walking [3]. The purpose of this abstract is to determine the asymmetricity of gait parameters including step length and step time during uphill, downhill and level walking outdoors.

## METHODS

Ten young adults (age: 22.4±2.5 yrs.) walked outdoors at preferred speed for 91.4 m in three conditions: level surface, uphill slope of 5°, and downhill slope of 5°. Two trials of each condition were collected. All participants were right leg dominant as assessed with four questions [4]. SmartGait, a smartphone-enabled camera-based system for gait assessment [3], was used to assess gait parameters; this abstract will focus on step time (ST) and step length (SL). Variability of SL and ST was quantified as the standard deviation of each measure. A one-way ANOVA was conducted for comparing SL and ST in three different conditions. To assess asymmetry, left and right SL and ST were compared with a t-test for each subject in each condition. Due to multiple t-tests, a conservative p-value was set at 0.01.

## RESULTS AND DISCUSSION

No significant differences were observed for ST ($p=0.53$) or SL ($p=0.68$) across the three walkway conditions. Similarly, no differences in gait parameters have been observed indoors for ST and SL during indoor walking with short distance (3.1 m) over a level surface, uphill and downhill slope [5]. Thus, adaptations to slopes are similar for indoor and outdoor walking.

On level ground, four of the ten participants (40%) demonstrated asymmetry in both SL and ST on level ground, and nine (90%) showed asymmetry in at least one of the two measures (Fig. 1). SL distribution demonstrates that both limbs have similar range of SL, but the left limb has a higher frequency of steps at a shorter SL (Fig. 2A). When uphill walking, five subjects (50%) demonstrated asymmetry in both measures, and seven subjects (70%) demonstrated asymmetry in at least one of the two measures. When downhill walking, seven subjects (70%) demonstrated asymmetry in both measures, and eight (80%) demonstrated asymmetry in at least one of the two measures (Fig. 1). However, the dominant limb did not always demonstrate the longest SL or the longest ST. This result is consistent with the result that limb dominance cannot be related predictably to SL and ST [6].

Of particular interest, the limb with longest SL in level walking, which would be defined as the propulsive limb, became the limb with significantly smaller SL values in the uphill and/or downhill conditions in three participants (Fig. 2A; 2B). For example, the right limb SL was longer then the left for level walking, but shorter than the left for downhill walking (Fig. 2). Therefore, if the SL asymmetry is functional, that is, resulting from a propulsive limb and a stabilizing limb [1] it appears that the propulsion task can be shared across limbs;

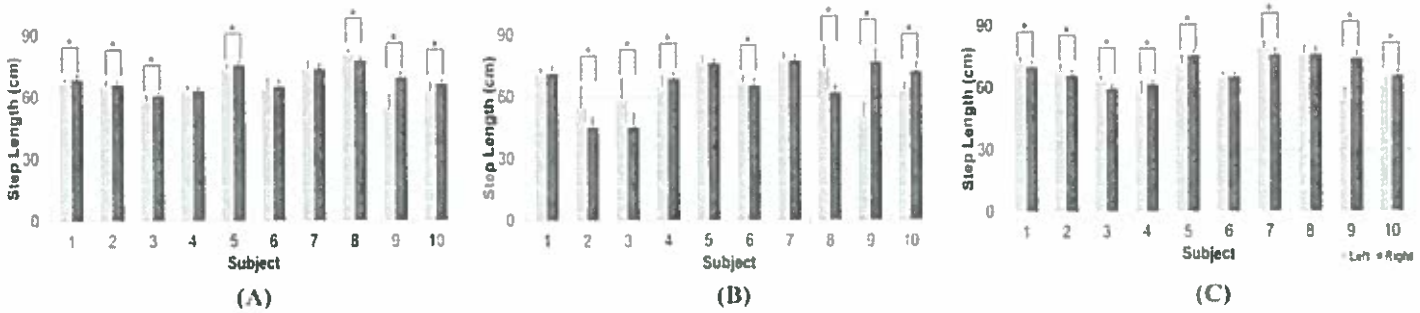


**Figure 1:** Step time plotted as a function of limb (left (gold) vs right (brown)) and the three gait conditions. A) Level walking, B) uphill walking, and C) downhill walking. Asterisk (*) indicates $p \leq 0.01$.

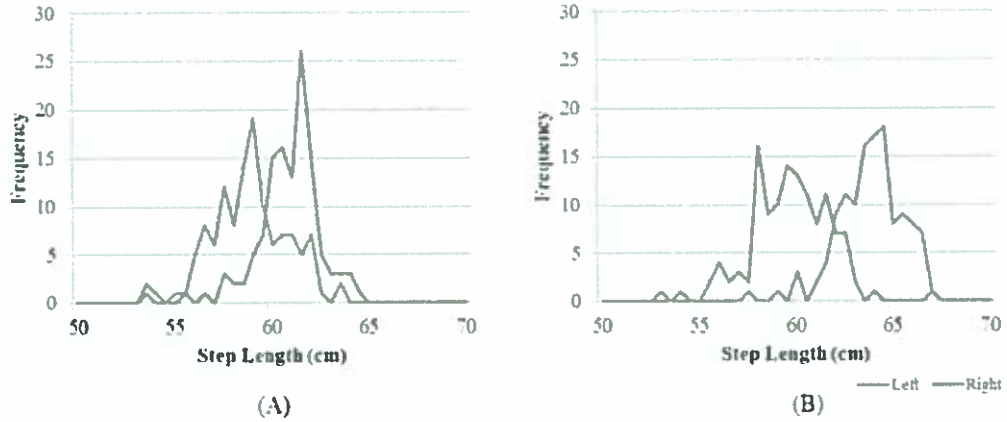


**Figure 2:** Distribution of step length as a function of limb (right vs left) for a single subject. A) Level walking and B) downhill walking. Red is right foot, blue is left foot.

each limb is not dedicated to a specific task. Future research should determine if this behavior is functional, that is, it provides benefit to the mobility. It is important to note that the measures reported here are kinematic, and it is known that kinetic measures provide a more accurate assessment of propulsion versus stability [2].

## CONCLUSIONS

Gait asymmetry was observed while walking outdoors in uphill, downhill, and level walking conditions. However, the so-called propulsive limb (longer step length and/or step time) was not always the dominant limb. In fact, the propulsive limb was observed to switch between left and right limbs across the different gait conditions. Thus, it appears that young, able-bodied adults readily adapt the behavior of the limb based on the environmental context. Hill walking is critical for community mobility, and further exploring the propulsive limb adaptation may lead to improved interventions for people with asymmetrical gait due to disease and disorder.

## REFERENCES

1. Sadeghi H, et al. *Gait Posture* **12(1)**, 34-45, 2000.
2. Patterson K, et al. *Arch Phys Med Rehab*, **89(2)**, 304-310, 2008.
3. Kim A, et al. *Gait Posture*, **42(2)**, 138-144, 2015.
4. Velotta J, et al. *Methods*, **11(2)**, 1035-1038, 2011.
5. Lay A, et al. *J Biomech*, **39(9)**, 1621-1628, 2006.
6. Gundersen L, et al. *Phys Ther*, **69(8)**, 640-650, 1989.

**Conflict of Interest Statement**: The SmartGait™ device used in this research was developed by SmartGait LLC; two of the co-authors (BZ & SR) are co-founders of SmartGait LLC.

# KINEMATICS OF SPRINTING AFTER ADAPTATION TO SPEEDMAKER RESISTANCE HARNESS IN TRACK ATHLETES

Mindie Clark, Randall L. Jensen and Sarah B. Clarke

Northern Michigan University, Marquette, MI, USA
www.nmu.edu/hhp
email: minclark@nmu.edu

## INTRODUCTION

Mechanical ergogenic aids are often used among athletes to improve muscle response and activation. The stretch-shortening cycle is a mechanical theory that muscular force will be increased if the muscle is stretched immediately prior to the contraction phase compared to relaxation before contraction. This concept is beneficial regardless of concentric or eccentric muscular contraction [1]. Therefore, coaches and trainers often include the stretch-shortening cycle component throughout an athlete's training program.

Resistance bands are widely used as mechanical aids that amplify the effects of the stretch-shortening cycle. Acute effects of elastic-cord towing bands improved the acceleration phase of sprinting 20 meters by increasing stride length and distance of center of mass between the foot and trunk in trained athletes [2]. Training effects of resistance on sprinting 20 m has been consistent across multiple studies by improving the acceleration phase of sprinting [3]. Research of sprint lengths over 20 m have not provided consistent results and kinematics regarding range of motion and stride length require further research. Can sprint kinematics, specifically range of motion be altered through training with resistance bands?

The purpose of the current study was to examine the effect of five weeks of training with the SpeedMaker (Elite Athletic Products Inc.; San Diego, CA) resistance device on hip and knee range of motion while sprinting. A secondary purpose was to investigate changes in sprint time. The researchers hypothesized that training with the SpeedMaker resistance harness will improve range of motion in the hip and knee angles, therefore improving running performance and sprint times.

## METHODS

Six female college track & field athletes were recruited and signed informed consent. One athlete was unable to complete post-testing due to an ankle injury. After submission of informed consent, height, weight, age and circumference of chest, waist and femur were measured for the fitting of the SpeedMaker device.

Pre- and post- tests described below were performed by five female track & field college athletes before and after five weeks of training. Athletes served as their own control group and wore the device during their training sessions on Mondays, Wednesdays and Fridays for five consecutive weeks.

A generalized self-selected warm-up including sprints, plyometrics and dynamic stretching was performed for five minutes. Following the warm-up, participants sprinted three 50 m lengths at 80, 90, and 100% maximum respectively with two-minute rests between each sprint. Three countermovement jumps were performed with one-minute rest between each. After conclusion of the jumps, reflective markers were placed on the participant's left shoulder, hip and knee joints and mid shank. Subjects then performed two 50 m sprints for time. Seven motion analysis cameras were used to record the markers in the sagittal plane for one full stride at 36.58 m (40 yards) to analyze hip and knee angles a maximum sprint stride [3]. Microgate (Bolzano BZ, Italy) timing gates were placed at 10, 20, 36.58 and 50 meters to measure sprint times. All split times were recorded following each sprint trial.

Following tests, data were digitized and filtered to 6Hz using Cortex Motion Analysis (Santa Rosa, CA) software. Minimum and maximum hip and knee angles were used to calculate range of motion of hip

and knee joints. Data were analyzed using a paired t-test.

## RESULTS AND DISCUSSION

Sprint times for the 10 m split improved significantly between testing ($p < .043$). Split times for 20, 36.58 and 50 m improved non-significantly (see Table 1). Significance for the latter split times may have been found if sample size was larger.

**Table 1:** Mean ± SD times for each sprint distance before and after training (N=5).
*=statistical significance.

| Distance | Pre Test (sec) | Post Test (sec) |
|---|---|---|
| **10 Meter*** | 1.96 ± .08 | 1.77 ± .19 |
| **20 Meter** | 3.41 ± .15 | 3.15 ± .23 |
| **36.58 Meter** | 5.52 ± .13 | 5.29 ± .29 |
| **50 Meter** | 7.36 ± .21 | 6.96 ± .36 |

Mean maximum knee extension angles decreased significantly after five weeks of training with the resistance harness ($p < .025$), suggesting an increased ROM, although it was not statistically significant ($p < .193$). ROM of the knee may have been significant with a larger sample population. There were no statistically significant differences between flexion/extension angles or ROM of the hip between pre and post-tests (see Table 2).

Participants served as their own controls for the five-week training study. Improvement in 10m acceleration may be the result of a general training adaptation and should be controlled for future studies. However, the athlete's training did not differ throughout the study and was consistent from the training that occurred prior to pre-testing. Therefore, adaptations are not likely influential of increased 10m acceleration.

Another limitation that should be noted is the difference in track events between participants. Because participants served as their own control, this factor should not be considered a confounding variable.

## CONCLUSIONS

The hypothesis that a change in range of motion of the hip and knee angles is rejected according to the present study's results. Although significance may occur in knee ROM with an increased sample size, there was no significant change found. 50 m sprint times did not improve significantly and therefore rejects the secondary hypothesis.

Knee extension improved significantly, inferring that increased knee ROM may be seen in future research. 10 m split times decreased significantly, supporting past researcher's conclusions that resistance devices improve initial acceleration in sprinters.

Future research involving the SpeedMaker device should include similar studies with greater sample populations and matched, control groups to provide better statistical power of effects of training with the SpeedMaker harness.

## REFERENCES


1. Komi PV. *Exerc Sport Sci Rev* **12**, 81-122, 1984.
2. Corn RJ & Knudson D. *J Strength Cond Res* **17**, 72-75, 2003.
3. LeBlanc KS & Gervais PL. *Proceeding of the XXII ISBS Congress*, Ottawa, Canada, 2004.


## ACKNOWLEDGEMENT


Sponsored in part by a Northern Michigan University PRIME grant and a contract with Elite Athletic Products Inc.


**Table 2:** Mean ± SD joint angles and ROM of the knee and hip before and after training (N=5).
[a]=statistical significance, [b]=negative values in the hip joint refer to hyperextension past zero degrees).

| Test | Joint Angle/Range of Motion (Deg) | | | | | |
|---|---|---|---|---|---|---|
| | **Knee Ext[a]** | **Knee Flex** | **Knee ROM** | **Hip Ext[b]** | **Hip Flex** | **Hip ROM** |
| **Pre-Test** | 23.43 ± 4.7 | 129.43 ± 6.7 | 106.00 ± 9.4 | -12.53 ± 14.5 | 30.62 ± 9.4 | 43.15 ± 20.1 |
| **Post-Test** | 18.00 ± 5.9 | 129.99 ± 7.3 | 112.08 ± 10.3 | -15.91 ± 3.1 | 28.88 ± 3.6 | 44.79 ± 6.1 |

# Studying Balance on an Active Balance Board with Controllable Stiffness and Time-delay

[1] Denise R. Cruise (drcruise@purdue.edu), [2]James R. Chagdes, [3]Joshua L. Liddy, [3]Shirley Rietdyk, [3]Jeffrey M. Haddad, [3]Howard N. Zelaznik, and [1]Arvind Raman

[1] School of Mechanical Engineering, Purdue University, West Lafayette, IN
[2] Department of Mechanical and Manufacturing Engineering, Miami University, Oxford, OH
[3]Department of Health and Kinesiology, Purdue University, West Lafayette, IN

## INTRODUCTION

Understanding how humans balance on unstable surfaces is critical for the development of methods to prevent falls and improve stability. A mathematical model of a human on a balance board was presented in Chagdes et al. [1]. Model simulations revealed two mechanisms of instability: a static instability resulting in "tipping" and a dynamic instability leading to limit cycle oscillations (LCOs). LCOs were also detected in balance-compromised populations standing on solid ground [2]. Muscular stiffness and neuromuscular time-delay were both important factors contributing to instability. However, while commercial balance boards manipulate torsional stiffness to explore one instability, time-delay is not utilized as a parameter.

First, we explore the relationship between upright stability and the adjustable board parameters with a model of a human on the active balance board. Simulations revealed both types of instability. Second, we design and fabricate an active balance board with controllable rotational board stiffness and board feedback time-delay. Initial testing of this active balance board is completed with a population of healthy college-aged adults, which also revealed both types of instability.

## METHODS

The model of human posture on a balance board from Chagdes et al. [1] was adapted by combining the 1-DOF inverted pendulum human model with a 1-DOF inverted pendulum balance board model with tunable rotational stiffness and time-delay (Figure 1, Equation 1).

$$[I(\theta)]\begin{Bmatrix}\ddot{\theta}\\ \ddot{\phi}\end{Bmatrix}+[C(\theta,\dot{\theta},\dot{\phi})]\begin{Bmatrix}\dot{\theta}\\ \dot{\phi}\end{Bmatrix}+[K(\theta,\phi)]\begin{Bmatrix}\theta\\ \phi\end{Bmatrix}=\begin{Bmatrix}M_{ankle}\\ M_{board}\end{Bmatrix} \quad (1)$$

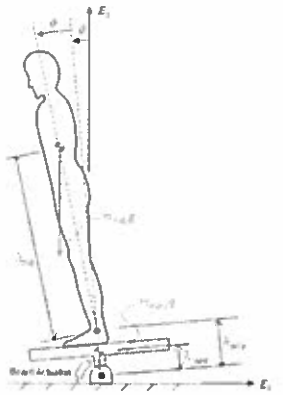

**Figure 1**: Diagram of a person on the balance board showing all external forces

A bifurcation analysis was completed by observing the variable space of equilibrium positions $(\theta^*,\phi^*)$ in the parameter space of $\tau$, $K_{board}$, $K_{\tau,board}$, and $\tau_{board}$ with all other parameters held constant. All values shown are ratios of $K^{cr} = m_{body}gh_{body}$. Equilibrium position and their stability were calculated using DDE-BIFTOOL MATLAB package and verified through 45 second time series realizations using the MATLAB (The MathWorks, Inc.) function dde23 [3].

A balance board with controllable stiffness and feedback time-delay was fabricated (Figure 2). For the initial testing, thirteen college-aged students (19.9 ± 1.7 yrs.; 65.4 ± 10.1 kg; 171.8 ± 9.1 cm) with no known balance issues participated in the study. The experimental procedure was approved by the local Institutional Review Board.

Participants stood with feet shoulder-width apart and ankles in line with the board's axis-of-rotation. The goal was to stay upright on the board and keep the board horizontal for each trial. Each participant performed 24 trials that were 45 seconds long, with a 60 second break between each.

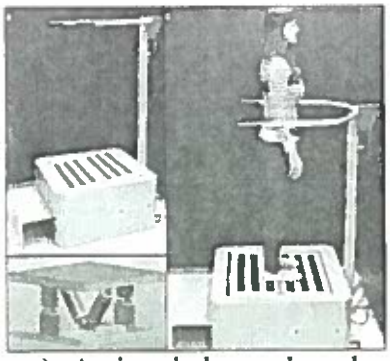

**Figure 2**: a) Active balance board with safety platform, b) primary mechanism of balance board, c) person standing in position on balance board.

## RESULTS AND DISCUSSION

Simulations of the model led to a stability plot (Figure 3). The vertical axis represents the board feedback time-delay, and the horizontal axis represents the active board stiffness, normalized by an individual's mass and the height of the center of mass. This plot shows the parameter combinations which lead to upright stability (grey), as well as the two types of instabilities. The blue line denotes a supercritical pitchfork bifurcation, which occurs when the stiffness is not large enough to maintain upright stance, leading to tipping forward or backward. The red line identifies a supercritical Hopf bifurcation which presents itself via LCOs of the person on the board.

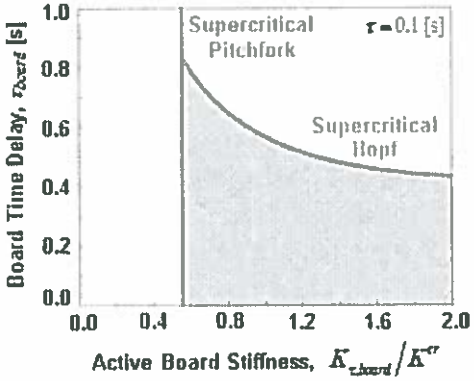


**Figure 3**: Stability plot showing stable (grey) and unstable (white) regions of upright stance on a 1-DOF balance board.

From human experiments, we identified the tipping point as well as the point when LCOs began for each participant, and then averaged the results to create a stability plot (Figure 4).

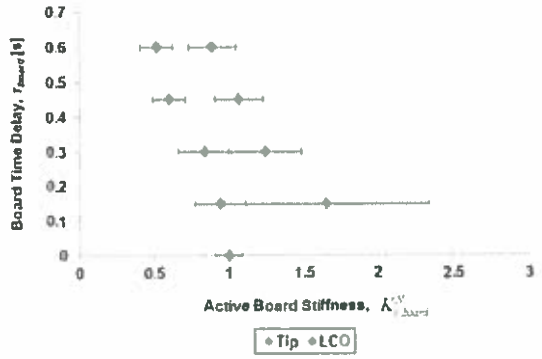


**Figure 4**: Average stability plot for all participants. The blue dots represent the tipping instability, and the red dots show the point at which limit cycle oscillations occur. The error bars represent the 95% confidence intervals for each of the points.

## CONCLUSIONS

We developed an active balance board capable of identifying two distinct mechanisms of postural instability previously predicted with theoretical modeling and simulations. We expect that this active balance board will allow for the early identification of increased fall-risk populations. In addition, having multiple variable parameters potentially allows for the creation of individualized balance training plans which will improve training efficacy.

## REFERENCES


1. Chagdes JR, Rietdyk S, Haddad J, Zelaznik H, and Raman A. *J Biomech* **46**, 2593-2602, 2013.
2. Chagdes JR, Rietdyk S, Haddad J, Zelaznik H, Cinelli ME, Denomme LT, Powers KC, and Raman A. *J Biomech* **49**, 1170-1179, 2016.
3. Engelborghs K, Luzyanina T, Samaey G. *DDE-BIFTOOL v 2.00: a Matlab package for bifurcation analysis of delay differential equations* **330**, 2001.


## ACKNOWLEDGEMENTS


The authors were supported by the National Science Foundation for the project provided through the grant CMMI-13

# BIOMECHANICS OF STERILE CHEVRON-STYLE POUCH OPENING IN A MEDICAL SETTING

Amber R. Cussen, Tony Trier, Laura Bix and Tamara R. Bush

Michigan State University, Lansing, MI, USA
email: cussenam@msu.edu, web: https://www.egr.msu.edu/reidtama/

## INTRODUCTION

Hospital-acquired infections (HAIs) are infections one acquires while receiving treatment for another reason. HAIs affect nearly 725,000 patients and result in the death of more than 10 % of these in the U.S [1]. A major cause of HAIs, surgical site infections, can arise from improper patient skin preparation, lengthy procedures, large incisions, and contaminated surgical tools and devices [2]. Although many of these are carefully monitored to prevent HAIs, surveillance of sterile package opening and guideline compliance is lacking. In addition, only some of the current guidelines are the result of evidence-based medicine. In this pilot study, we propose a motion capture method to evaluate the human factors associated with aseptic package opening guidelines.

## METHODS

*Recommended Guidelines:* To identify best practice recommendations related to package opening, Association of peri-Operative Registered Nurses and Association of Surgical Technologists guidelines were reviewed by two of the authors. The following guidelines were identified to be related to human factors of package opening and thus were evaluated: a) Unscrubbed team members should avoid leaning or reaching over the sterile field b) Motions should be simple, productive, minimal and non-repetitive, and c) The potential for airborne contamination increases with the length of time a sterile field has been open.

*Testing:* Nine health professionals trained in sterile package opening and scrub procedures were recruited to open two package sizes in duplicate wearing 13 reflective markers to detect movement (Figure 1). Participants included residents, surgical technicians, medical and nursing students; all had been trained in aseptic technique during the course of their education. Packages included two sizes of chevron pouches (7.6 cm x 20.3 cm (small) and 40.64 cm x 26.7 cm (large)) (IRB 09-179).

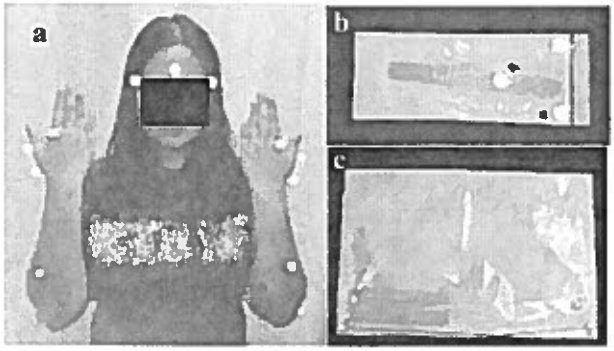


**Figure 1:** Markers on a) participant, b) small pouch, and c) large pouch.

## RESULTS AND DISCUSSION

a) Crossing the sterile field. No participant was able to present all 4 packages without crossing the field. Each participant opened each size package twice, and in all cases at least one was opened over the sterile field. Surprisingly, package size did not appear to play a role in the participants' ability to maintain a distance from the sterile field (Figure 2a).

b) Minimal and non-repetitive motion. Participants performed more repetitive motions when opening large sized packages than small ones (Figure 2b). These motions included more pulls (3.13 pulls/large package ± 2.15 and 1.88 pulls/small package ± 0.94), more repositioning of their hands along the package seal (2.1 repositions/large package and 0.93 repositions/small package), and removal of the corner tack (corners are tacked down to ease manufacturing; 0/18 large sized packages, and 7/18 small sized packages were detacked). Participants also pulled open the large sized packages to a greater degree (larger pull distance) than small size packages.

c) Time spent handling package. Participants spent more total time handling large sized packages than

small sized packages (Figure 2c). However, a similar amount of time was spent pulling open a pouch regardless of the package size (26 % of handling time for large package and 30 % of handling time for small package).

In this proof of concept study, we show that aseptic package guideline compliance can be evaluated using simple motion capture techniques. In our sample population, we found that participants spent more time handling large sized packages, and used more repetitive, and larger motions to open these packages. Participants had difficulty opening and dispensing package contents without crossing the sterile field when opening packages of either sizes, although participants spent more time over the sterile field when opening the large sized packages.

Taken together, this work suggests that participants deviate from recommended guidelines more frequently when opening large sized packages. We previously have shown that sterile contents expelled from large sized chevron packages have a greater risk of contact with the non-sterile exterior of the package than contents expelled from a small sized package [3]. Future studies should combine this methodology with concurrent contamination data collection to link compliance of these guidelines with risk of contamination.

## CONCLUSIONS

In this study, we suggest a methodology which can be used to track guideline compliance and train employees. Our method can also be used to identify handling behaviors that deviate from historical practice and existing guidelines, and can be combined with contamination methods to study the relationship between these specific behaviors and contamination. Finally, our method can be used in conjunction with contamination data to help healthcare providers build an evidence basis for new training and opening techniques. Additionally, these measures could be used to evaluate the effect of package design on the opening process.

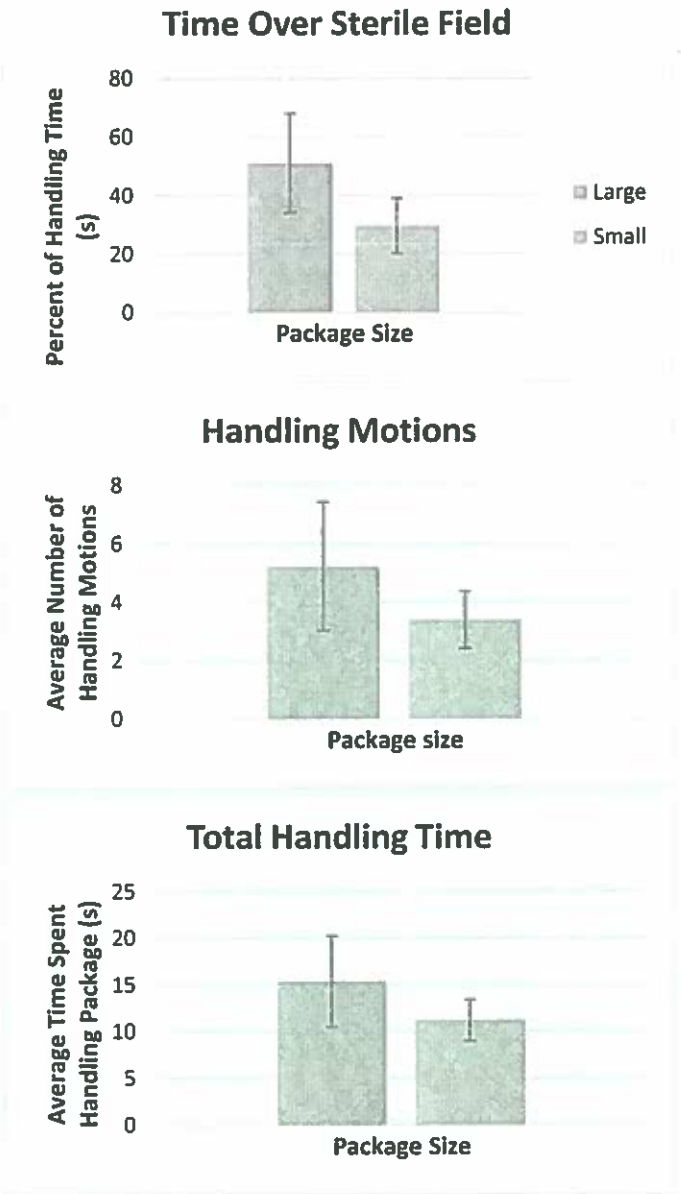


**Figure 2: top:** Average percent of time participants spent with their hands or package over the sterile field, **middle:** the average number of handling motions including pulls, repositioning of hands on package and detack, and **bottom:** the average spent handling the package.


## ACKNOWLEDGEMENTS

Funding for this project was provided by Michigan State University, and in-kind donations provided by Oliver-Tolas Healthcare Packaging, Kimberly Clark, Cardinal Health, and DePuy. We would also like to thank Sam Leitkam, Josh Drost, Pan Wu, Megan Luzenski for their help.


## REFERENCES


1. Magill SS et al. *NEJM*, **370,** 1198-1208, 2014.
2. Mangram et al. *Am J Infect Control,* 1999.
3. Trier T et al. *PLOS ONE*, **9(7),** e100414, 2014.

# The Heterogeneity of the Elastic Properties of the Pectoralis Major Fiber Regions Across Postures and Volitional Contractions

[1] David Desmet, [1]Joshua M. Leonardis, and [1,2] David B. Lipps

[1] Department of Kinesiology, University of Michigan, Ann Arbor, MI, USA
[2] Department of Biomedical Engineering, University of Michigan, Ann Arbor, MI, USA
email: jleo@umich.edu, web: http://www.kines.umich.edu/research/mbil

## INTRODUCTION

The pectoralis major consists of two distinct fiber regions. The sternocostal region originates on the sternum and costal cartilage and constitutes roughly two-thirds of the muscles volume. The remaining muscle volume originates on the clavicle (e.g. the clavicular region). Either region can be harvested to provide structural support to the glenohumeral joint in many surgical cases including irreparable rotator cuff repairs [1]. Physicians often assume that any function lost due to disinsertion will be compensated by the remaining shoulder musculature when determining which pectoral region to harvest [2]. No consideration is given to the biomechanical consequences of choosing one region over the other.

This lack of consideration is in part due to the limited knowledge regarding how the elastic properties of each region may differ, which will ultimately change how each pectoral region produces force and stabilizes the shoulder [3]. Assessing the passive and active elastic properties of each fiber region may provide new insights into how disinserting a specific fiber region influences shoulder function. The present project utilized ultrasound shear wave elastography to characterize the *in vivo* elastic properties of the sternocostal and clavicular fiber regions of the pectoralis major as a function of shoulder position and shoulder torque direction.

## METHODS

The right shoulder of ten male subjects (mean (SD) age: 24 (5) yrs., weight: 81 (14) kg, height: 177 (8) cm) with no history of shoulder injury was placed in a removable fiberglass cast and attached to a rotary motor instrumented with a six-degree of freedom load cell. Subjects were positioned in a combination of two shoulder abduction angles (60° and 90°) and two external rotation angles (neutral and 90°) for a total of four experimental shoulder positions (Figure 1). At each experimental position, participants were asked to produce isometric shoulder torques for 5 sec equivalent to 0, 15, and 30% MVC in the vertical and horizontal adduction directions. Visual feedback was provided to assist with force accuracy, and surface electromyography data were collected from key shoulder muscles to validate that subject's activated their muscles in a similar fashion across trials.

During each isometric force task, an Aixplorer ultrasound elastography machine connected to an SL-15 linear transducer array was used to measure the mean shear wave velocity (SWV) of the clavicular and sternocostal regions of the pectoralis major (Figure 2). SWV along a muscle's fiber direction is directly related to a tissue's shear elastic modulus [4]. Two images were collected from both regions for each isometric force task, resulting in approximately 80 images per subject.

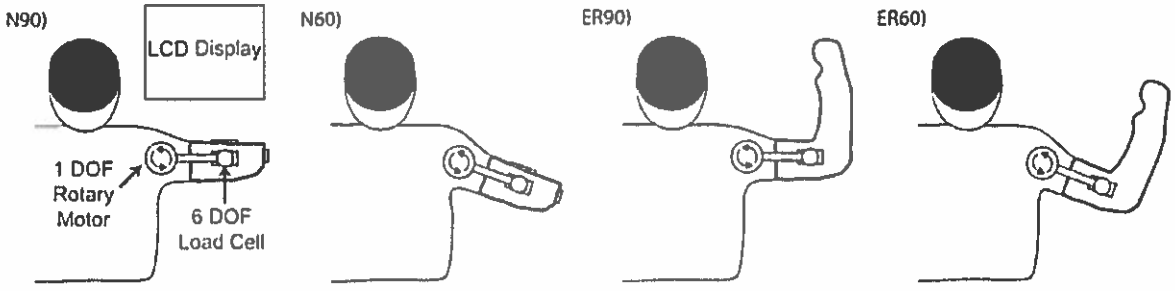


**Figure 1**: Schematic of the experimental setup. Subjects were attached to a rotary motor while their arm was elevated 60 degrees (60) or 90 degrees (90) and externally rotated in a neutral position (N) or 90 degrees (ER).

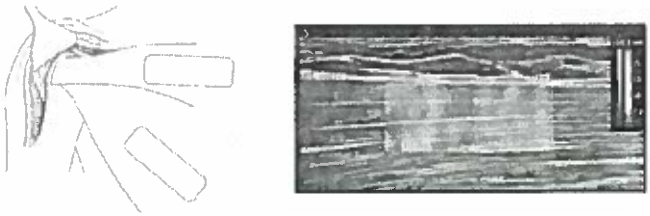

**Figure 2:** Probe location and representative B-mode ultrasound image of the clavicular fiber region with the shear wave elastography color map

A four-factor mixed model was used to assess differences in SWV between fiber regions (clavicular, sternocostal), shoulder positions (N60, N90, ER60, ER90), torque directions (horizontal, vertical adduction), and torque levels (0, 15, 30% MVC). All significances are reported at $\alpha$=0.05.

## RESULTS AND DISCUSSION

SWV increased with increasing activation for each fiber region and shoulder position (all $p<0.001$). Within the clavicular region, SWVs were higher at every experimental shoulder position and torque level when torque was produced in the horizontal direction (all $p<0.001$). Within the sternocostal region, horizontal adduction torques resulted in higher SWVs at every experimental position (all $p<0.05$) except N60 ($p > 0.90$).

Resting SWVs were higher in the clavicular region for all four experimental shoulder positions (Figure 3) (all $p<0.001$). When the shoulder was externally rotated 90°, there were no differences between the regions for either torque direction at any torque level greater than passive. When the shoulder was in neutral external rotation, the clavicular region exhibited significantly higher SWVs than the sternocostal region at 15% and 30% MVC in horizontal adduction (Figure 4). During vertical adduction, SWVs were higher in the sternocostal region, but only at 30% MVC (Figure 4).

Our results indicate that harvesting the clavicular region may affect passive shoulder stiffness to a greater degree than harvesting the sternocostal region especially at greater abduction and rotation angles [5]. Disinsertion of either region may impact torque-generation in horizontal adduction in a similar manner, while disinsertion of the sternocostal fibers may result in additional impairments when producing vertical adduction torques [6].

Changing shoulder joint position and torque direction underscores the heterogeneous elastic properties of the pectoralis major muscle. These results suggest that each fiber region uniquely contributes to isometric shoulder stability, but future work is needed to identify exactly how each region contributes to shoulder dynamics.

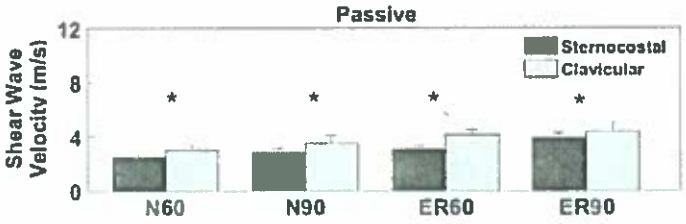


**Figure 3:** Passive shear wave velocities across fiber regions and experimental conditions. Errors bars indicate 1 SD. * signifies $p < 0.05$.

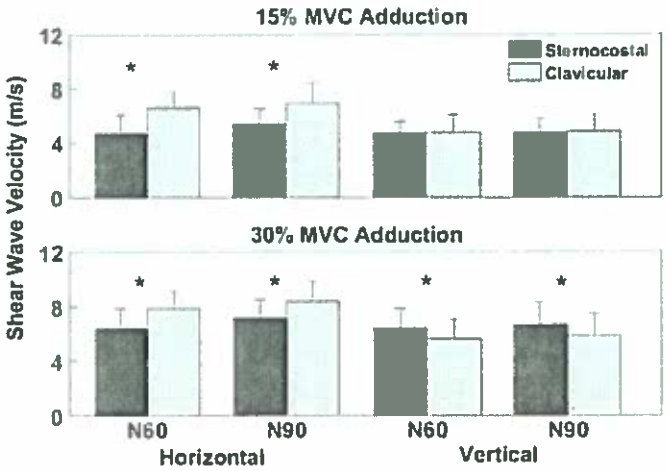


**Figure 4:** Fiber region differences in active shear wave velocities for N60 and N90 experimental conditions when producing torques in horizontal or vertical adduction. Errors bars indicate 1 SD. * signifies $p < 0.05$.

## CONCLUSIONS

The pectoralis major has distinct fiber regions that exhibit markedly different elastic properties.

## REFERENCES


1. Valenti et al., *Int Orthopaedics,* **39**:477-483, 2015
2. Carlson et al., *Oral Max Surg*, **15**:565-575, 2003
3. Hu et al., *J Neurophysiol*, **105**:16300-1641, 2011
4. Bercoff et al., *IEEE Trans*, **51**:396-409, 2004
5. Koo et al., *J Biomech*, **46**:2053-2059, 2013
6. Hug et al., *J EMG & Kines*, **25**:703-708, 2015

# MODELING FUNCTION OF THE HAND AND THE EFFECT OF OSTEOARTHRITIS ON FORCE

Joshua P. Drost, Tamara Reid Bush
Michigan State University, East Lansing, MI, USA
email: drostjos@msu.edu, reidtama@msu.edu

## INTRODUCTION

Our hands are used constantly for crucial tasks such as eating, dressing and toileting. When the hand is impaired, it is critical that we understand how much function was lost and where so that the best possible treatment can be provided. Currently, changes in hand function are measured using surveys and radiological exams, both of which are subjective; objective methods to quantify changes in hand function are needed [1, 2]. A model that includes the total *force and motion abilities* will allow health care experts to easily compare changes in hand function, and better rehabilitate and treat the individual.

Previously, we modeled changes in the motion abilities of the hand caused by arthritis [3]. This model included the full range of motions of the hand; however, force data for each finger were not incorporated into that model. Both motion and forces are necessary to generate a comprehensive hand model for clinical use. The goal of this work was to develop a model that could predict the forces over the kinematic workspace of participants with and without reduced hand functionality.

## METHODS

Sixteen participants (7 female and 9 male, average age 25.6 years, SD 6.1 years) without any reported injury or arthritis, termed "Healthy", and fifteen participants (13 female and 2 male, average age 73.5, SD 4.8 years) with doctor diagnosed arthritis, termed "Arthritic", were included in this study.

Forces due to changes in flexion/extension of the index finger (no adduction or abduction) were measured using a "U-shaped" metal bracket placed in seven positions along a line, each 15mm apart. The participant was asked to push on the bracket, and then pull on the bracket with maximum force using the pad of the index finger (Figure 1 A&B).

Maximum abduction/adduction forces were also measured in six positions. Three of the positions were at maximum extension (called "Adduction/Abduction Push"—Figure 1C) and the other three were at a mid-range flexion of the interphalangeal joints (called "Adduction/Abduction Pull"—Figure 1D). During data collection participants were asked to continually grip a cylindrical handle with the other fingers to isolate the finger forces and to maintain a consistent orientation of the wrist.

After collection, the data were analyzed in terms of the 1) fingertip posture (x,y,z coordinate) 2) the direction of the force applied, and 3) the magnitude of the force applied. A linear mixed effect model was then created for each health and gender population. The model included the covariates of normalized distal displacement, normalized palmer displacement, angle and angle squared along with their interactions. Subject number was used as a random variable to remove error between subjects.

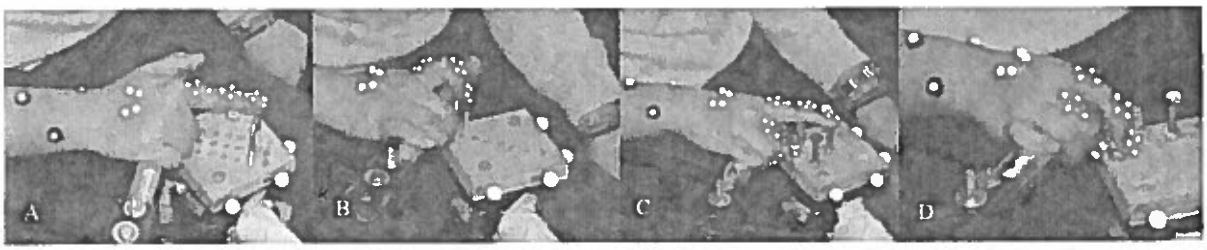


**Figure 1: Experimental setup and force data for (A) flexion/extension push, (B) flexion/extension pull, (C) adduction/abduction push and (D) adduction/abduction pull trials**

## RESULTS AND DISCUSSION

Sagittal plane views of the force data are presented in Figure 2 (Left). Forces were plotted based on the finger posture in 3D space and normalized based on the length of the individual's finger. The origin for all data was at the MCP (metacarpal phalange) joint of the index finger. The plots are oriented so that a fully extended index finger would sit along the horizontal axis with the pad of the index finger pointing in the positive vertical direction.

Predicted forces are also shown in a sagittal plane view (Figure 2 Right). The covariates are the same as the observed data, but the forces have been predicted using the model. This model can closely predict the forces over the range of motion. Of the covariates the most accurate are the three way interactions between the displacements and the angle and the three way interactions between the displacements and the angle squared ($p=0.01$).

This prediction model is the first step in being able to use limited clinical measures to create a complete mapping of the forces of the hand. Such a model will give clinicians an additional tool for diagnosing disorders, tracking therapy and identifying treatment to help the patient gain back function.

Currently the model has only been developed for a portion of the index finger. Future work will include forces and associated models for all fingers. Also, measures of motion and force will be gathered prior to intervention; mid-way through rehabilitation and after rehabilitation is complete to test its usefulness in a clinical situation.

There is a need for an objective method for diagnosing loss in hand function. We are working to model the force and motion abilities of the hand and how they change with arthritis. This model is highly innovative and useful: comparisons with these models will be able to determine what level of function was lost and how much was restored due to treatment.


## ACKNOWLEDGEMENTS

The authors would like to thank the Pearl J. Aldrich Endowment in Aging Related Research for their funding as well as Sam Lietkam, Wu Pan, and Jessica Buschman for assistance in capturing data.


## REFERENCES


[1] Chung K C., et al The Journal of Hand Surgery, 575-587. 1998.

[2] Katz S, et al. Journal of the American Medical Association, 914-919. 1963.

[3] Leitkam S, Bush TR. ASME Journal of Biomechanical Engineering. 2015.


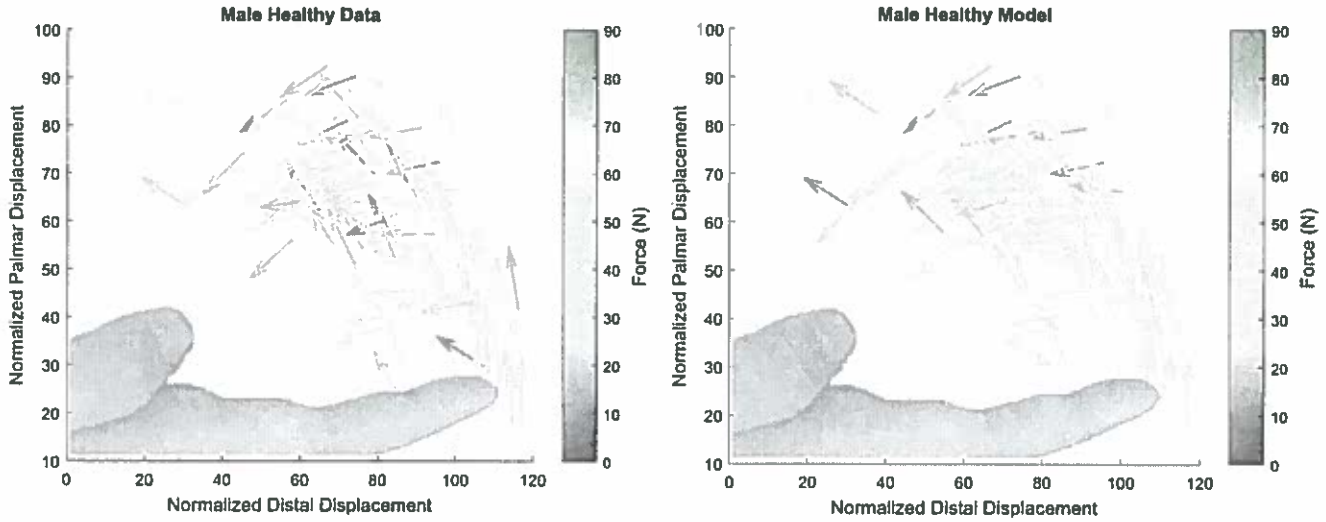


**Figure 2: Sagittal projection of force data for healthy male subjects. A finger has been superimposed over the image to help represent position and direction of forces. Left: observed forces. Right: model prediction of forces.**

# An Investigation of the Effect of Gear Ratio on Manual Wheelchair Kinetics

[1] Elizabeth Gacek, [1]Abby Pakeltis, [2] Omid Jahanian, [1] Alan Gaglio, [3] Scott Daigle
[1] Ian Rice, [2] Brooke Slavens, and [1] Elizabeth T. Hsiao-Wecksler

[1] University of Illinois at Urbana-Champaign, Urbana, IL, USA
[2] University of Wisconsin-Milwaukee, Milwaukee, WI, USA
[3] IntelliWheels, Inc., Champaign, IL, USA
email: egacek2@illinois.edu, web: www.hdcl.mechanical.illinois.edu

## INTRODUCTION

In the United States, there are approximately 3.26 million manual wheelchair users (MWUs) [1]. Manual wheelchair use exposes the user to excessive loading of the upper extremity joints. As a result, MWUs commonly report upper extremity joint pain, most notably in the shoulders and wrists. Approximately 58.5% of users report shoulder pain, which is most commonly attributed to manual wheelchair mobility [1].

Multiple design modifications have been proposed to reduce the excessive loading experienced by MWUs including pushrim-activated power-assist and lever-driven wheelchairs. Drawbacks of these assistive wheelchairs include bulkiness, inaccessibility, and high cost. IntelliWheel, Inc. has developed geared wheels that incorporate a planetary gear train between the hand rim and the wheel for different gear ratios. These geared wheels provide MWUs with a low cost, discrete assistive device aimed at reducing upper extremity loading and joint pain while maintaining the aesthetics and weight of a standard wheelchair. Specifically, geared manual wheelchair wheels allow a MWU to adjust gear ratio based on the terrain over which the user is propelling.

Although geared manual wheelchairs have the potential to reduce upper-extremity joint biomechanical demands [2] and pain [3] in MWUs, their kinetic effects on propulsion biomechanics remain untested. A reduction in peak force on the wheelchair hand rim has been shown to reduce net muscle stress [4]. To investigate the effects of lower gear ratio on wheelchair biomechanics, an instrumented wheelchair hand rim was developed [5]. The hand rim can be attached to a standard wheel or an IntelliWheels geared wheel. The applied forces and torques during standard and geared manual wheelchair mobility were examined for two conditions (over level ground and up a short ramp).

## METHODS

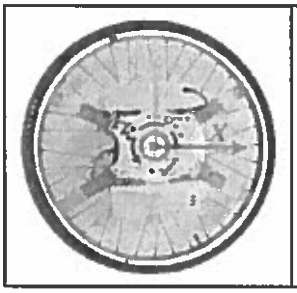

**Figure 1: Orientation of the coordinate system on the direct drive and geared wheels.**

For this study, the instrumented hand rim (IHR) measures forces applied to the rim in three axes and wheel rotation angle. The IHR coordinate system is a global frame, denoted by *XYZ*, at the axis of the wheel (Fig. 1). A positive moment in the XY plane is denoted as a counter-clockwise torque, $M_z$, applied in the direction of the Z-axis.

The IHR was attached to an IntelliWheel (IW) multi-gear wheel capable of two gear ratios: direct drive (DD, 1:1) and a low gear ratio (G, 1:1.5). The IW+IHR wheel was attached to the right side. A dummy IW wheel with 3D balance weights was on the left. The wheelchair was set with a camber angle of 0 degrees. Forces and torques are measured locally at the center of the wheel and converted to the hand rim point of contact [5].

Propulsion trials were conducted at the Mobility Lab at the University of Wisconsin-Milwaukee for both gear ratios in two scenarios: overground on level tiled floor and up an inclined ramp. Five trials in each condition (DD, G) were recorded for each scenario. The subject propelled approximately 30 feet for overground trials, and approximately 8 feet up an ADA compliant incline (~4.8 degrees) for ramp trials. Preliminary data are from a novice able-bodied young adult male (24 yr) propelling at a self-selected speed. Standard

kinematic equations were used to determine linear speed of the subject.

To eliminate forces and torques due to the weight of the hand rim, dynamic offset vectors were constructed by collecting dynamic trials without an applied load [6]. To do this, a researcher pushed the chair while the subject kept his hands in his lap to prevent the application of an external force on the hand rim. Forces and torques due to start up and braking were eliminated from all propulsion trials. Specific peak forces ($F_x$, $F_y$) and torque ($T_z$) for each condition and gear ratio were emphasized due to their large influence on manual wheelchair propulsion.

## RESULTS AND DISCUSSION

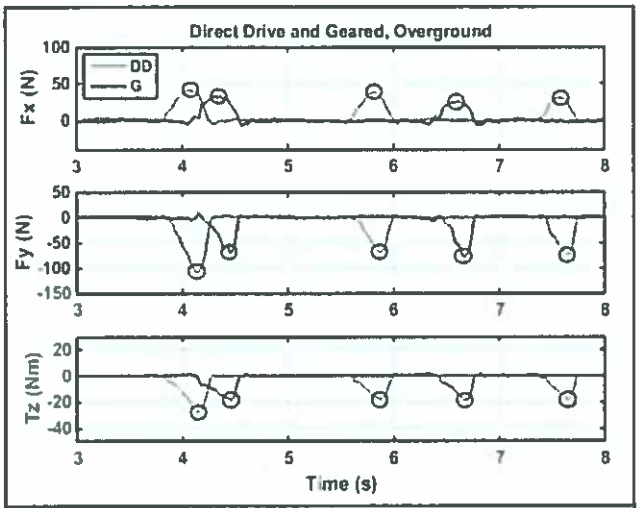


**Figure 2:** ***Sample peak XY forces and Z torque for a single overground direct drive (DD) or geared (G) trials.***

The total force, $F_{tot}$, was larger for DD than G, both during propulsion on level floor and up the ramp. The force applied in the x-axis, $F_x$, was notably lower for G than DD during overground (30%) and ramp (19%) propulsion. Furthermore, $T_z$ was lower for the G than the DD wheel (Table 1). The linear speed of the subject was higher for DD than G for OG trials and similar for R trials (Table 2). These findings indicate that decreasing gear ratio decreased the amount of force necessary for manual wheelchair propulsion on level floor.

**Table 2: Self-selected linear speeds of a novice able-bodied subject when overground (OG) or up a ramp (R) using either direct drive (DD) or a lower gear ratio (G).**

| Gear Ratio | Mean Speed OG (m/s) | Mean Speed R (m/s) |
|---|---|---|
| DD | 1.15 (0.12) | 0.39 (0.23) |
| G | 0.99 (0.13) | 0.39 (0.21) |

## CONCLUSIONS

Geared manual wheelchairs with lower gear ratios offer an alternative to assistive technologies aimed at reducing excessive loads experienced by MWUs. The presented results preliminarily demonstrates that reducing the gear ratio on a manual wheelchair wheel reduce handrim forces. This suggests that geared manual wheelchair wheels can be used as an interventional tool. Future direction will include a larger investigation to be conducted at the University of Wisconsin-Milwaukee aimed at examining the effect of lower gear ratio on upper extremity joint biomechanics in MWUs with spinal cord injury.

## REFERENCES


1. LaPlante, M. P., & Kaye, H. S. *Assist Technol: The Official Journal of RESNA*, *22*(1), 3–17, 2010.
2. Jahanian, O., et al. *EMBC IEEE 38th Annual International Conference*, Orlando, FL, August, 2016.
3. Finley, M. A., Rodgers, M. M.. *Arch. Phys. Med. Rehabil.*, 88, 1622-1627, 2007.
4. Lin, G. G., & Scott, J. G. *Clin Biomech*, 27(9), 879-886, 2012.
5. Gaglio A, et al. *J Med Dev Trans ASME*, 10(3), 030956, 2016.
6. Woods KR, et al. *RESNA 27th International Annual Conference*, Orlando, FL, June 18-22, 2004.


## ACKNOWLEDGEMENTS


Supported by NIH SBIR II #R44 HD071653-02


**Table 1: Overground (OG) and Ramp (R) average (std) forces and torques for manual wheelchair propulsion from a single, novice user.**

| Gear Ratio | Mean Peak $F_x$ (N) | | Mean Peak $F_y$ (N) | | Mean Peak $T_z$ (Nm) | | Mean Peak $F_{tot}$ (N) | |
|---|---|---|---|---|---|---|---|---|
| | OG | R | OG | R | OG | R | OG | R |
| DD | 44.6 (1.5) | 82.2 (7.0) | -90.3 (13.6) | -73.3 (30.0) | -23.7 (4.4) | -28.5 (1.8) | 126.8 (18.2) | 104.2 (29.1) |
| G | 31.7 (5.8) | 67.5 (7.1) | -77.6 (8.1) | -79.3 (19.6) | -19.9 (2.1) | -23.9 (1.9) | 97.2 (11.8) | 93.5 (20.6) |

# A COMPARISON OF PREFERRED AND REQUESTED STEP LANDING STRATEGIES

[1] Emily Gerstle, [1]Kazandra Rodriguez, [1]Stephen Cobb

[1] University of Wisconsin-Milwaukee, WI, USA
email: egerstle@uwm.edu

## INTRODUCTION

The transition steps to level walking is where 70% of trips and falls on steps occur [1]. With the cost of treating fall related injuries estimated at $31.3 billion in the United States [2] determining modifiable risk factors associated with transition step negotiation is needed.

Depending on the height of the step, walking speed, and the age of the participant, the preferred landing strategy of the step onto level ground varies. Freedman and Kent [3] found most healthy young adults prefer to land with the heel on steps up to 10cm (91%), while on 20cm steps landing with the forefoot was preferred (81%). van Dieen and Pijnappels [4], examining the effect of age, speed, and step height on step mechanics also found young adult landing preference to be with the heel regardless of walking speed on a 5cm step, however, on a 10cm step the preference was split between the heel and forefoot strategies. The majority of young adults switched to a forefoot landing at faster speeds. With a 15cm step at the fastest speed (5km/h) only 20% of young participants landed with a heel strike. The majority of older adults in van Dieen and Pijnappels [4] study preferred a forefoot strike even on the 5cm step with the exception of the faster speeds (4 and 5 km/h) on the 5cm step. On all other steps and speeds more than 80% of the older adults landed with the forefoot. The difference in landing preference between young and older adults may be due to the need to rely more on the skeletal system for stability and less on the muscular system [5]. However, to determine stepping mechanic differences between groups (e.g. young and older adults), it is important to compare the groups during the performance of similar landing strategies. The question then becomes, if participants are asked to land with their non-preferred strategy, will the planned landing influence their stepping mechanics.

The purpose of this study was to determine if there are differences in foot posture at initial contact between healthy young individuals preferred versus non-preferred landing strategy on a 15cm step.

It was hypothesized that comparing initial contact angles of participants that landed with the heel without landing instructions (preferred heel) would not be significantly different than those that landed with the forefoot but were requested to land with the heel (requested heel).

## METHODS

Participants:
Sixteen participants (8 female, 8 male; age = 25.8 ± 5.3 years; height = 173 ± 9.5 cm; mass = 72.6 ± 14.7 kg) were recruited for the study. All subjects had weight bearing ankle dorsiflexion ROM $\geq 25°$, did not wear bifocals, and had no history of lower extremity surgery or recent injury.

Gait analysis:
A 10 camera motion analysis system was used to capture 3D positions of clusters of retroreflective markers placed on the foot and leg to define five functional articulations [Rearfoot complex (RC), Lateral midfoot (LMF), Medial midfoot (MMF), Medial forefoot (MFF), and Lateral forefoot (LFF)].

At a self-selected pace, participants walked along a level 5 m walkway, stepped down a height of 15 cm and continued walking. After completing practice trials to establish a consistent self-selected pace, trials were recorded until 10 of the same (preferred) landing strategy were achieved. Participants were then asked to continue but with the opposite landing strategy until 10 of the requested trials were recorded.

The calibrated anatomical systems technique was used to reconstruct 3D segment positions and orientations. Joint angles between adjacent segments were calculated using the joint coordinate system technique.

Data analysis:
Independent t-tests were performed between the preferred and requested heel landing examining the initial contact angles of the rearfoot in all three planes, and in the sagittal plane of the medial and lateral midfoot and medial and lateral forefoot. Significance level for all tests was set at $\alpha$=0.05.

## RESULTS AND DISCUSSION

The preferred versus requested heel landing strategy did not have any significant differences at any of the articulations in any of the planes examined (Table 1).

As the difference between preferred and requested heel landing strategies in young adults is not significantly different, it is possible to ensure similar landing strategies when examining step landing across groups. In this group of young healthy adult participants, the majority preferred a heel strike, however, the preferred landing strategy of individuals with pathologies may indicate a possible compensation. Thus the ability to match landing strategy between control and experimental groups may clarify differences that may otherwise be lost if only preferred strategies are used. Further analysis needs to be done to determine if preferred and requested forefoot strategies are similar within healthy young adults.

## REFERENCES


1. Templer J. *The staircase* MIT press, 1992.
2. Burns ER, et al. *J Safety Res* **58,** 99-103, 2016.
3. Freedman W and Kent L. *J of Motor Behavior* **19,** 214-226, 1987.
4. Van Dieen JH and Pijnappels M. *Gait Posture* **29,** 343-345, 2009.
5. DeVita P and Hortobagyi T. *J Gerontol A Biol Sci Med* **55,** B593-600, 2000.
6. Skalska A. et al. *Exp Gerontol* **48.** 140-146, 2013.
7. Koepsell TD. et al. *J Am Geriatr Soc* **52** 1495-1501, 2004.


**Table 1:** Heel landing strategy Initial contact angles.

| Articulation & plane | Preferred heel (degrees) mean (SD) | Requested heel (degrees) mean (SD) | p-value |
|---|---|---|---|
| Rearfoot sagittal plane | 7.2 (4.6) | 11.4 (4.5) | 0.091 |
| Rearfoot frontal plane | 4.5 (3.4) | 1.8 (2.1) | 0.113 |
| Rearfoot transverse plane | -2.8 (5.2) | -4.4 (3.5) | 0.514 |
| Medial Midfoot sagittal plane | -9.1 (11.1) | -8.6 (7.1) | 0.924 |
| Lateral Midfoot sagittal plane | 0.4 (4.5) | -0.3 (8.5) | 0.833 |
| Medial Forefoot sagittal plane | 10.6 (9.5) | 9.7 (3.6) | 0.844 |
| Lateral Forefoot sagittal plane | 2.6 (3.4) | 2.6 (4.2) | 0.999 |

# KINETIC DIFFERENCES DURING STANCE PHASE OF GAIT WHEN WEARING AN ORTHOPEDIC WALKING BOOT

Heather R. Gulgin

Grand Valley State University, Allendale, MI, USA
email: gulginh@gvsu.edu

## INTRODUCTION

Walking boots or short-leg rigid immobilization devices have been widely used in place of traditional fiberglass casts for orthopedic injuries such as severe ankle sprains, stress fractures, complete foot and ankle fractures, chronic tendinopathy, and post- surgical interventions. These orthopedic walking boots create a leg length discrepancy (LLD). LLD has been shown to alter the kinematics and kinetics of gait [1-2] and has been associated with lumbar and lower limb conditions such as: foot over pronation, low back pain, scoliosis, and osteoarthritis of the hip and knee joints [3]. Research on the biomechanics of gait when wearing an orthopedic walking boot is very limited [4-5]. Thus, the purpose of the study was to examine the kinetics of the stance phase of gait with and without an orthopedic walking boot.

## METHODS

Ethics approval was obtained from the Human Research Review Committee. Forty healthy participants (m = 20, f = 20, mean age 20.7 yrs., ht. 171.6 cm, wt. 73.2 kg) without history of previous lower extremity surgeries or recent physical therapy volunteered. Eight Vicon cameras (MX-T40) capturing at 120 Hz, and floor-embedded AMTI force plates (Advanced Mechanical Technology Inc., Watertown, MA) capturing at 1,200 Hz were utilized to record the kinematics and kinetics during all walking trials. The Vicon full body PIG model was used for the three conditions: (1) tennis shoes on each foot, (2) orthopedic boot on right foot, tennis shoe on left foot – creating a 2.4 cm leg length difference, and (3) orthopedic walking boot on right foot and barefoot on left foot – creating a 5 cm leg length difference. Vicon Nexus 2.2.3 was used to reconstruct, label, and filter marker trajectories (Woltring, MSE 15) prior to exporting three walking trials for each participant for each condition to Visual 3D software (C-Motion Inc., Germantown, MD) for analysis. A one-way ANOVA was run to test for significance across conditions, with follow-up paired t-tests to test for significance differences between left and right limbs.

## RESULTS AND DISCUSSION

Peak sagittal knee moments for left and right limbs are shown in Figures 1 & 2. For both figures, Black = Cond 1, Red = Cond 2, and Green = Cond 3.

Figure 1. Left Knee Extensor Moment

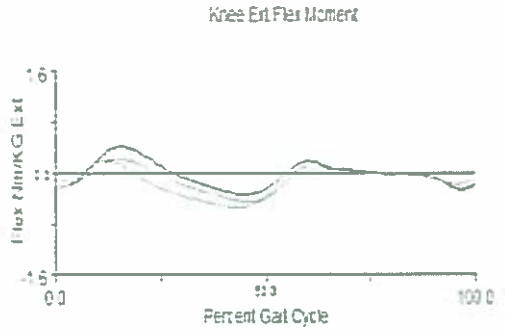


Figure 2. Right Knee Extensor Moment

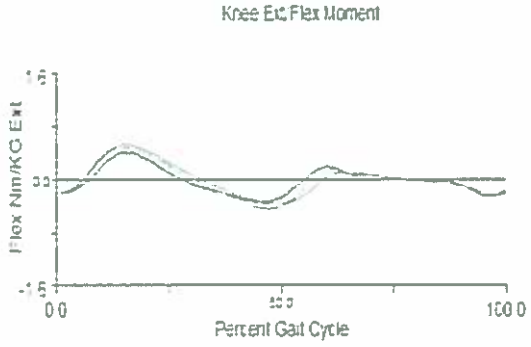


Since the walking boot makes the right limb longer, there is an increase in right hip and knee flexion and a decrease in left hip and knee flexion across the conditions. This side to side difference creates an asymmetrical gait pattern that may alter the joint moments. The current study found a significant increase in the right knee extensor moment and significant increase in the left flexor knee moment. Thus, the sagittal plane loading on the knee joint changes significantly as a result of wearing an orthopedic walking boot. There was little change in the frontal plane kinetics across conditions at the hip, but the right knee has an increased adductor moment when wearing the boot.

## CONCLUSION

Biomechanists and clinicians should be made aware of how the LLD created by the walking boot changes the sagittal and frontal plane knee joint moments as result of the asymmetrical gait pattern.

## REFERENCES

1.Kakushima, M., Miyamoto, K., Shimizu, K. (2003). The effect of leg length discrepancy on spinal motion during gait. Spine, **28(21):**2472- 2476.

2. Wretenberg, P., Hugo, A., Brostrom, A. (2008). Hip joint load in relation to leg length discrepancy. *Medical Devices: Evidence and Research*, **1**, 13-18. 3. Murray, K., Azari, M. (2015). Leg length discrepancy and osteoarthritis in the knee, hip, and lumbar spine. J Can Chiropr Assoc, **59(3):**226-238. 4. Pollo, F., Gowling, T., Jackson, R. (1999). Walking boot design: A gait analysis study. *Orthopedics*, **22(5),** 503-507.

5. Zhang, S., Clowers, K., Powell, D. Ground reaction force and 3D biomechanical characteristics of walking in short-leg walkers. (2006). *Gait & Posture*, **24**, 487-492.

## ACKNOWLEDGEMENTS

The authors would like to acknowledge the donation of the tennis shoes by the Grandville, MI New Balance store. The authors would also like to acknowledge Gordy Alderink and Lauren Hickox for their assistance with the Visual 3D software.

# TEXTING DURING STAIR NEGOTIATION AND IMPLICATIONS FOR FALL RISK

[1]Rami Hashish, [2]Megan E. Toney-Bolger, [3]Sarah Sharpe, and [3]Ben Lester

[1] National Biomechanics Institute, Los Angeles, CA, USA
[2] Exponent, Detroit, MI, USA
[3]Exponent, Phoenix, AZ, USA
email: mtbolger@exponent.com

## INTRODUCTION

Walking in complex environments requires integration of the sensory and motor systems. Cognitive distractions have been shown to interfere with negotiation of complex walking environments, especially in populations at greater risk for falls, such as the elderly. Use of mobile phones for texting has been shown to disrupt gait patterns in healthy individuals during level walking, but no study has identified the effect texting has on navigating complex walking environments.

Texting has been shown to alter cognitive attention, modify mechanical demands, and reduce the visual field in ways that may negatively affect gait performance. Existing research reports gait changes that may indicate adoption of strategies to increase stability while simultaneously texting and walking over level ground, including reduced walking speed, wider stance width, and increased minimum margin of stability. Conversely, other studies have reported changes that suggest increased potential for gait disruption and falls while texting and walking on level ground, including deviation from a straight path and reduction of swing leg toe clearance. These findings suggest that the potential for unintended interactions with obstacles and trip initiation may increase while texting. Additionally, Smith et al. (2013) found that 78% of injuries associated with cell phone use while walking resulted from a fall, suggesting that distraction with cell phone use could lead to changes in walking biomechanics that could result in greater fall and injury potential.

Current research has not investigated the effects of texting while negotiating complex walking environments frequently encountered in daily life, such as stairs. Stair ascent and descent are inherently complex both in physical execution and motor control, with increased potential to produce trips, slips, and subsequent falls. Stairs by nature are elevated structures, and falls in these environments have a greater potential to be from increased height, resulting in potentially higher impact forces and more severe injuries than falls on level ground. The effects of texting that may increase the potential for trips, compounded with the inherent hazards associated with stair negotiation, may lead to greater safety concerns should individuals choose to text while negotiating stairs.

The purpose of this study was to investigate how the cognitive distraction and additional motor demands associated with texting while walking influence execution of the complex locomotor task of stair negotiation. We hypothesized that participants would walk more slowly, foot clearance would be reduced, and stance width would increase when participants negotiated a stair obstacle while texting compared to navigating the same obstacle without performing a texting task.

## METHODS

Twenty participants were recruited from the Phoenix, AZ area. Participants met the following criteria for inclusion: 1) 25-55 years old; 2) not currently taking medications that influence balance or walking; 3) no musculoskeletal or cardiovascular issues that might compromise balance or walking; 4) daily use of a mobile device for texting. The average age of the participants was 39 years, with an average height and weight of 64.8 inches and 174.2 pounds, respectively. The study procedures were approved by Exponent's IRB.

Three-dimensional kinematic data were collected using an 8-camera OptiTrack system (Corvallis, OR). A series of markers were placed directly on body suits worn by the participants according to the standard OptiTrack 51-marker set, which included a toe marker placed near the top of the third distal phalange and a heel marker placed near the

calcaneus. Participants used their personal mobile device for the texting task.

A step-deck obstacle, mimicking the beginning of stair accent and end of stair decent, was positioned in the middle of a straight walking space. Participants were instructed to walk at a comfortable pace toward the stair obstacle and ascend/descend by placing one foot on each step. Participants performed an 8-trial block consisting of 4 texting trials and 4 non-texting trials. The texting vs. non-texting trial structure was randomized for each participant. During each texting trial, participants iteratively subtracted 7 from a double-digit number an experimenter texted them prior to beginning the trial. The participant texted their final answer back to the experimenter before coming to a stop at the end of the trial.

Kinematic information of interest was calculated using custom code (Matlab, Mathworks, Natick, MA). Stance and swing foot toe clearance during ascent of the first stair and stance and swing foot heel clearance during descent of the last stair were considered for the analysis. Clearances were calculated as the vertical and horizontal distance from the toe or heel marker to the stair edge, at a time when the marker was directly above or in front of the stair nose.

A repeated-measures ANOVA was used to evaluate differences between non-texting and texting trials ($p \leq 0.05$). Statistical analyses were conducted using NCSS Version 10.0.10.

## RESULTS AND DISCUSSION

When texting during stair ascent, participants demonstrated slower ascent ($\Delta$=0.11±0.01s; $p<0.05$), reduced swing-leg vertical toe clearance ($\Delta$=0.01±0.002cm; p=0.03), and reduced swing-leg horizontal toe clearance ($\Delta$=0.03±0.0005cm; p=0.001). No significant differences were found in stance leg variables.

When texting during stair descent, participants demonstrated slower descent ($\Delta$=0.10±0.01s; $p<0.05$), reduced stance-leg vertical heel clearance ($\Delta$=0.02±0.002cm; p=0.0004), and reduced stance-leg horizontal heel clearance ($\Delta$=0.06 ±0.005cm; $p<0.05$). Participants also demonstrated reduced swing-leg horizontal heel clearance that approached significance ($\Delta$=0.01±0.002cm; p=0.051) when compared to the non-texting task. No significant differences were observed in the swing-leg's vertical heel clearance.

## CONCLUSIONS

Our findings suggest that texting during stair negotiation results in changes to gait kinematics that may result in an increased risk for gait disruption and subsequent fall and injury. Reduced swing-leg toe clearance during stair ascent and stance-leg heel clearance during stair descent suggest an increased potential for interaction with the stair lip, potentially disrupting the base of support, which could lead to a subsequent trip and fall.

This study is the first to examine the effect of texting on gait kinematics during stair negotiation. We found that texting while ascending and descending a stair obstacle resulted in changes to gait kinematics that may result in an increased potential for gait disruption and could lead to fall and injury. Our findings are consistent with prior work indicating that the additional cognitive and motor demands associated with secondary task performance negatively affect execution of a primary locomotor task. These findings are particularly important for inherently hazardous tasks in which failure to perform the primary locomotor task could lead to potential injury. Future work should investigate the effects of playing augmented reality games while walking, which present similar challenges as texting and may also affect gait kinematics. Attention should also be given to understanding the effects of texting during task execution in elderly and other high risk populations.

## REFERENCES


1. Schabrun SM, et al. *PLOS One* **9**(1), 2014.
2. Parr ND, et al. *J. Applied Biomech.* 30, 685-688, 2014.
3. Marone, JR, et al. *Gait & Posture* 20, 243-246, 2014.
4. Smith DC, et al. *J. Safety Research* 47, 19-23, 2013.

# Accurately Quantifying Cartilage Using MicroCT and Magnetic Resonance Imaging

David J. Heckelsmiller, Barbara J. Laughlin, Mothana Saad Eldine, Dan R. Thedens, Douglas R. Pedersen, Douglas C. Fredericks, Jessica E. Goetz
The University of Iowa, Iowa City, IA

**INTRODUCTION:** Osteoarthritis is a degenerative joint disease that is characterized by gradual, progressive loss of articular cartilage. Accurate and precise quantification of these changes is of great interest for evaluating osteoarthritic patients in the clinic, testing disease-modifying treatments, and studying the disease process. Micro-computed tomography (microCT) and magnetic resonance imaging (MRI) are appealing methods of non-destructive, three-dimensional (3-D) assessment of articular cartilage. While microCT confers cartilage resolution at the micrometer-level, permitting its use as a gold standard measure of cartilage morphologic parameters such as volume, thickness, and area [1][2], scanner size limits its use to the following: *in vivo* research in small animals, analysis of *ex vivo* specimens, or as a substitute for histology [3]. In contrast, MRI can be used to image large animals or humans for *in vivo* whole joint characterization, but is limited to lower resolution due to scanning time constraints. This work assessed the validity of cartilage thickness measures acquired from MRI to those measured from gold standard microCT scans.

**METHODS:** Following an IACUC-approved protocol, 20 skeletally mature, castrated male goats were anesthetized and underwent an operation to introduce traumatic joint injury to the left knee. The procedure consisted of a partial meniscectomy of the anterior horn of the medial meniscus followed by a blunt impact to the weight bearing region of the medial femoral condyle using a hand-held impaction device [4][5]. The original impact was approximately 6 mm in diameter. At 168 days post-surgery, the animals were euthanized and the hind limbs disarticulated and imaged using a battery of standard clinical MRI protocols. A 3-Tesla research scanner (Siemens, Erlangen, Germany) was used for image acquisition. Following imaging, the operative and non-operative femurs and tibiae were dissected and soaked in formalin. Prior to microCT scanning, the specimens were thoroughly rinsed and dissected further to separate the medial and lateral tibial plateaus and femoral condyles. To assist with the task of cartilage identification, the specimens were incubated in a 30% dilution of the ionic contrast agent Hexabrix (Mallinckrodt, Hazelwood, MO) in phosphate buffered saline (PBS). MicroCT scans were acquired at 9-micron resolution (voxel size: 9 x 9 x 9 $\mu m^3$) using a Skyscan 1176 (Bruker; Billerica, MA) for a sample of right and left medial condyles.

For analysis of the MRI acquisitions, cartilage and subchondral bone interfaces in the medial femoral compartments of both knees were segmented manually from Double Echo Steady State images (voxel size: 0.5 x 0.5 x 0.5 $mm^3$). An, automatic threshold-based segmentation algorithm implemented in MATLAB (TheMathworks; Natick, MA) served to extract the cartilage and subchondral bone interfaces from the microCT scans. Surface models were generated using MATLAB and Geomagic Studio (3DS; Rock Hill, SC). Following surface generation, the MRI and microCT models were registered to one another.

A ray casting algorithm was implemented in MATLAB to calculate cartilage thickness, defined as the distance between cartilage and subchondral bone surface models. To evaluate the efficacy of MRI versus microCT, mean cartilage thickness was calculated for 1-mm diameter discs at 15 randomly selected control points in the weight bearing region on both models. Differences were evaluated using the standard deviation of the mean difference between models.

**RESULTS:** The standard deviation of the mean difference between thicknesses measured for each of the modalities was calculated to be approximately 0.3 mm. A figure illustrating the microCT segmentation before surface model generation and the control points is pictured below.

**DISCUSSION:** Differentiation of cartilage surfaces in contact with one another presents a unique challenge associated with articular cartilage segmentation of an intact joint. Not only are the boundaries of each surface difficult to identify, but compression resulting from passive tension of the joint ligaments during scanning may lead to thinner thickness measurements in the region of contact. In spite of this segmentation challenge, the calculated standard error between thickness measures from microCT and MRI across the medial compartment was less than the expected error from image resolution (+/- 0.5 mm). Therefore, it is reasonable to conclude that clinically available MRI sequences and scanning constraints are of sufficient quality to accurately measure cartilage thickness in the intact human or large animal joint.

**SIGNIFICANCE:** Standard clinical MRI is an accurate modality to acquire quantitative measures of cartilage morphology.

**ACKNOWLEDGEMENTS:** This work was funded by NIH/NIAMS AR055533.

**REFERENCES:** [1] Das Neves Borges, P. et al (2014). Osteoarthritis Cartilage, **22**, 1419-1428. [2] Siebelt, M. et al (2011). J Orthop Res, **29**, 1788-1794. [3] Xie, L. et al (2009). Osteoarthritis Cartilage, **17**, 313-320. [4] Heckelsmiller, DJ et al. A Handheld Device for Creating Cartilage Blunt Impact Injuries [abstract]. In: 62nd Annual Meeting of the Orthopaedic Research Society; 2016 Mar 3-5; Orlando, FL. [5] Heckelsmiller, DJ et al. Changes in Joint Contact Mechanics after an Anterior Partial Meniscectomy in a Large Quadrupedal Animal Model of Osteoarthritis [abstract].

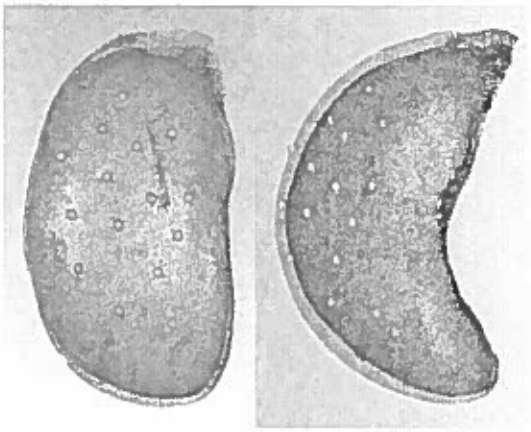

(Left) Control points (orange) overlaid on the microCT segmentation prior to surface model generation. (Right) Segmented microCT points corresponding to the outer cartilage (red) and subchondral bone interfaces (black).

# NEUROMUSCULAR REFLEX CONTROL CAN DESCRIBE HUMAN LOCOMOTION AND RESPONSES TO PERTURBATION

Sandra K. Hnat and Antonie J. van den Bogert

Cleveland State University, Cleveland, OH, USA
email: s.hnat@csuohio.edu, web: http://hmc.csuohio.edu

## INTRODUCTION

A more humanlike actuation system, including muscle dynamics and spinal reflex control, may be able to better replicate able-bodied motor control in lower-limb prostheses or exoskeletons [1]. Currently, the parameters of these reflex models are manually tuned until realistic walking patterns are observed in both simulation and hardware [2]. Here, we investigate the possibility of using a Virtual Muscle Reflex (VMR) system to determine if muscle reflexes can reproduce able-bodied walking and replicate the variations in human joint torques under the effect of random perturbations.

## METHODS

Walking data from 15 participants (4 females and 11 males, age: 24 ± 4 years, height: 1.75 ± 0.09 m, mass: 74 ± 13 kg) was used in the study [3]. The test subjects walked for 8 minutes on an instrumented treadmill at 0.8, 1.2, and 1.6 m/s and were perturbed using random belt acceleration signals generated from discrete-time Gaussian white noise. The variance of the signal was adjusted until the perturbations were within 10% of the mean walking speed. Joint torques were calculated through standard inverse 2D analysis using joint positions from motion capture and the measured ground reaction forces after compensating for inertial artifacts [4].

A planar, lower-leg model with three muscle groups (Gastrocnemius, Soleus, and Tibialis Anterior), representing a lower-limb prosthesis, was used in the VMR controller. Muscles were represented by a standard 3-element Hill-type model: contractile element (CE), series/parallel nonlinear elastic elements (SEE/PEE), and viscous damping. Muscle contraction and activation dynamics were formulated as a set of first-order implicit differential equations (IDE) and were simulated in MATLAB® using a first-order, implicit Rosenbrock solver [5]. Ankle torque was obtained from the VMR model by multiplying the force generated by each muscle with the moment arms.

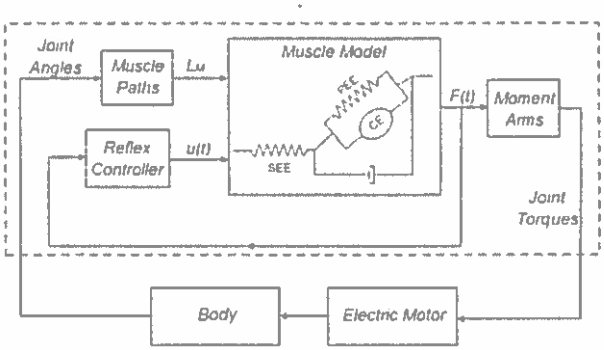


**Figure 1**: Block diagram describing the inputs (muscle length, $L_m$, and neural excitation signals, $u$) and outputs (torque) of the muscle model, in which the red box indicates the scope of this study

Neural excitation signals ($u$) were generated by an autonomous muscle reflex model using positive sensory feedback [1]. The control parameters were optimized in MATLAB using Particle Swarm Optimization (PSO) [6]. A multi-objective cost function minimized the norm between the VMR ankle torque ($\tau_{VMR}$) and measured ankle torque ($\tau_{exp}$), while the effort term was modeled as the mean of the squared muscle activation ($a$):

$$C = W_1\left(\sqrt{\frac{1}{N}\sum\left(\tau_{VMR}-\tau_{exp}\right)^2}\right) + W_2\left(\sqrt{\frac{1}{N}\sum a^2}\right)$$

Statistical significance was calculated by separating each of the gait cycles was into 100 different points. The coefficient of determination ($R^2$) was calculated for all gait cycles at each point to correlate how well the reflex controller can describe that particular

instance of the gait cycle compared to the torque exhibited by the test subject at the same time. The correlation between the measured and predicted joint torques was plotted for each of the 100 points.

## RESULTS AND DISCUSSION

Results from one test subject (male, age = 22, mass = 81 kg, speed = 1.2 m/s) are presented here. The VMR system produces variations in peak moment between gait cycles and the predicted joint torque consistently matches the timing of ankle push-off.

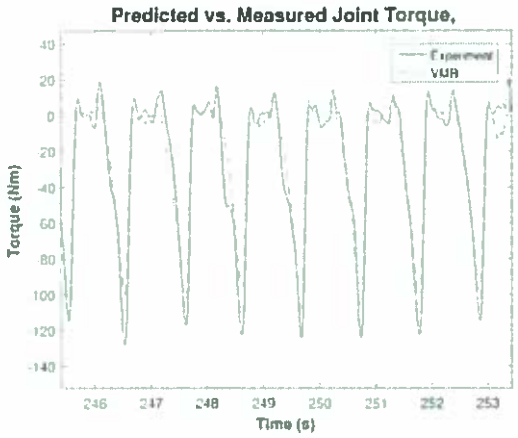


**Figure 2**: Experimental joint torque (black) and Virtual Muscle Reflex (VMR) joint torque using optimized reflex control parameters (red). Negative torque corresponds to plantarflexion.

The statistical analysis shows that the response of the VMR system to mechanical perturbations is similar to the response of the human subject. The $R^2$ value was calculated using 470 gait cycles. The highest correlation occurs during ankle push-off and early swing.

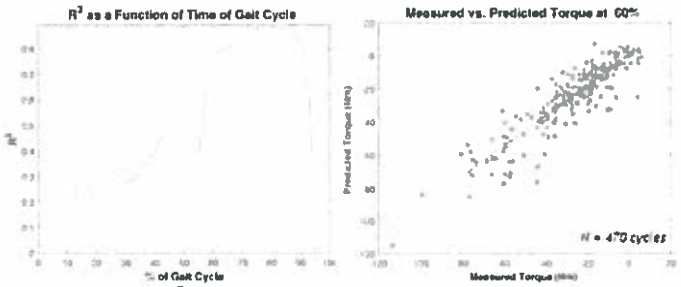


**Figure 3**: $R^2$ as a function of the gait cycle (left) and the correlation between experimental joint torque vs predicted joint torque at 60% of the gait cycle

## CONCLUSIONS

The reflex controller of Geyer et al. [1] is capable of producing realistic joint moments in a powered prosthesis or exoskeleton. Further research includes completing the optimizations and statistical analysis for all subjects and all speeds, as well as performing cross-validations.

## REFERENCES


1. Eilenberg MF, et al. *IEEE Trans. on Neural Syst. and Rehab. Eng.*, **18**, 164-173, 2010.
2. Geyer H, et al. *IEEE Trans. Neural Syst. Rehab. Eng.*, **18**, 263-273, 2010.
3. Moore JK, et al. *Peer J*, **3:e918**, 2015.
4. Hnat SK, et al. *Journal of Biomechanics*, **47**, 3758-3761, 2014.
5. Van den Bogert AJ, et al. *Procedia IUTAM*, **2**, 297-316, 2011.
6. Simon D. *Evolutionary Optimization Algorithms: Biologically Inspired and Population-Based Approaches to Computer Intelligence*, John Wiley & Sons, Ltd., 2013


## ACKNOWLEDGMENTS


This research is supported by the Parker Hannifin Graduate Research Fellowship Program and the National Science Foundation under Grant no. 134495.

# BALANCE CHARACTERISTIC OF HOCKEY PLAYERS

Audrey Hoffmeister[1], Caroline Church[1], Andrew Wallace[1], Joshua Haworth[2], Mark Walsh[1]
Miami University[1], Oxford, OH, USA
Whittier College[2], Whittier, CA. USA
email: hoffmea@miamioh.edu

## INTRODUCTION

Ice hockey players have a unique set of balance parameters. The blade on their skate foot produces a fulcrum that allows for rotation around the longitudinal axis of the foot with a point of rotation well below the plantar surface of the foot. In most land based sports the point of rotation is either the inside or outside edge of the athletes shoe. Additionally, because of the low friction characteristic of the skate blade on ice the skate can easily glide both in front and behind their center of pressure easily without being lifted from the ground. Furthermore ice hockey players do not typically have a flight phase when skating which leads them to either have single leg or double leg support throughout almost the entire game.

Because of the unique balance requirements of ice hockey are unique we hypothesize that hockey players develop different balance characteristics, particularly when standing on one foot when compared with other athletes or physically active college students. The purpose of this study is to examine the postural swat characteristic of hockey players and a comparison group during several balance tasks and determine if hockey players demonstrate unique balance abilities.

## METHODS

To test this we recruited 16 NCAA division 1 ice hockey players, 47 Division 1 football players and 16 physically active college students. All subjects provided their informed consent to participate in this project. Descriptive data of the participants can be seen in Table 1. On data collection day subjects reported to the biomechanics lab where we collected descriptive data. Each subject was then asked to perform 3 balance tasks, a double leg stand, and single right and left leg stands. The balance tasks were performed in a counterbalanced order. For each trial, participants were asked to stand still, barefoot on a 60 x 90 cm in-ground forceplate (Bertec, USA, model #6090-15) with feet placed approximately shoulder's width apart and arms crossed over the chest. While in this position, COP was recorded in the AP and ML directions at a sampling rate of 100 Hz for trials of 30 s. During all trials participants were asked to direct their visual attention towards a 5 x 5 cm piece of cardboard fixed at eye level.

| Group | Age (yrs) | Height (cm) | Body mass (kg) |
|---|---|---|---|
| Physically active | 21.6 (1.0) | 180.5 (7) | 81.8 (13) |
| Ice Hockey | 21.4 (1.3) | 184.6 (5.4) | 86.8 (10) |
| Football | 19.3 (1.0) | 184.4 (6.3) | 97.8 (15) |

**Table 1.** Descriptive data of the subjects

If a participant lost their balance during a trial the trial was repeated until the subject successful performed the trial.

The data was analyzed in both AP and ML directions. Analysis of the data included use of standard balance measures of path length and range of the center of mass postural sway movement as well as sample entropy (SEn) to examine the nature of the postural sway. ANOVAs with post hoc Tukey Tests were used to detect differences between the groups for the different conditions.

## RESULTS AND DISCUSSION

There were no significant differences among the groups for AP or ML range for double or single leg stance. Significant differences were detected for AP and ML path length for all conditions. Exact

values and significant differences are presented in table 2.

| | Physically active | Ice Hockey | Football |
|---|---|---|---|
| Measure | mm | mm | mm |
| AP path double leg | 1036 (158) | 319.(59)[1] | 369 (255) [1] |
| AP path left leg | 1428 (222) | 1557 (293) | 856 (179) [1,2] |
| AP path right leg | 1450 (269) | 1407 (275) | 888 (210) [1,2] |
| ML path double leg | 1426 (208) | 448 (50) [1] | 367 (144) [1] |
| ML path left leg | 1823 (318)) | 1433 (310) [1] | 829 (186) [1,2] |
| ML path right leg | 1797 (447) | 1288 (182) [1] | 866 (232) [1,2] |

**Table 2.** Results for single and double leg path length measures. [1] and [2] note significance with other groups.

Since the instructions were to stand still lower path length values indicate the subjects are performing the assigned task better. As expected the athletes tended to perform better than the non-athletes with the football players with the football players producing significantly lower values that the control group in every condition and the ice hockey players producing lower values that the control group in most conditions. These results agree partially with our hypothesis that ice hockey players would develop a unique balance characteristic medio-laterally due to the unique demands of the sport of ice hockey. Of the groups we anticipated the ice hockey players producing the best results. It's possible that since during the game of ice hockey, ice hockey players balance on a thin blade during single leg support that they are more sensitive to mediolateral deviations and are constantly correcting their center of pressure deviations resulting in more movement back and forth past the center of the skate blade while other athletes (in this case football players) are comfortable having their center of pressure over a range of widths between the medial and lateral sides of the foot and don't feel the need to immediately return the center of pressure to a specific position.

The SEn results show that the athlete groups produced significantly different SEn values than the control group for each condition and that the ice hockey and football groups produced similar values for all mediolateral measurements but significantly different values for all AP conditions. Exact values and significant differences are presented in table 3.

| | Physically active | Ice Hockey | Football |
|---|---|---|---|
| AP SEn double leg | 0.55 (0.32) | 0.09 (0.04) [1] | 0.22 (0.12) [1,2] |
| AP SEn left leg | 0.31 (0.08) | 0.22 (0.04) [1] | 0.18 (0.04) [1,2] |
| AP SEn right leg | 0.27 (0.05) | 0.21 (0.04) [1] | 0.18 (0.04) [1,2] |
| ML SEn double leg | 0.39 (0.20) | 0.06 (0.02) [1] | 0.07 (0.03) [1] |
| ML SEn left leg | 0.27 (0.13) | 0.11 (0.04) [1] | 0.10 (0.04) [1] |
| ML SEn right leg | 0.25 (0.08) | 0.11 (0.02) [1] | 0.11 (0.03) [1] |

**Table 3.** Results for single and double leg Sample Entropy measures. [1] and [2] note significance with other groups.

A higher SEn value indicates a more complex pattern. More complex and more chaotic postural sway patterns have been associated with better balance (Schmit, 2005). It is unclear why the ice hockey and football players produced lower values in this case.

## CONCLUSIONS

Our hypothesis was partially confirmed that hockey players develop unique balance strategies than non-athletes and other athletes. More research needs to be performed to better explain the mechanisms behind these different strategies.

## REFERENCES

1. Schmit J. et al. Exp Brain Res.163. 370-378 2005.

# THE INFLUENCE OF CARBON COMPOSITE AND PLASTIC ANKLE FOOT ORTHOSES ON BALANCE, GAIT AND FATIGUE IN INDIVIDUALS WITH MULTIPLE SCLEROSIS

Sarah Hollis, Hannah Clark, Paige Ingram, Tamara Erlich, Tessa Hill, Dr. Kurt Jackson, and Dr. Kimberly Bigelow,

University of Dayton, Dayton, OH, USA
Email: holliss2@udayton.edu

## INTRODUCTION

There are an estimated 400,000 Americans with multiple sclerosis, many of whom suffer from debilitating mobility impairments [1]. Multiple sclerosis (MS) is a neurological disease due to the breakdown, or demyelination, of myelin sheaths that coat the nerves. When demyelination happens, the axons of nerves get damaged. This damage to the axons causes a disruption of transmission between the brain and the desired action of the body [2]. This affects function throughout the body, with one of the most common complaints associated with the disease being mobility impairments and balance deficits [3]. Muscle weakness, balance problems, and sensory deficits further contribute to these difficulties and increases the risk of falls in this population [2].

These mobility impairments caused by MS may be appropriate to treat with orthoses. Ankle foot orthoses (AFO) are braces worn on the lower leg and foot. They are usually prescribed to individuals with foot drop to help stabilize the ankle due to muscle weakness; and also prevent the individual from falling or injuring themselves. Although individuals with Multiple Sclerosis do not typically have foot drop, there may be other advantages to prescribing AFOs to those individuals.
Two of the most common AFOs are carbon-fiber anterior shell and polypropylene posterior leaf spring. AFOs can provide different features and benefits to improve gait, balance, and fatigue management. Some of the common benefits include increasing toe clearance and support in the swing stage of the gait cycle, force management during heel strike, and energy storage [4]. However, there could potentially be some tradeoffs to wearing the orthotics.

The purpose of this in-progress study is to take a comprehensive look at ankle foot orthoses; and more specifically, evaluate the influence of carbon composite and plastic ankle foot orthoses on balance, gait, and fatigue in individuals with MS.

## METHODS

Twenty study participants with MS (18-85 y/o) will participate in this study. The inclusion criteria for the study participants included a diagnosis of relapsing remitting or secondary progressive MS and the ability to ambulate a minimum of ten meters with or without an assistive device no greater than contact guard assistance. Individuals must also not be currently using an AFO.

Each of the study participants will come to the on-campus laboratory for a total of three visits to complete all tests under three conditions: a baseline visit with no AFO, and two additional visits with randomized brace conditions between carbon-fiber anterior shell and polypropylene posterior leaf spring AFOs. During the initial visit, a neurological exam is conducted, including various clinical assessments. The outcomes of these assessments will be incorporated into the final overall conclusions on AFO effectiveness, however the focus of this paper will be on the more biomechanical aspects of the study.

To measure the effects of the AFOs on balance, quiet standing posturography tests were done under different conditions using a Bertec balance plate. The tests were conducted with eyes open, eyes closed, with foam, and without foam. Another test conducted on the balance plate is limits of stability to examine the possible negative effects of AFOs on dynamic motion. A 10 meter walk and Instrumented Timed Up and Go (iTUG) are two gait assessments performed using APDM Wearable Opal Sensors. These assessments are used to examine the effects of the AFOs on mobility.

After the data collection process is completed for the 20 study participants, data will be analyzed. For the purpose of this abstract, the focus will be on the data from the quiet-standing and limits of stability posturography assessments. Center of pressure data from these assessments will be analyzed using a MATLAB code to calculate anterior-posterior sway range, mediolateral sway range, and mean velocity. SPSS statistical software will be used to carry out a MANOVA to examine the effect of the braces ($p<0.05$).

## RESULTS AND DISCUSSION

Three individuals have completed their study participation to date. While statistical analysis is not appropriate until the study is completed, preliminary results have not suggested a single effective AFO across individuals. For example, Figure 1 shows that each individual exhibited a difference response to the various AFOs.

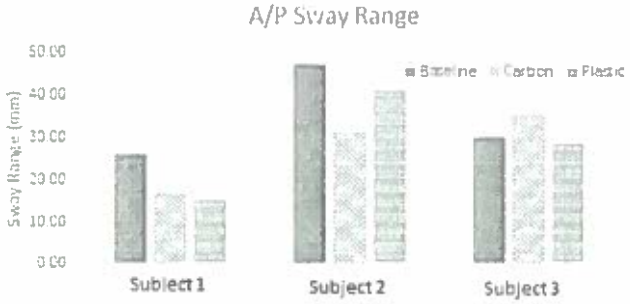


**Figure 1.** A/P Sway Range for Eyes Open, Flat Plate for the first three study participants in all of the brace conditions.

The next step in the study is to finish up testing, which is expected to be complete by early spring.

## CONCLUSION

Understanding the effects of various AFOs on gait, balance, and fatigue for those with Multiple Sclerosis is a step in the direction of helping these individuals manage the effects. Results from postural control studies such as ours can contribute to this understanding. MS has on important aspects of daily life and the benefits and trade-offs different styles might have for different individuals.

## REFERENCES

1. National Multiple Sclerosis Society. http://www.nationalmssociety.org/
2. Multiple Sclerosis Foundation. https://msfocus.org/
3. Heesen C et as. *Multiple Sclerosis.* 14;988-991:2008.
4. Össur. https://www.ossur.com/americas

# A Proposed Study of Core Shift in Human Walking

U. Huzaifa[1], A. LaViers[2],
Department of Mechanical Sciences and Engineering, University of Illinois at Urbana-Champaign, IL, USA
[1]mhuzaif2@illinois.edu [2]alaviers@illinois.edu

## Introduction

Humans are remarkable movers. There are a number of ways to analyze human movement. In the proposed work, we are trying to reconcile findings about one movement, human walking, from a number of disciplines and use them for applications in motion planning of robots.

From embodied movement analysis perspective, Irmgard Bartenieff developed basic movement exercises [1], termed as the Basic Six during her work on rehabilitating polio patients. Out of these six, three are related to walking: Thigh Lift, Forward Pelvic Shift and Lateral Pelvic Shift (Fig. 1a). In the proposed work, we are exploring the nature of pelvic shift in forward and lateral directions in human walking. Along this line of thought, authors have tried to replicate these movements in robots and an initial bipedal robot model for walking was presented in [2] (Fig 1b) where the walking motion was achieved using an open loop control scheme. Building up on that, a simplified model was developed that focused on two of these movements (i.e. Forward Pelvic Shift and Thigh Lift) and achieved walking using state-of-the-art closed-loop control techniques [3] (Fig 1c).

In the biomechanics literature, evidence for pelvic shift during walking has been found in numerous works. The pelvis as mentioned in Bartenieff's walking exercises essentially means the core along with the pelvic girdle. The core constitutes the musculature surrounding the *lumbopelvic region* [4] : *rectus abdominis*, *transverse abdominis* and *interior and exterior oblique muscles*. In [5] and [6], it was concluded that the pelvic rotation and the lateral pelvic displacement were two of the essential determinants of walking. According to some related studies, measurements made from the muscles during walking show activity in the core musculature [7], [8].

## Methods

There has been work done in recording human movements to guide designing and motion planning of a bipedal robot [9]. Inspired by that, it is proposed here to take measurements of translational core shift in forward and lateral directions. For this, VICON motion capture system will be used by attaching reflective markers to the core region of subjects for tracking movements in sagittal and frontal planes during walking. In this regard, marker placement will follow as described in [10] but with more markers in the upper femoral and lower torso regions. As a result, a new kinematic model with more degree of freedom between lumbar and sacrum will be generated to clarify temporal resolution around where walking is initiated. For a start, we want to record as many as ten rigid body movements in the core region to have a detailed account of the core movement. These rigid bodies will be placed corresponding to the spinal region between T12 and the pubic bone. In the test environment, movements will be recorded for the following cases:

- Normal Walking:
  On a treadmill, subjects will be asked to walk at the normal speed of 3 mi/ hr without any extraneous effort done on the legs and the abdomen.
- Brisk Walking:
  Based on the subjects health and build, a target speed will be given to achieve in walking.
- Walk with style:
  This mode of walking will be for studying sway in motion for which dancers will be invited to perform the movement.
- Recover from a push:
  This mode of movement will be the most complex and hard to record as compared to others. Here, the subjects will be given a considerable push to recover from during walking.

The recorded data will be analyzed to find a correlation between the marker output from the core in the normal walking and the rest of the cases.

## Results and Discussion

This is an ongoing work and is motivated by the idea of generating different styles of walking in human-like robots. In the controller design phase of [3], and [2], it was a difficult task to come up with a desired trajectory for the core to follow. Since we did not have exact data about the core motion profile, we designed a desired trajectory for the core, with trial and error. Although we have achieved stable walking motion as a result of feeding this desired trajectory and designing a feedback controller for it, for three-dimensional extension of this robot, more refined knowledge from this study about translational movement of the core will be helpful.

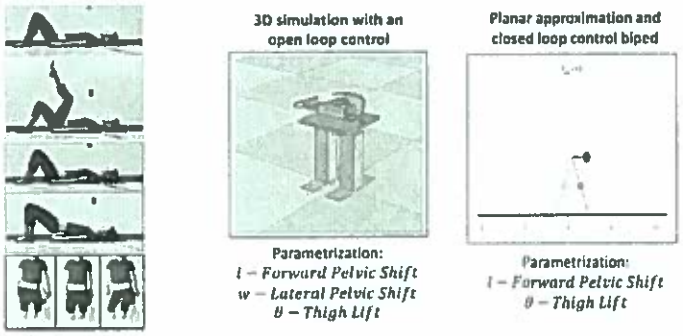


(a) (b) (c)

Figure 1: 1a)- Three exercises within Bartenieff's Basic Six. Thigh Lift in the upper panel; Forward Pelvic Shift in the middle; and an exaggerated Lateral Pelvic Shift, both sides (right and left) are shown in the lower panel. 1b, 1c)- Initial 3D robot model with parametrization of the three movements and a simplified model in plane with two parametrized movements. (Recreated from [2] and [3])

From the point of view of robot design, having a core-like structure to shift the overall center of mass of the robot can be beneficial as well. In most of the designs, leg actuators are responsible for bearing the load and carrying robot in the direction of travel. This load can be distributed between legs and the core if such a structure is designed.

## Conclusions

The Three walking exercises (Thigh Lift, Forward Pelvic Shift, and Lateral Pelvic Shift) from Bartenieff's Basic Six give some insight into embodied human movement analysis of walking. We are investigating these movements and for that, a study is planned for recording core movements in the subjects. In this study, we want to reconcile the theory between the disciplines about the role played by the core in different styles of walking. The recorded data will be used to perform motion planning for a robot using core-located actuation to produce diverse walking motions that are more consistent with human walking than the current robotic systems.

## References


[1] I. Bartenieff and D. Lewis, *Body Movement: Coping with the Environment.* Gordon and Breach Science Publishers, 1980.

[2] U. Huzaifa *et al.*, "Embodied movement strategies for development of a core-located actuation walker," in *Proceedings of the IEEE International Conference on Biomedical Robotics and Biomechatronics*, 2016.

[3] U. Huzaifa and A. LaViers, "Control design for planar model of a core-located actuation walker," in *Proceedings of the IEEE International Conference on Biomedical Robotics and Biomechatronics*, 2016.

[4] L. S. Bliss and P. Teeple, "Core stability: The centerpiece of any training program," *Current Sports Medicine Reports*, vol. 4, no. 3, pp. 179–183, 2005.

[5] J. B. d. M. Saunders, V. T. Inman, and H. D. Eberhart, "The major determinants in normal and pathological gait," *The Journal of Bone & Joint Surgery*, vol. 35, no. 3, pp. 543–558, 1953.

[6] T. McMahon, *Muscles, Reflexes, and Locomotion.* Princeton paperbacks, Princeton University Press, 1984.

[7] J. P. Callaghan, A. E. Patla, and S. M. McGill, "Low back three-dimensional joint forces, kinematics, and kinetics during walking," *Clinical Biomechanics*, vol. 14, no. 3, pp. 203 – 216, 1999.

[8] J. F. Veneman, J. Menger, E. H. van Asseldonk, F. C. van der Helm, and H. van der Kooij, "Fixating the pelvis in the horizontal plane affects gait characteristics," *Gait & Posture*, vol. 28, no. 1, pp. 157 – 163, 2008.

[9] S. Kolathaya, R. Sinnet, W. Ma, and A. Ames, "Human-inspired walking in amber 1.0 and amber 2.0," *IEEE Transactions on*, vol. 18, no. 3, pp. 263–273, 2010.

[10] C. Mandery, O. Terlemez, M. Do, N. Vahrenkamp, and T. Asfour, "The kit whole-body human motion database," in *International Conference on Advanced Robotics (ICAR)*, pp. 329–336, July 2015.

# LOWER EXTREMITY GAIT BIOMECHANICS IN INDIVIDUALS WITH BIPOLAR DISORDER

[1] Gu Eon Kang, [1,2] Brian J. Mickey, [1] Melvin G. McInnis and [1] M. Melissa Gross

[1] University of Michigan, Ann Arbor, MI, USA
[2] University of Utah, Salt Lake City, UT, USA
email: guekang@umich.edu

## INTRODUCTION

Bipolar disorder (BD) is a mood disorder that is defined by mood instability and changes in energy and motor behavior. Previous studies suggest that BD may be associated with changes in gait kinematics [1,2] but investigating lower extremity gait kinetics may be useful for more precisely understanding changes in energy and motor behavior that occur during different phases of BD. We aimed to investigate joint moments and powers in the lower extremity during gait in BD.

## METHODS

Patients with BD (n=18) and healthy controls (HC; n=13; age=41.9±13.1 years; BMI=25.7±5.3 kg/m$^2$) recruited from the Heinz C. Prechter Longitudinal Study of Bipolar Disorder at the University of Michigan Depression Center participated after giving informed consent. All participants had no history of neurological or orthopedic illnesses. Furthermore, HC had no history of personal or familial psychiatric illnesses.

We used the Altman Self-Rating Mania Scale (ASRM) and the Patient Health Questionnaire (PHQ-9) to classify patients with BD by phase into hypomanic (HG; n=3; age=51.7±13.7 years; BMI=24.5±2.4 kg/m$^2$; ASRM=13.7±5.7; PHQ-9=1.3±1.5), euthymic (EG; n=6; age=35.8±7.0 years; BMI=25.2±3.9 kg/m$^2$; ASRM=2.7±1.8; PHQ-9=2.0±1.3) and depressed (DG; n=9; age=37.8±10.6 years; BMI=25.3±4.2 kg/m$^2$; ASRM=2.2±1.6; PHQ-9=13.4±7.5) groups.

Participants performed gait on level ground at comfortable, slow and fast speeds. Gait data were obtained using a 3D motion capture system (Motion Analysis, Santa Rosa, CA) at 120 Hz and a force plate (AMTI, Watertown, MA) at 1200 Hz. Kinematic and kinetic data were low-pass filtered at 6 Hz and 50 Hz, respectively.

We used Visual 3D (C-Motion, Germantown, MD) to compute gait parameters and joint kinematics, including ranges of motion (ROM) in the hip, knee and ankle during one gait cycle. We also computed peak antero-posterior (AP) and vertical (VT) ground reaction forces (GRF), and joint moments and powers in the hip, knee and ankle during stance. One-way repeated measure ANOVA with Tukey correction was used to compare differences in mean between groups ($p$<.05).

## RESULTS AND DISCUSSION

For comfortable speed, gait parameters, GRF, and joint moments and powers differed between HG, and EG, DG and HC, but joint ROM were similar among groups (Table 1). Gait speed, minimum APGRF (peak braking force), the 1$^{st}$ peak VTGRF, maximum flexion knee moment, and maximum knee and ankle powers were greater for HG than for EG, DG and HC ($p$<.05). VTGRF valley was less for HG than for EG, DG and HC ($p$<.05). Stride length, maximum APGRF (peak propulsive force) and maximum knee extension moment were greater for HG than for DG and HC ($p$<.05). Cadence was greater for HG than for EG ($p$<.05).

For slow speed, gait parameters (gait speed = 0.79±0.21 m/s), joint ROM and GRF were similar among groups. For joint moments and powers, maximum knee flexion moment was greater for HG (0.50±0.11 Nm/BW) than for DG (0.27±0.11 Nm/BW) ($p$<.05). Maximum knee power was greater for HG (0.79±0.65 Nm/BW) than for EG (0.29±0.09 Nm/BW), DG (0.31±0.19 Nm/BW) and HC (0.27±0.14 Nm/BW) ($p$<.05).

For fast speed, gait parameters (gait speed = 1.80±0.25 m/s), joint ROM, GRF, and joint moments and powers were similar among groups.

## CONCLUSIONS

The results suggest that lower extremity gait kinetics may be mood-specific, particularly at the knee. The results also suggest that assessing knee moments and powers may provide information about changes in energy due to mood symptoms in BD, especially with regard to understanding body movement characteristics associated with hypomania. Further investigation of gait in BD with larger sample size is warranted.

## REFERENCES


1. Hausdorff JM, et al. *BMC Psychiatry,* 4:39, 2004.
2. Kang GE, et al. *Proceedings of GCMAS'16,* Memphis, TN, USA, 2016.


## ACKNOWLEDGEMENTS


This study was funded by the American Society of Biomechanics, the Blue Cross Blue Shield of Michigan Foundation, and the Horace H. Rackham School of Graduate Studies at the University of Michigan. The authors thank Dr. Deanna Gates and Barry Krembs for their help with data collection.


**Table 1:** Mean kinematic and kinetic values for comfortable speed across participants in each group.

| | HG | EG | DG | HC |
|---|---|---|---|---|
| Gait Parameters | | | | |
| Gait Speed (m/s) | 1.59 (0.16)$^{EG*,DG,*HC*}$ | 1.22 (0.13)$^{HG*}$ | 1.18 (0.28)$^{HG*}$ | 1.23 (0.11)$^{HG*}$ |
| Stride Length (m) | 1.58 (0.03)$^{DG,*HC*}$ | 1.44 (0.11) | 1.32 (0.18)$^{HG*}$ | 1.35 (0.10)$^{HG*}$ |
| Cadence (steps/min) | 120.2 (10.0)$^{EG*}$ | 101.4 (9.1)$^{HG*}$ | 106.0 (11.3) | 109.6 (7.2) |
| Joint ROM (deg) | | | | |
| Hip | 37.2 (13.7) | 46.4 (5.3) | 42.3 (4.5) | 42.8 (12.3) |
| Knee | 42.6 (4.2) | 43.6 (2.7) | 40.8 (4.8) | 43.9 (4.7) |
| Ankle | 30.4 (3.0) | 27.3 (3.7) | 25.8 (3.9) | 28.8 (4.2) |
| GRF (N/BW) | | | | |
| Max. APGRF | 0.27 (0.01)$^{DG,*HC*}$ | 0.21 (0.03) | 0.19 (0.04)$^{HG*}$ | 0.20 (0.03)$^{HG*}$ |
| Min. APGRF | 0.29 (0.03)$^{EG*,DG,*HC*}$ | 0.18 (0.03)$^{HG*}$ | 0.17 (0.05)$^{HG*}$ | 0.18 (0.03)$^{HG*}$ |
| 1$^{st}$ Peak VTGRF | 1.34 (0.08)$^{EG*,DG,*HC*}$ | 1.09 (0.07)$^{HG*}$ | 1.09 (0.10)$^{HG*}$ | 1.07 (0.06)$^{HG*}$ |
| 2$^{nd}$ Peak VTGRF | 1.20 (0.08) | 1.13 (0.07) | 1.08 (0.11) | 1.09 (0.07) |
| VTGRF Valley | 0.54 (0.06)$^{EG*,DG,*HC*}$ | 0.73 (0.07)$^{HG*}$ | 0.75 (0.11)$^{HG*}$ | 0.76 (0.07)$^{HG*}$ |
| Max. Flexion Joint Moments (Nm/BW) | | | | |
| Hip | 0.70 (0.86) | 1.23 (0.22) | 1.13 (0.41) | 0.98 (0.33) |
| Knee | 0.69 (0.20)$^{EG*,DG,*HC*}$ | 0.42 (0.07)$^{HG*}$ | 0.38 (0.13)$^{HG*}$ | 0.44 (0.08)$^{HG*}$ |
| Ankle | 0.33 (0.09) | 0.24 (0.07) | 0.22 (0.09) | 0.24 (0.07) |
| Max. Extension Joint Moments (Nm/BW) | | | | |
| Hip | 0.59 (0.45) | 0.75 (0.11) | 0.70 (0.30) | 0.83 (0.24) |
| Knee | 0.81 (0.30)$^{DG,*HC*}$ | 0.52 (0.18) | 0.43 (0.22)$^{HG*}$ | 0.45 (0.14)$^{HG*}$ |
| Ankle | 1.61 (0.20) | 1.42 (0.12) | 1.34 (0.18) | 1.35 (0.14) |
| Max. Joint Powers (W/BW) | | | | |
| Hip | 0.60 (0.52) | 1.18 (0.38) | 0.95 (0.54) | 0.90 (0.34) |
| Knee | 2.42 (0.86)$^{EG*,DG,*HC*}$ | 0.91 (0.23)$^{HG*}$ | 0.77 (0.57)$^{HG*}$ | 0.98 (0.32)$^{HG*}$ |
| Ankle | 5.26 (0.88)$^{EG*,DG,*HC*}$ | 3.07 (0.54)$^{HG*}$ | 3.17 (1.33)$^{HG*}$ | 3.52 (0.53)$^{HG*}$ |

*Note:* Values in parentheses mean standard deviations. Superscript letters represent significant differences between groups: *$p < .05$.

# BETTER SAFE THAN SORRY: FOOT CLEARANCE IS LARGER IN NOISY PREDICTIVE SIMULATIONS OF GAIT

Anne D. Koelewijn and Antonie J. van den Bogert

Cleveland State University, Cleveland, OH, USA
email: a.koelewijn@csuohio.edu, web: hmc.csuohio.edu

## INTRODUCTION

Predictive simulations of human movement, such as walking, do not always predict realistic gait cycles when muscular effort is minimized [1]. These simulations ignore all noise and solve the problem in a deterministic environment. Recent studies suggest that humans prefer strategies that are safe, rather than theoretically optimal, and take uncertainty into account when planning their movements (e.g. [2]). Thus, predictive simulations may better reflect human movement when performed on a stochastic dynamic model.

Recently, we developed a method to solve trajectory optimization problems in a stochastic environment. This approach was first applied to a pendulum swing-up problem and to show that co-contraction of muscles can be optimal in a stochastic environment [3]. In the current study, this approach was applied to find predictive simulations of gait. It was hypothesized that in a stochastic environment, foot clearance will be larger during the swing phase than in a deterministic environment.

## METHODS

Predictive simulations of gait were found using a sagittal plane model with nine degrees of freedom. The model was operated by six torques in the hip, knee, and ankle joints. A trajectory optimization problem was formulated over 10 gait cycles to find open-loop and closed-loop control inputs that minimize the tracking error and the squared torque, similar to [4]. A periodicity constraint was added between the first and final gait cycle under the assumption of left-right symmetry.

Noise was added to the control torque to model the stochasticity of human control. The standard deviation of the noise was varied between 0 Nm (deterministic environment) and 20 Nm. The noise was sampled with a sampling rate of 0.037 s.

Ground contact was modeled using contact points at the heel and toe of the foot. To study the foot clearance, the clearance of the heel and toe during the swing phase will be compared. It is expected that the clearance of the foot will increase in the stochastic model to avoid tripping.

## RESULTS AND DISCUSSION

Figure 1 shows the foot clearance at the heel and toe. A more detailed graphs of the final part of the swing phase is given in the smaller graphs. These graphs show that in this phase the foot clearance increases when the noise has a larger standard deviation.

Table 1 shows the minimum foot clearance of the toe and the heel during the phase that is plotted in the detailed graphs. Both the clearance of the heel and toe increase around 5 mm when the standard deviation of the noise increases.

**Table 1:** Minimal foot clearance of the heel and toe during the swing phase using different standard deviation.

| Standard Deviation [Nm] | Toe Clearance [mm] | Heel Clearance [mm] |
|---|---|---|
| **0** | 0.01 | 4.76 |
| **0.1** | 0.09 | 5.29 |
| **0.5** | 0.03 | 5.35 |
| **1** | 0.12 | 5.42 |
| **5** | 0.44 | 5.98 |
| **10** | 0.89 | 6.56 |
| **15** | 1.38 | 5.58 |
| **20** | 1.89 | 6.26 |
| **30** | 2.72 | 7.63 |
| **40** | 3.05 | 8.21 |
| **50** | 3.86 | 8.72 |
| **60** | 4.54 | 9.14 |

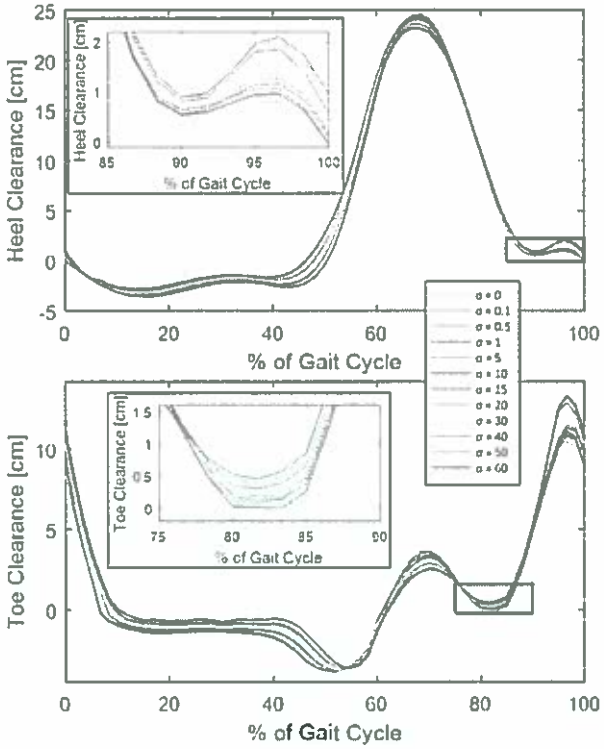


**Figure 1:** Foot clearance of the heel and toe. The figures on the right zoom in on the part in the black square.

Figure 1 and Table 1 show a clear trend towards increased foot clearance with increasing control noise. This means that in a stochastic environment, a less energy efficient strategy is favored, since the most energy efficient strategy is riskier due to the small ground clearance.

Occasionally, contradicting results were seen (e.g. the heel clearance at 10 Nm vs. 15 Nm). This might be an artifact of the noise, which was sampled only for 10 gait cycles. To avoid this, the number of gait cycles should be increased. It is expected that a larger number of gait cycles is required to correctly estimate the effect of the noise, since a convergence analysis on a problem with one degree of freedom showed that at least 30 episodes were required for that problem [3], and this problem has more degrees of freedom.

However, even with the small number of gait cycles, it was already possible to confirm our hypothesis. It is expected that the effect of the noise on the foot clearance will be larger when the optimization is solved over a larger number of gait cycles, since then the optimal solution will have a smaller chance to take advantage of the noise.

Using 10 gait cycles yields an optimization problem with 7000 optimization variables. This problem was solved in approximately four hours on a standard laptop computer. A larger number of gait cycles will increase the required solution time. Therefore, parallel computing will be employed for the convergence analysis to determine how many gait cycles are required to correctly estimate the effect of the noise in this problem.

An additional advantage of the solution method is that, besides the optimal trajectory, an optimal feedback controller is found as well. When a predictive simulation is solved in a deterministic environment, only an optimal trajectory is found. The controller is found separately, for example by linearizing around the trajectory.

## CONCLUSIONS

Our stochastic trajectory optimization approach shows that foot clearance in gait increases in a stochastic environment. Next, this approach will be applied to a musculoskeletal model of a person with a transtibial amputation, to find if a stochastic environment can explain co-contraction reported in subject studies.

## REFERENCES

1. Ackermann M and Van den Bogert AJ. *J Biomech,* 43, 1055-1060 2010.
2. Donelan JM, et al. *J Biomech* **37**, 827-835, 2004.
3. Koelewijn AD and Van den Bogert AJ. *BANCOM 2016 Program and Abstracts*, Mt. Sterling, OH USA, 2016.
4. Van den Bogert AJ, et al. *Proc Inst Mech Eng, Part P: J Sports Eng. Technol.*, 1-11, 2012.

## ACKNOWLEDGEMENTS

This research was supported by the National Science Foundation under Grant No 1344954 and the Parker Hannifin Scholarship program.

# CORRELATION PROFILES BETWEEN LOWER EXTREMITY NET JOINT TORQUES AND WHOLE BODY POWER DURING THE POWER CLEAN

[1] Sangwoo Lee, Ph.D., [1] Kyle D. DeRosia, [1] Landon M. Lamie, and [2] Erin Carlson

[1] Western Michigan University, Kalamazoo, MI, USA
[2] CrossFit Azo, Portage, MI, USA
email: sangwoo.lee@wmich.edu

## INTRODUCTION

The power clean (PC) is a bilateral weightlifting technique that generates explosive power output by vertically accelerating a heavy load as quickly as possible. Several studies investigated how individuals generated power during the PC with different conditions, such as different starting positions, loads, and pull techniques [1, 2, 3]. The studies primarily focused on determining an optimal load generating peak power and identifying the timing of peak power occurrence during the PC.

A critical review of literature on power generation during the PC elicits one observation. The whole body power can be significantly related to lower extremity joint kinetics (e.g., net joint torques (NJT)) during the PC. It is because a primary movement during the PC is the deadlift that involves all lower body joints simultaneously moving against a resistance. In spite of its potential correlations, however, there is a paucity of research investigation on the correlations.

Therefore, the purposes of this study were 1) to investigate the relationship between lower extremity NJT and whole body power and 2) to identify how well each lower extremity NJT predicted whole body power during the PC.

## METHODS

Ten participants (five males and five females) with at least two years of prior PC experience were recruited for this study. The participants performed five PC trials with their 60% of 1 repetition maximum of the PC (Comfort et al., 2011).

A 200-Hz six-camera VICON motion capture system and two AMTI forceplates were used to collect three-dimensional coordinates of the retro-reflective markers and ground reaction force (GRF), respectively. Fifty-nine markers were placed on the participant's anatomical landmarks and a group of additional secondary points (e.g., joints and whole body center-of-mass (CM)) were also defined using the markers captured (Fig. 1). Both combined GRF and independent GRFs were collected (Fig. 1). Whole body power was calculated by the product of the combined vertical GRF and whole body CM vertical velocity and lower extremity NJT was computed using an inverse dynamics procedure.

For statistical analysis, Pearson correlation coefficients were obtained to observe the relationships between lower extremity NJT (hip, knee, and ankle) and whole body power. To identify how well each joint NJT predicted to the whole body power, multiple-regression (stepwise) analysis was conducted with the hip, knee, and ankle NJT being the independent variables. The $\alpha$ level was set at .05.

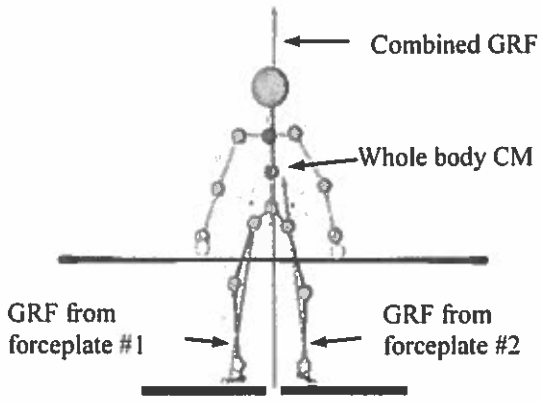


**Figure 1**: A stick figure showing marker placement, secondary points (joints and whole body CM), and GRF vectors.

## RESULTS AND DISCUSSION

Hip and knee NJT showed significant positive correlations with whole body power ($r = .29$ - $.33$, $p < .05$; Table 1), but no significant intercorrelation was observed among lower extremity NJT. Both hip

and knee NJT were identified as significant predictors of PC performance with up to 19% of the variance in whole body power explained, and knee NJT appeared to the best predictor of whole body power during the PC, followed by hip NJT (Table 2).

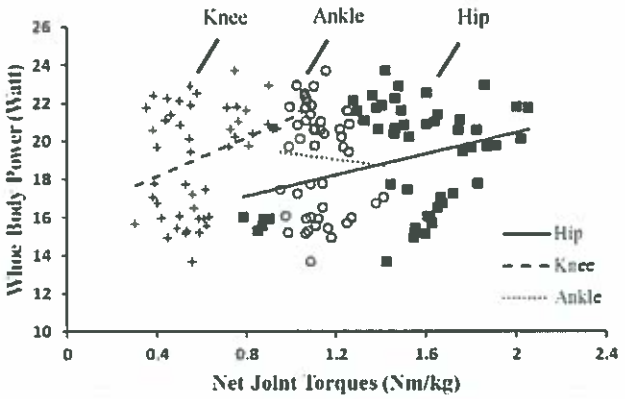


**Figure 2**: A scatter plot of the whole body power versus hip, knee, and ankle NJT. Linear trend lines of hip and knee NJT are also presented.

It could be, therefore, suggested that the developments of hip and knee extensor muscle action help individuals increase their whole body power during the PC. Although ankle NJT did not appear to be a significant predictor of whole body power during the PC, it would be beneficial for individuals to practice training skills that allow them to utilize ankle NJT for power enhancement because ankle NJT value was relatively high (Fig. 2). These findings, however, were somewhat inconclusive due to large intraclass variability (Fig. 2). The variability might be due to either the number of participants or the influence of gender-induced heterogeneity. Therefore, further investigations on the correlation profiles with a larger number of participants and with gender by gender are warranted. Nonetheless, the correlation profile results reported in this study provide new biomechanical insights into how to optimally produce whole body power during the PC performance.

## REFERENCES


1. Kipp L, et al. Lower extremity biomechanics during weightlifting exercise vary across joint and load. *J Strength Cond Res* **25**, 1229-1234, 2011.
2. MacKenzie PC, et al. A biomechanical comparison of the vertical jump, power clean, and jump squat. *J Sports Sci* **32**, 1576-1585, 2014.
3. Moolyk AN, et al. Characteristics of lower extremity work during the impact phase of jumping and weightlifting. *J Strength Cond Res* **27**, 3225-3232, 2013.


**Table 1:** Summary of the correlations among whole body power and net joint toques.

| | **Whole body power** | **Hip NJT** | **Knee NJT** | **Ankle NJT** |
|---|---|---|---|---|
| Whole body power | 1.00 | .29* | .33* | -.06 |
| Hip NJT | .29* | 1.00 | .01 | .05 |
| Knee NJT | .33* | .01 | 1.00 | -.07 |
| Ankle NJT | -.06 | .05 | -.07 | 1.00 |

**Table 2:** Summary of the multiple-regression (stepwise) results.

| **Model** | **Variable** | **B** | **SE** | **β** | **t** | **$R^2$** |
|---|---|---|---|---|---|---|
| 1 | Constant | 16.10 | 1.33 | | 12.10 | .10 |
| | Knee NJT | 5.13 | 2.15 | .33 | 2.39* | |
| 2 | Constant | 11.98 | 2.27 | | 5.27 | .19 |
| | Knee NJT | 5.06 | 2.07 | .32 | 2.45* | |
| | Hip NJT | 2.71 | 1.24 | .29 | 2.19* | |

# COMPARISON OF THE BENCH PRESS USING A STANDARD BAR AND A POWERGLIDE BAR

Kelsey Loss, Ryan Shick, Brand'n Byrd, Mark Walsh

Miami University, Oxford, OH, USA
email: Losskd@miamioh.edu

## INTRODUCTION

The bench press is a commonly utilized multi segment lift. The bench press is primarily used to load the pectoralis major but also involves other muscles of the shoulder joint, shoulder girdle and elbow joint. Because the bench press is a multi-segment lift that utilizes several different muscle groups various combinations of muscle involvement could contribute to a successful lift.

Recently, a new exercise bar, the Powerglide bar, for here referred to as the test bar, was developed that has a sliding grip that allows subjects to change their grip width during a given lift.

When performing the bench press exercise with a standard bar, the distance between the hands is fixed. Because of the fixed hand width an increased activation of the elbow extensor muscles would cause elbow extension which should aid in lifting the weight. The test bar has a bearing system which allows the user to widen their grip during the lift. Because of this the distance between the hands is not fixed and elbow extension may not necessarily aid in lifting the weight, but would rather cause the distance between the hands to increase when using the test bar. The test bar can be seem in Figure 1. Because of this difference we

Figure 1. The test bar

hypothesize that using the test bar will result in less relative elbow extensor activity. The purpose of this study is to compare muscle activation between the standard bench press exercise and the bench press using the test bar.

## METHODS

Three subjects gave their informed consent to participate in this study. Subjects performed strength training regularly and were familiar and proficient in the bench press exercise. Subjects were invited to come to the laboratory on 3 occasions before the testing session to use the powerglide bar and become familiar with it. On the 3rd visit each subject's 3 rep maximum was established. On the 4th visit subjects were asked to perform reps using each bar at 70% of their max.

Surface EMG was used to quantify muscle activity for the right pectoralis major (RPM), the left pectoralis major (LPM), Right triceps brachii (RTB) and left triceps brachii (LTB) using an 8-channel fixed shielded cabled, Noraxon TeleMyo 2400 G2 EMG system (Noraxon U.S.A. Inc. Scottsdale, AZ). The input impedance is $10^{15}\ \Omega$ with a common mode rejection ratio of >80 db. Bipolar, disposable, surface EMG electrodes with a 2.0-cm interelectrode distance were placed on the medial portion of the RPM, LPM, RTB, LTB muscles Skin preparation included shaving hair, abrading, and cleaning the surface of the participant's skin with alcohol. Elastic tape was applied to ensure electrode and cable placement, and to provide strain relief.

Surface electrodes were connected to an amplifier and streamed continuously through an analog-to-digital converter (Noraxon U.S.A. Inc.) to a laboratory notebook computer. All data was filtered with a bandpass filter allowing 10 Hz high pass and 450 Hz low pass frequencies, saved, and later analyzed with the use of computer software. Data was then cut to only the 2nd rep of lifting and Root Mean Squares were calculated of the duration of that repetition.

Electromyography was collected using a Noraxon telemetry electromyography system. Data was collected at 1000 Hz, smoothed and rectified. Subjects were asked to perform multiple sets of the exercise at different speeds so that we could compare reps of the two conditions performed at the same tempo.

## RESULTS AND DISCUSSION

Figures 1 show the ration of muscular activation between the test bar and the standard bar. Since we only have a n f 3 we did not test for significance but the data from these three subjects supports our hypothesis that using the test bar results in a lower relative triceps activation

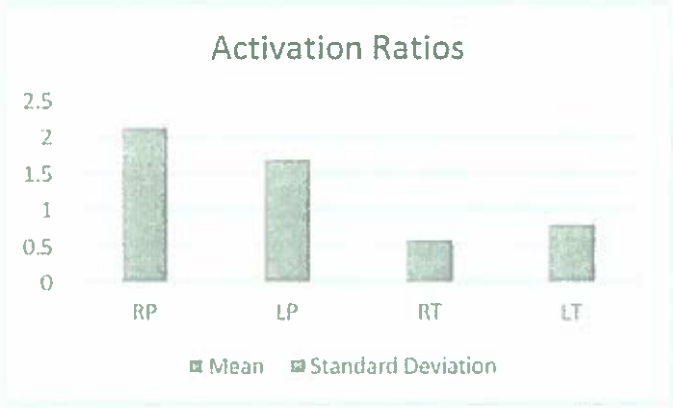


**Figure 1:** Relative muscle activation (test bar/standard bar) of the pectoralis major to triceps brachii activation during a bench press

In addition to a decrease in relative triceps brachii activation while using the test bar we also see an increase in relative pectoralis major activity. The moving grip width of the test bar seems to shift part of the load from the triceps brachii to the pectoralis major, and likely the other muscles that work as shoulder horizontal abductors.

## CONCLUSIONS

For the 3 subjects who participated in this experiment the test bar was found to load the upper extremity muscles differently during a bench press exercise than a normal bar. If this is an advantage or a disadvantage would depend on a person's training goals. A limitation of this study was the number of subjects.

# IDENTIFYING THE SPATIAL TUNING OF MUSCLE ELASTICITY AND EMG ACTIVITY FOR THE STERNOCLEIDOMASTOID MUSCLES

Bhillie Luciani, David Desmet, Amani Alkayyali, David Lipps

School of Kinesiology, University of Michigan, Ann Arbor, MI, USA
email: dlipps@umich.edu, web: www.kines.umich.edu/research/mbil

## INTRODUCTION

The neck is composed of a complex layering of musculature that allows the neck to move in flexion, extension, lateral flexion, and axial rotation. This complexity allows the neck muscles to be precisely tuned to have preferred directions where their muscle activity will be greatest during isometric tasks [1-3]. The specificity of neck muscles like the sternocleidomastoid (SCM) are reduced in pathologies like chronic neck pain [2]. Such pathologies are also associated with increases in neck muscle stiffness [4]. Assessments of *in vivo* muscle stiffness have been limited in the past to qualitative assessments such as manual palpations. However, recent advances in ultrasound shear wave elastography (SWE) present a method to assess the elastic properties of muscle. Eby et al. (2013) has shown ultrasound SWE provides a reliable, quantitative, and noninvasive estimation of muscle elasticity. In this study, we utilized SWE to investigate in healthy individuals whether the elasticity of the SCM muscles exhibit the same directional specificity as their muscle activation patterns.

## METHODS

Three healthy adults (2 males, 1 female) with no history of neck dysfunction participated in this experiment. The mean age of participants was 21 years old. Recruitment for the study is ongoing at the time of abstract submission

Surface electromyography (EMG) electrodes (Bagnoli system, Delsys, Natick, MA) were placed bilaterally on the SCM muscles (Fig. 1A). The electrodes were placed parallel to the muscle fibers. Once the EMG electrodes were place, subjects were seated with their head secured within a wall-mounted halo attached to a load cell modeled after Falla et al. (2013) (Fig. 1A). Subject heads were secured in the device before running maximum voluntary contractions (MVCs) in flexion, extension, left flexion, and right flexion.

Subjects were asked to generate isometric forces set to 20% of the maximum MVC in 16 axial directions (Fig. 1B). Visual feedback of the desired target was provided as subject matched isometric targets in a randomized order during this ramp and hold (RH) protocol. After collecting EMG data during these trials, the EMG electrodes were removed to image the SCM. The EMG data was collected at 1 kHz, gained at 1 kHz, detrended, rectified, and low-pass filtered (7 Hz). EMG values during each contraction were average over 500 ms.

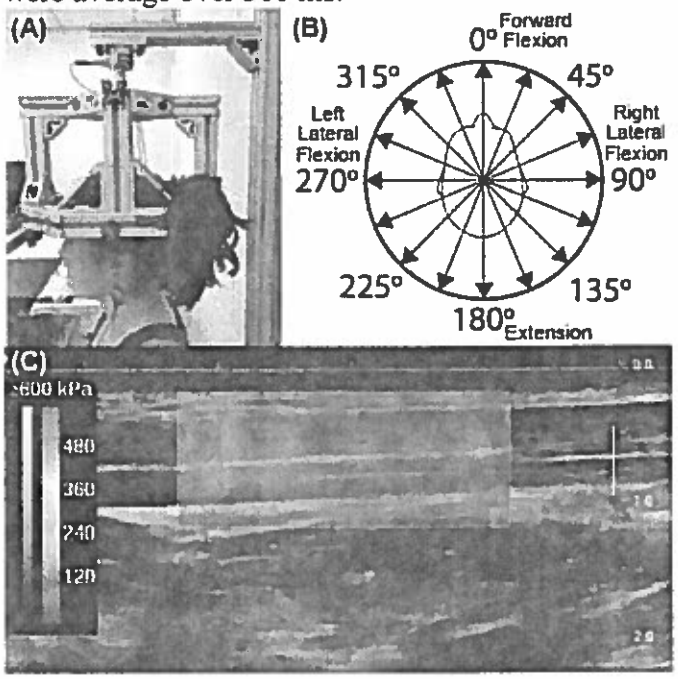


**Figure 1:** (A) Metal halo with embedded force sensor. (B) Experimental procedure involves generating forces in 1 of 8 directions to examine neck strength imbalances. (C) A representative image of the SCM muscle using ultrasound shear wave elastography. The B-mode ultrasound image is superimposed with a color map of tissue elasticity.

SWE ultrasound images were acquired from the muscle bellies of both SCM muscles using an Aixplorer system (Supersonic Imagine, Aix-en-Provence, France) (Fig. 1C). Images were aquired as subjects performed the same isometric force matching task as the EMG collection. Muscle elasticity was estimated as the mean shear wave velocity within the SWE color map [5].

The specificity of muscle activity was determined by computing tuning curves from the EMG data [3]. We computed specificity from these tuning curves as the mean vector direction, which is equivalent to the vector sum of the normalized EMG data across all force target directions. These procedures were modified to calculate the specificity of the tuning curves produced by the SWE data.

## RESULTS AND DISCUSSION

Representative EMG and muscle elasticity tuning curves for the left and right SCM muscles are represented in Fig. 2-3. The specificity of muscle activity and muscle elasticity was unique between the left and right SCMs. The representative subject shows similar patterns of specificity for both EMG activity and muscle elasticity.

Across all 3 subjects, the mean (± SD) vector direction for the left SCM was 345° ± 18° for EMG activity and 332° ± 28° for muscle elasticity. For the right SCM, the mean vector direction was 15° ± 24° for EMG activity and 27° ± 15° for muscle elasticity. The directional specificity of both the left and right SCM were consistent, with muscle elasticity having a mean vector that was oriented more towards lateral flexion than the mean vector for EMG activity.

The SCM muscles showed similar directional specificity as previously reported [3]. The finding that the preferred direction of muscle activity and elasticity are similar for the SCM muscles is consistent with muscle stiffness increasing with greater activation [6]. Future work will increase the number of subjects in this study to reduce the variability of our data. Future work will also investigate how muscle activation and elasticity are related in neck pathologies.

## CONCLUSIONS

The directional specificity of SCM muscle elasticity as indicated by ultrasound SWE is similar to the directional specificity of muscle activation determined by EMG.

## REFERENCES


1. Blouin JS, et al. *J Neurophysiol*, **98**, 920-928, 2007.
2. Falla D, et al. *Eur J Pain*, **17**, 1517-1528, 2013.
3. Vasavada AN, et al. *Exp Brain Res*, **147**, 437-448, 2002.
4. Kuo WH, et al. *Ultrasound Med Biol*, **39**, 1356-1361, 2013.
5. Eby SF, et al. *J Biomech*, **46**, 2381-2387, 2013.
6. Rack PM & Westbury DR. *J Physiol*, **240**, 331-350, 1974.


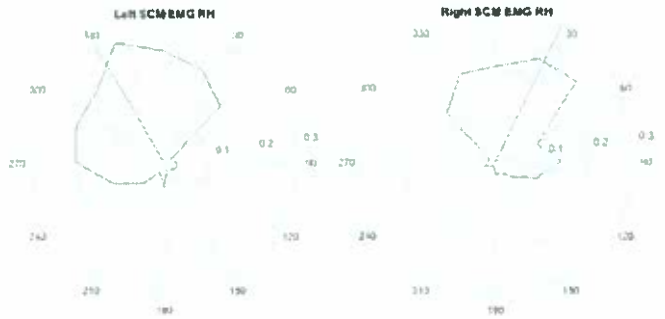

**Figure 2:** Representative tuning curves of left and right SCM EMG activity for one subject. Red indicates the EMG activity across 16 RH trials, while the blue line indicates the directional specificity of the EMG activity.

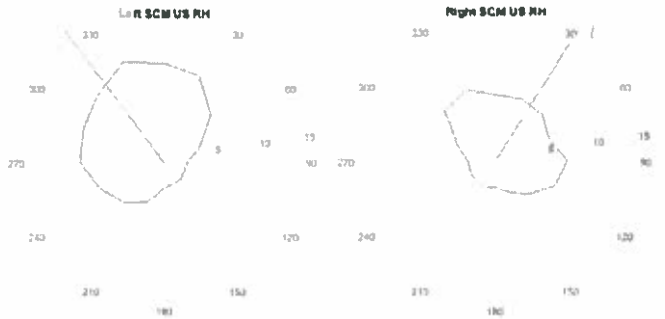

**Figure 3:** Representative tuning curves of left and right SCM muscle elasticity for one subject. Muscle elasticity was estimated as the mean shear wave velocity from the SWE images. Red indicates the mean shear wave velocity across 16 RH trials, while the blue line indicates the directional specificity of muscle elasticity.

# MEDIAL VS LATERAL HAMSTRING INNERVATION STRATEGIES

[1]Arden McMath, [1]Eric Slattery, [2]Justin Waxman, [1]Mark Walsh

[1]Miami University, Oxford, OH, USA
[1]Highpoint University, High Point, NC, USA
email: mcmathal@miamioh.edu

## INTRODUCTION

Female athletes have a greater incidence of ACL injuries than males in the same sport. One possible contributing factor that is considered by strength and conditioning coaches/athletic trainers of athletic teams is muscular imbalances. Because the quadriceps muscle group pulls the tibia anteriorly and the hamstring muscle group pulls the tibia posteriorly the hamstrings are believed to support ACL function. Because of this the hamstring/quadriceps (H/Q) strength ratio is sometimes considered when planning training or rehabilitation of athletes.

Recently, Zebis (2009) reported that ACL injuries in elite female handball players may be more likely in subjects with a reduced semitendinosus (ST) pre activation electromyography (EMG). They speculate that ST, because of its location on the medial side of the knee, may be important to compress the medial knee joint and thereby reduce valgus collapse and external knee rotation. These results may indicate that when designing ACL injury prevention programs, exercises should be chosen that upregulate ST activation. The purposes of this study were to examine typical strength training and rehabilitation exercises and determine 1) H/Q activation ratios for these exercises, and 2) ST/Biceps Femoris (BF) activation ratios for those exercises, which represent medial vs lateral hamstring activation relative to the knee.

## METHODS

After granting informed consent, 21 participants who regularly perform strength training were show the technique of the 6 exercises. A 6 rep max was determined for each exercise (squat (SQT), prone leg curl (LC), stiff leg deadlift (SLD), single leg stiff leg deadlift (SLSDL), good morning (GM), and the Russian curl (RC)). The exercises selected are frequently used and are commonly believed to be effective at training the hamstrings. The SQT has been included in this study because it serves as a useful reference for H/Q activation ratios under conditions where the quadriceps are typically dominant.

Electromyography: Surface EMG was used to quantify muscle activity for the vastus lateralis (VL), vastus medialis (VM), rectus femoris (RF), BF, and ST using an 8-channel fixed shielded cabled, Noraxon TeleMyo 2400 G2 EMG system (Noraxon U.S.A. Inc. Scottsdale, AZ). The input impedance is $10^{15}\ \Omega$ with a common mode rejection ratio of >80 db. Bipolar, disposable, surface EMG electrodes with a 2.0-cm interelectrode distance were placed on the medial portion of the VL, VM, and RF muscles of the quadriceps femoris muscle, and on the BF and ST muscles representing the lateral and medial hamstring muscle groups, respectively.
Skin preparation included shaving hair, abrading, and cleaning the surface of the participant's skin with alcohol. Elastic tape was applied to ensure electrode and cable placement, and to provide strain relief.

Surface electrodes were connected to an amplifier and streamed continuously through an analog-to-digital converter (Noraxon U.S.A. Inc.) to a laboratory notebook computer. All data was filtered with a bandpass filter allowing 10 Hz high pass and 450 Hz low pass frequencies, saved, and later analyzed with the use of computer software. Data was then cut to only the 2nd rep of lifting and Root Mean Squares were calculated of the duration of that repetition.

Although previous studies (Ebben, 2009) used only the rectus femoris and medial hamstring muscles to determine H/Q activation ratios we thought including mono articular muscles to represent Q activity was important because most of the extension force at the knee joint is produced by the vasti muscles.

## RESULTS AND DISCUSSION

Figure 1 shows the H/Q ratios for the chosen exercises. These results show a similar basic pattern to those of previously published ratios (Ebben, 2009). The ratios determined in the present study are skewed toward more quadriceps activity. This is likely because we used 3 Q muscles and 2 H muscles for our ratio as opposed to Ebben (2009) who used 1 H and 1 Q muscle.

As expected the exercises with the highest ration were the single joint exercises that require only flexion of the knee.

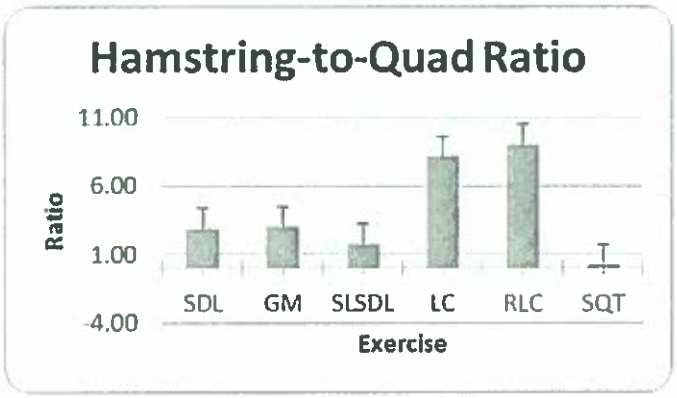


**Figure 1**:Hamstring/Quadriceps activation ratios.

Significant differences in H/Q activation ratios was found between exercises. The SQT showed a significantly lower H/Q ration than all other exercises. The LC and RLC had significantly higher H/Q ratios than the other exercises. SDL, GM and SLSDL ratios were all similar.

**Figure 2**:Semitendinosus/Biceps Femoris activation ratios.

Figure 2 shows the trends in ST/BF activation ratios. Although no significant differences were identifies some trends emerge. The exercises that only involve movement at the knee joint show a light trend towards lower ST/BF ratio. It is not clear at this time if this trend is important.

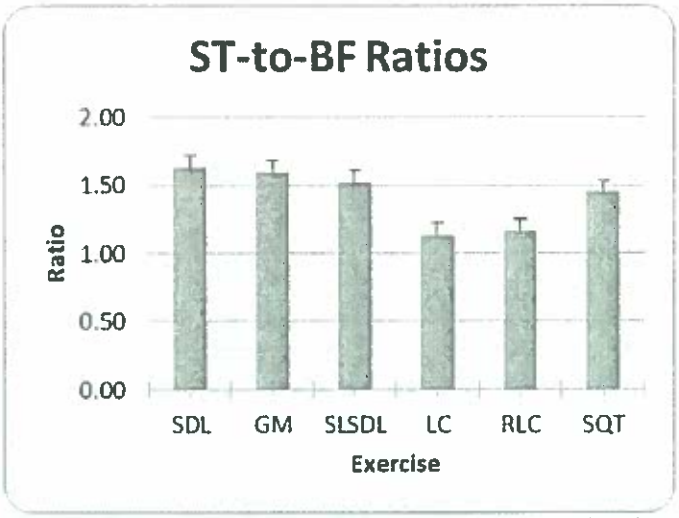


**Figure 2**:Semitendinosus/Biceps Femoris activation ratios during the chosen exercises.

## CONCLUSIONS

As with the causes many injuries, those ACL injuries are likely multifactorial. If upregulating medial hamstring activity proves to be a strategy in ACL injury prevention programs exercises it will be important to be identify exercises that better target the medial hamstring muscle group. This study shows some trends but does not clearly identify exercises that result in significant changes in medial hamstring activation relative to lateral hamstring activation. As of now strengthening the entire hamstring muscle group seems to be part of a reasonable strategy.

## REFERENCES

1. Ebben et al. *Int J Sport Phy and Perf. (4) 84-96*, 2009.
2. Zebbes et al. *The Amer J Sports Med.* 37(10), 1967-1973, 2009.

# A Case study of Adaptations to Activity After Inactivity

[1] Ryan L. Meidinger and [2]Marisa Heckendorn

[1] Northern Michigan University, Marquette, MI, USA
Email: rmeiding@nmu.edu
[2]University of Basel, Basel, Switzerland
Email: mheckend@nmu.edu

## INTRODUCTION

When a person is inactive the skeletal and neuromuscular systems adapt to the decreased stress, which is called detraining (7). In the present study inactivity was defined as exercise of less than 150 minutes a week, according to ACSM general guidelines (2). It is expected that when activity is initiated after a period of inactivity there will be improvements in body composition, neuromuscular control and fitness (2). The primary purpose of this study was to examine a single participant's adaptations to endurance training after a period of inactivity.

## METHODS

A single participant was the focus of this experiment. Prior to the study the participant was considered inactive for five months. The participant noted he attempted to change his diet to a high protein, high fat diet during this inactive period.

The current study consisted of an eight week training regimen. The regimen consisted of runs ranging from 4 to 45 minutes for up to four days a week. The regimen consisted of increasing duration of activity from the beginning to the end. Prior to the study the participant was tested for ankle and knee strength, balance, sprint agility and body composition measurements.

Ankle and knee isokinetic flexion and extension concentric strength were tested on a Biodex System 4 dynamometer at 60 degrees per second. Balance was tested with the Y and Bess balance tests. In the Y balance test the participant was assessed bilaterally in the anterior, posterior medial and posterior lateral positions. In the Bess test the participant was tested on a firm and foam surface in the double leg, single leg and tandem stances on the non-dominant leg. Leg dominance was assessed with the Lateral Preference Inventory (1). Sprint agility was tested with a T-test and body composition was estimated via DEXA scan.

## RESULTS AND DISCUSSION

During the inactive period the participant had a decrease in bone mineral density (BMD) of 4.2%, increase in lean tissue of 2.5%; a 2.4% decrease in percent body fat and a 15.7% change towards android in the android to gynoid ratio. From start to end of the training regimen, the participant increased BMD 2.2%; lean tissue volume decreased 1.4%, total mass decreased 2.3% and 3.8% change towards android in the android to gynoid ratio.

There was a decrease in muscle volume, measured by a DEXA scan, which supports previous research that has shown fiber size and/or type decreases or change from endurance training (5). In contrast previous research (7), the current participant increased lean mass during detraining.

There was a 1.9% improvement between pre and post testing in the t-test. This is a rather small change and it may be an effect of endurance training on musculo-tendinous stiffness. This was not measured so it cannot be shown to be the cause but it may factor in

as it has been shown to be improved during endurance training. (3)

In the Y balance test the participant's dominant leg had a 2.8% increase in the anterior; 1.6% increase in the posterior medial and 7.8% increase in the posterior lateral measurement. The participant's non-dominant leg had a 22.0% increase in the anterior; 1.2% increase in the posterior medial and 2.4% decrease in the posterior lateral measurement.

For strength measures there was a range of change from a decrease of 31.6% to an increase of 11.3% in plantar and dorsi flexion. There were modest changes in knee flexion and extension strength ranging from increases of 13.3% to decreases of about 3.4%.

In the Y balance test there were some differences in the performance of the dominant and non-dominant leg in this test. The majority of the Y balance test measurements became more similar. In the anterior test there was a difference of 7.7cm prior to training and 3.3cm post training. In the anterior test the participant had a farther reach with the dominant leg in the pretest and a farther reach in the non-dominant leg in post testing. In the posterior medial test the participant had a difference of 0.7cm prior to training and 1.2cm after training, with a minimal difference between legs. In the posterior lateral test the participant had a difference of 9.2cm; with the non-dominant reaching farther and 2cm difference, with the dominant reaching farther.

The greatest changes in this study were found in the Bess balance tests and strength measurements. There was a change of 53.9% and 33.3% in the single leg and tandem stances respectively. The changes on the foam pad were more modest, where the tandem stance had an increase in errors compared to the pretest trial. The strength changes were surprising but could be caused by from a loss in lean mass, and/ or changes in the nervous system (5).

The current data suggests that the participant may respond well to trail run training and could primarily benefit in balance. It is possible that the changes in this study were mostly neural improvements in postural control (4). The present study was lacking electromyography assessment to support this hypothesis but the balance improvements could be related to neuromuscular adaptations (2). The participant did adapt to the training stimulus as would be expected.

## REFERENCES


1. Coren, S. *Bulletin of Psychonomic Society*, 1-3, (1993).
2. Garber, CE. et al., *Medicine & Science in Sport & Exercise, 30*(6), 1334-1359, (2011).
3. Grosset, JF., *European Journal of Applied Phsiology, 105*, 131-139, (2009).
4. Horak, FB. *Age and Aging, 35*(S2), ii7-ii11, (2006).
5. Kraemer, WJ. et al., *Journal of Applied Physiology, 78*(3), 976-989 (1995).
6. Robinovitch, SN. et al., *Journal of Neurophysiology, 88*, 613-620, (2002).
7. Zhong, H. et al., *Journal of Applied Physiology, 99*(4), 1494-1499, (2005).


## ACKNOWLEDGEMENTS


The authors would like to thank Northern Michigan University for allowing them to use the Exercise science facility.

# VALIDITY OF WIRELESS SENSORS FOR ASSESSING SENIOR FITNESS TEST MEASURES

Kennady Miller, Abigail Matsushima, Uriel Ibarra-Moreno, Megan Salvatore, DPT, Nathan W. Saunders, PhD

University of Mount Union, Alliance, OH, USA
email: saundenw@mountunion.edu, web: www.mountunion.edu

## INTRODUCTION

In the cross sectional analysis for Senior Fitness Testing we will use APDM Opal sensors to measure and collect data of three tests, including a 30 Second Chair Stand Test, an 8 Foot Timed Up-and-Go (TUG), and a 6 Minute Walk Test (6MWT). We will be analyzing the validity of the sensors by using stopwatches and observation during each test. The importance of validating this equipment is to show that only using stopwatches and observation could lead to human error. Using the APDM Opal sensors will help to eliminate human error upon collecting data during testing. When researching we found one study analyzing the validity of Opal sensors used during an 8 Foot Timed Up-and-Go [1]. Testers found that a strong correlation existed between the Opal sensors timing and timing using a stopwatch. However, the Opal sensors were found to overestimate the time-to-completion by approximately 2 seconds longer than when using the stopwatch. This was due to the Opal sensors detecting different starting and ending points [1]. This aspect didn't have an effect on the relative times, but it is something to be aware of when comparing to other sources that may have used stopwatches. Another study conducted showed that use of sensors allows for in depth, more accurate data collection during testing [2]. Not only do sensors keep track of time as a stopwatch would, they also make specific observations such as arm swing [2]. These specific observations serve to be very useful to the researchers during the testing period.

## METHODS

A total of at least 30 participants, including both males and females, will be recruited for this study. The participants should be older adults, age 65 and up, and should be apparently healthy with no known cognitive or balance disorders. They should also be able to walk unassisted. Participants will be recruited from the Alliance area from places such as churches, YMCAs, community centers, and independent living facilities.

Participants will complete three tests; those including a 30 Second Chair Stand, an 8 Foot Up-and-Go, and a 6 Minute Walk Test. These three tests are protocols originally created by researchers Rikli and Jones [3]. These specific protocols by Rikli and Jones have been altered to fit the research protocol that is to be conducted. Testing will be conducted in a long hallway measuring at least 25 meters in length. For the 30 Second Chair Stand Test and the 8 Foot Timed Up-and-Go, the chair used will be 17 inches in height.

We will be using 6 APDM Opal sensors positioned on both wrists, the top of both feet, lower back, and chest, which will measure and give us data from the 30 Second Chair Stand Test, 8 Foot Timed Up-and-Go, and 6 Minute Walk Test for each of the participants [3]. To determine the validity of the sensors we will use stopwatches and observe the participants as they perform the tests. For the 30 Second Chair Stand Test we will observe how many times the participants get from a seated position to fully extended knees and standing then return to a seated position. A stopwatch will be used for the 8 Foot Timed Up-and-Go. The stopwatch will begin when the tester says "go" and will be stopped when the participant returns to a seated position. The stopwatch will again be used for the 6 Minute Walk Test as we will be able to observe the total distance traveled, gait speed, and stride length frequency. By timing the tests manually with stopwatches, we will be able to validate the data collected and the accuracy of the APDM Opal sensors. The distance traveled will be determined by counting the number of times each participant is able to walk back and forth along the 25 meter area in 6 minutes. Gait speed will be calculated by using a stopwatch to the middle 20 meters of the 25 meter walkway (to eliminate the acceleration and deceleration phases). Stride frequency will be determined by the tester 10

consecutive strides. The relative agreement between the APDM system and manual data collection will be made using Pearson Product Moment Correlations. We will also perform paired sample t-tests to test for significant differences between the two methods.

## RESULTS AND DISCUSSION

Research and data collection will begin on February 1st, 2017.

## CONCLUSIONS

Research and data collection will begin on February 1st, 2017.

## REFERENCES


1. Coulthard, Jason T., Treen, Tanner T., Oates, Alison R., & Lanovaz, Joel L. (2015). Evaluation of an inertial
sensor system for analysis of timed-up- and-go under dual-task demands. *Gait & posture, 41*(4), 882-887.
2. Mancini, M., King, L., Salarian, A., Holmstrom, L., McNames, J., & Horak, F. B. (2011). Mobility Lab to Assess Balance and Gait with Synchronized Body-worn Sensors. *Journal of bioengineering & biomedical science, Suppl 1*, 007. doi: 10.4172/2155-9538.S1- 007 [doi]
3. Rikli, Roberta E., & Jones, C. Jessie. (1999). Functional fitness normative scores for community-residing older adults, ages 60-94. *Journal of Aging and Physical Activity, 7,* 162-181.

# EVALUATION OF USING AN ACCELEROMETER TO ASSESS FRONTAL PLANE KNEE MECHANICS DURING A DROP LANDING

Alexander M. Morgan and Kristian M. O'Connor

Department of Kinesiology
University of Wisconsin-Milwaukee, Milwaukee, WI, USA
email: morgan28@uwm.edu

## INTRODUCTION

Non-contact anterior cruciate ligament (ACL) injuries account for around 70% of all ACL injuries annually, and are two to eight times more prevalent in women [1]. Prior studies have examined neuro-mechanical factors that contribute to this prevalence and have found increased knee abduction angles, increased external knee abduction moments, and decreased knee flexion to be main contributors to developing an ACL injury [2,3]. Furthermore, thigh angular velocity in the frontal plane as determined through inertial measurement units (IMUs) have been associated with the external knee abduction moments [4]. A biofeedback protocol intended to increase knee flexion and decrease thigh angular velocity in the frontal plane also displayed a significant decrease in knee abduction moment [4]. However, the IMUs being utilized above contain both an accelerometer and a gyroscope, and as such are more expensive. A less expensive IMU measuring only accelerations may also be useful in evaluating ACL injury risk.

Thus, the purpose of this study was to compare accelerations in the frontal plane near the knee during a drop landing maneuver with commonly assessed kinematic and kinetic risk factors for ACL injury using only an accelerometer.

## METHODS

Ten subjects (four male and six female) participated in this study (average: 23.3 years, 1.70 m, 66.2 kg). Three-dimensional kinematic data were collected for the right leg using a Motion Analysis Eagle motion capture system (Santa Rosa, CA) at 200 Hz. Kinetic data were collected with a Bertec force plate (Columbus, OH) at 1000 Hz. Medial-lateral accelerations at the tibial tuberosity of the right leg were collected using a Noraxon DTS 3D Accelerometer (Scottsdale, AZ). Positive accelerations indicated acceleration of the knee medially. Reflective markers were placed on the pelvis and dominant leg at relevant anatomical landmarks for three-dimensional kinematic analysis.

A standing calibration trial was captured, after which subjects were instructed to stand on a 30-cm tall box located next to the force plate. Subjects were instructed to perform a bilateral drop landing task in which the individual stepped off of the box and landed on the ground. Subjects were instructed to land with the foot of the right leg on the force plate, with the left foot off of the force plate. Ten drop landing trials were collected.

All data reported occurred in the frontal plane. Peak positive knee acceleration, knee angle at initial contact, peak external knee abduction moment, and knee linear range of motion from initial contact to maximum knee flexion across the ten trials were reported. Pearson product-moment correlation coefficients were computed to assess linear relationships between variables.

## RESULTS AND DISCUSSION

A mild negative association between frontal plane knee angle at initial contact and peak external abduction moment was found (Table 1 and Figure 1). This finding suggests that, as knee angle moves towards abduction at initial contact, a larger peak external abduction moment during landing will be present. This is to be expected. No significant correlation was found between frontal plane peak positive knee acceleration and peak external knee abduction moment (Figure 2). No other correlations

of note were found between variables. Overall, it appears that between subjects, peak positive knee acceleration in the frontal plane does not predict kinematic or kinetic variables at the knee in the frontal plane.

## CONCLUSIONS

Peak acceleration was not related across subjects to the peak knee abduction moment, the frontal plane knee angle at initial contact, or the linear range of motion of the knee in the frontal plane. It was hypothesized that frontal plane acceleration of the knee might predict kinematic and kinetic variables at the knee associated with ACL injury, as thigh angular velocity had previously displayed this relationship [4]. However, this was not evident in the reported findings. While it is possible that the velocity calculated by integrating the accelerometer signal could provide a similar result as the previous IMU study [4], the lack of a baseline velocity and potential gravitational drift make such calculations difficult. It is also possible that accelerometer data is more effective in detecting within subject variation in moments, which was not explored in this study. Further work is necessary to determine the full applicability of using this accelerometer to assess ACL injury risk.

## REFERENCES


1. Agel J, et al. *Am J Sport Med* **33**(4), 524-531.
2. Hewett TE, et al. *Am J Sport Med* **33**(4), 492-501.
3. Myer GD, et al. *Brit J Sport Med* **49**(2), 118-122.
4. Dowling AV, et al. *Am J Sport Med* **40**(5), 1075-1083.


**Table 1:** Pearson product-moment correlation coefficients for knee kinematic, kinetic and acceleration-based variables in the frontal plane.

| | External Abduction Moment | Peak Positive Acceleration | Angle at Initial Contact |
|---|---|---|---|
| **Range of Motion** | **0.179** | **0.287** | **0.008** |
| **External Abduction Moment** | | **-0.083** | **-0.589** |
| **Peak Positive Acceleration** | | | **0.026** |

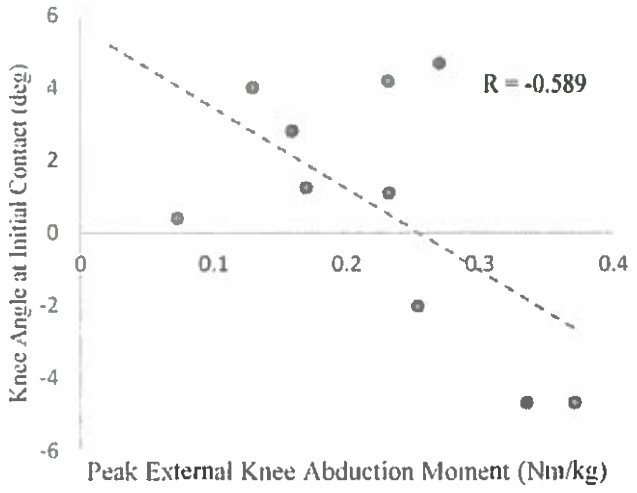


**Figure 1:** Frontal plane knee angle at initial contact displays a mild negative correlation with peak external knee abduction moment.

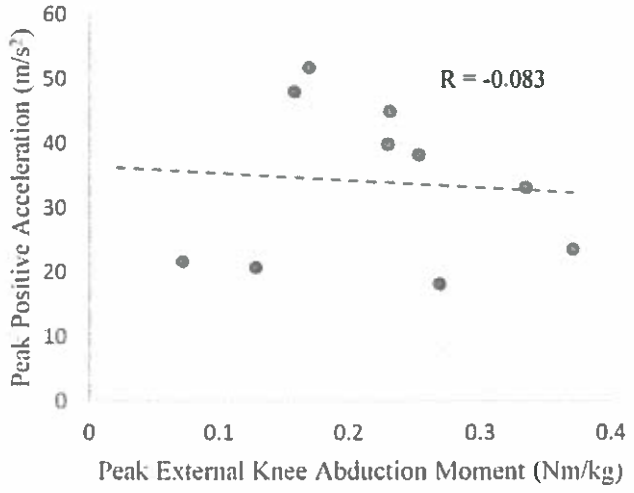


**Figure 2:** Peak positive acceleration does not display a significant correlation with peak external knee abduction moment.

# Analyzing the Use of Visual Feedback Provided by Limb Mounted Lasers for Improving Lower Extremity Movement in Individuals With Neurological Disorders

[1]Kevin Nowaki, [1]Bridget Dues, [1]Luke Schepers, [1]Kurt Jackson, PhD, PT, [1]Megan Reissman, PhD, [1]Kimberly Bigelow, PhD

[1]University of Dayton, Dayton, OH, US

## INTRODUCTION

Movement disorders of the lower extremities are common for many individuals who have experienced various neurological conditions including stroke, multiple sclerosis, anoxic brain injury, and spinal cord injury. Research[1-4] has suggested that visual or audio cues can help improve mobility for these individuals. There have been multiple studies[1-4] showing individuals have an increase in mobility or motor control function after receiving some form of corrective visual feedback during rehabilitation or training. For example, a portable virtual reality apparatus was used to improve walking speed in individuals with multiple sclerosis and resulted in an average improvement of 13.46%[2]. Another study[4] used colored tape lines and a ball moving machine to improve gait speed and stride length in individuals with incomplete spinal cord injury and reported a mean improvement in gait speed of 0.17m/s.

Recently a wearable laser light system that provides real-time visible feedback on movements has emerged as a commercially available rehabilitation tool[5]; however, research examining the use of lasers for visual feedback has been more limited. Research examining the use of lasers has been limited, though what has been done has shown promise for future research. Wearing a laser that is carefully positioned on the body can provide feedback about the movement trajectory on a nearby wall. An individual can then observe if their movement strategy results in a path that would be desirable for reducing extraneous movement, ensuring better weight distribution, and improvement of overall movement efficiency. Such a system could be ideal for at-home training, especially if using target lines.

The purpose of our study is to determine if the use of a limb mounted laser during leg raises can reduce pathologic frontal plane motion and result in a more desirable lower limb motion. Specifically, our team is interested to determine if participants can make improvements when a laser is used compared to baseline (no feedback) movements. With the laser feedback, we predict the participants will have increased knee and hip flexion, decreased hip abduction and circumduction, and decreased extraneous frontal plane movement of the knee joint center.

As a secondary goal, we will also examine immediate carry-over effects in motion improvement. Following movement practice with the laser, a trial of step-ups or knee raises will be performed without the laser. We hypothesize that immediate carry-over effects will be observed. If so, this will indicate that laser biofeedback may be an effective form of visual feedback. This outcome would also suggest that prolonged use of the lasers will have lasting effects on the participants. If the wearable laser system is found effective this would provide support for an inexpensive therapy device for both traditional clinic training sessions and extra rehabilitation training at home.

## METHODS

A minimum of six individuals will participate in this study. Inclusion criteria include diagnosis of a neurological disorder or injury that has caused a loss of lower extremity motor control in one or both lower limbs, such as stroke, multiple sclerosis, anoxic brain injury, or spinal cord injury.

Research participants who meet study criteria will make two visits to the University of Dayton

campus. On the first visit, University of Dayton Physical Therapy students and professors will be administering a series of clinical tests to measure the cognitive and movement abilities. These tests consist of a Berg Balance test, Lower Extremity Fugl-Meyer test, Mini Mental Status Exam, and Snellen eye test. The Berg Balance and Lower Extremity Fugl-Meyer tests will not be used as exclusion criteria for the study, but rather will be used in analysis of results. The Mini Mental and Snellen eye tests will be used as exclusion criteria, excluding participation if corrected vision is worse than 20/60 or if the Mini Mental test score is less than 24.

On the second visit, research participants will come to the Motion Analysis Laboratory at the University of Dayton. Twenty-six individual markers as well as four marker plates will be placed on the study participant. The markers are placed in specific bony landmarks that allow us to recreate body segments of the participant. These skeleton recreations are then used to quantify the movement response and support whether or not visual feedback helps the participant to make movement corrections.

The participant will perform a series of tests that we have developed that will allow them to see their movement in real time and make corrections. We use laser guidance systems made by Motion Guidance and attach them to the leg of participant. They will perform box step ups and max knee raises with and without the laser turned on.

Kinematic outcomes including joint angles and center of mass position will be determined using Visual-3D software (C-Motion, MD, USA) and established biomechanics modeling methods. Center of pressure response will be determined from a single force plate. Behavior of the feedback endpoint relative to the target line (tracking error) will be determined using motion capture of the target board, target line, and feedback laser device to determine the projection of the feedback on the target board.

Results will be statistically analyzed for both the box step task and the knee raise task using a repeated measures analysis of variance (ANOVA) model. Within factors will include condition: baseline, with guidance, post-guidance.

For both tasks we will examine maximum excursion of the center of mass and center of pressure. For both tasks we will examine frontal plane movement behaviors using maximum lateral position of the feedback endpoint and total area between the feedback endpoint trajectory and the target line. For the knee raise task we will assess task specific kinematic outcomes of sagittal knee and hip angles, and height of knee joint center.

## RESULTS AND DISCUSSION

Currently, Institutional Review Board approval has been secured and study participant recruitment is underway. We anticipate collecting data from approximately six individuals by February 2016. The first study participant, an individual with an anoxic brain injury, has completed his first visit and will be finishing the study later this week.

If we determine promising results from certain populations after the study, we plan to develop a longitudinal training study focusing on the population that benefitted most.

## REFERENCES


1. Cheng P, et al., *Clin Rehabil,* 18.7, 747-753, 2004.
2. Baram Y, et al., *Neurology,* 66.2, 178-181, 2006.
3. Walker C, et al., *Phys Ther,* 80.9, 866-895, 2000.
4. Amatachaya S, et al., *Spinal Cord*, 47.9, 668-673, 2009.
5. Motion Guidance.


## ACKNOWLEDGEMENTS


We wish to thank [1]Jenifer Westover, [1]Gina Lausin, [1]Victoria Marchant[1] and [1]Courtney Golembiewski for their help with the study.

# MEDICAL PACAKGE DESIGN AND BIOMECHANICAL OPENNING TECHNIQUES AS THEY RELATE TO DEVICE CONTAMINATION

[1] Wu Pan, [1] Paula Perez, [1] Laura Bix, [2]Larissa Miller [1]Tamara Reid Bush

[1] Michigan State University, East Lansing, MI, USA
[2]Health and Human Services Division, Lansing Community College, MI USA
email: panwu@egr.msu.edu, reidtama@egr.msu.edu

## INTRODUCTION

Healthcare Acquired Infections (HAIs)—are infections that were neither present nor incubating at the time of hospital admission. HAIs have been listed as one of the top 10 leading causes of morbidity and mortality in the United States. It has been reported that 1 in 25 hospital patients has had at least one healthcare-associated infection [1]. Indirect contact contamination, defined as the transfer of infectious agents though an intermediate object (e.g. hospital surfaces) or a person, is one transfer mechanism of HAIs [2]. Indirect contamination can also occur when a packaged device is opened and comes into contact with the outside of the package or the healthcare provider's hands (non-sterile surfaces). However, transfers of infectious agents via indirect contact with packaging can be minimized with proper package design and opening techniques

Hence, the goal of this study is to quantify influences of different package designs and modifications to opening techniques on the rates of contact with non-sterile surfaces (termed contamination in this work). Previous studies suggested that the material curling of the package as well the handling of the package during opening significantly impacted the contamination rate [3] therefore we focused our package designs on these factors.

## METHODS

Standard chevron pouches were used as the design base. A series of modifications were made so that when the layers were peeled apart during opening they 1) curled inward, or 2) curled outward. Additionally, a new design was created to reduce handling, the standard package was cut so a single large tab was located in the top center to facilitate center opening (Fig.1). Therefore a total of four package designs were tested: Inward, Outward, Standard, and Tab.

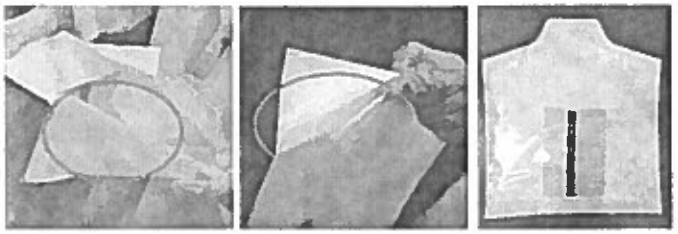


Figure 1. Three additional design modifications of a standard chevron package.

In order to investigate the impact of opening technique (aseptic technique) on contamination, two different protocols were performed: 1) Open the package with the technique learned in school and practiced as a healthcare provider ("Standard"); 2) Grab the package in top center, pull the package apart in one large movement and dump the content onto the sterile field ("Modified").

To simulate contamination, a lotion that fluoresces under a black light was coated on the outside of each package and on the back of the gloves worn by the participant. The palmer side of the hand and fingertips were not coated, so as not to change the interaction with fingers and package. (Fig. 2 a,b). Participants were asked to open and transfer the simulated sterile medical device (a set of 12 tongue depressors taped together) using "Standard" and "Modified" aseptic techniques (Fig. 2 c). Then the device was scanned with UV lights to identify whether it had been in contact with the non-sterile

surfaces. Contact is indicated by the presence of the contaminant on the tested device and was a binary outcome (Fig.2d).

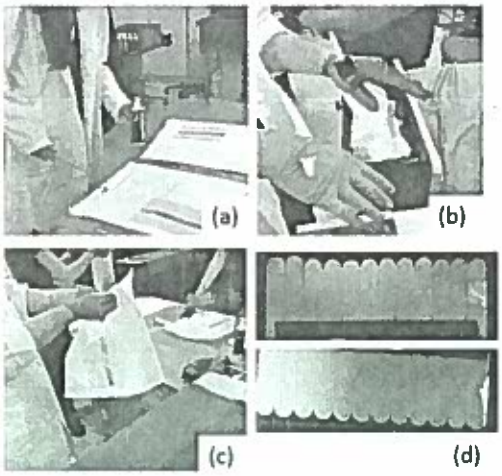


Figure 2. Contamination testing: a) coating the outside of the package, b) coating the dorsum side of participant's hand, c) participant opening package using aseptic technique, d) contamination fluoresced under UV light

The participants for this study included individuals trained in aseptic technique such as nursing professionals and nursing students. Each participant was asked to open 8 packages (2 for each design) using the "Standard" method and 8 packages using the "Modified" method. A post-test survey was conducted to evaluate participant preferences on the package designs.

## RESULTS AND DISCUSSION

Seventy four participants were tested with an average of 5.24 years of aseptic technique experience. Rates of contamination for each package and for the techniques of all four package designs are shown in Figure 3. As can be seen, indirect contact through package opening ranged from 32% to 11% contamination rates (Fig. 3). Data show that with the "Modified" method, the contamination decreased the most in the outward curling, followed by the standard and tab designs. Even though the tab design did not show a decrease in the contamination rate from the standard package, 74% of the participants reported preference of that design. A statistical analysis of these data is underway.

The second most common feedback was the commercial package did not leave enough material to grab on top center forcing them to grab along the sides (45%). Participants tended to reposition their hands and move along to the area. From our prior work, we know that an increase in this repositioning led to higher levels of contaminations.

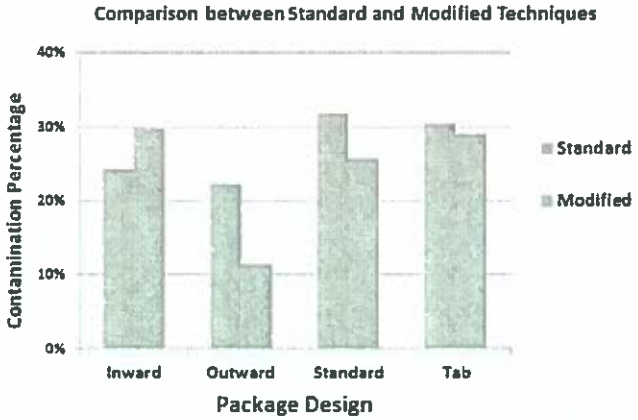


Figure 3 Comparison of contamination rates between package designs and techniques (Data are binary, contamination or no contamination).

## CONCLUSIONS

Indirect contact contamination, with packaging as a vehicle, has been largely ignored. Our preliminary work indicates that indirect contamination can be reduced through modified package design and training. Through training the contamination rates were decreased in three out of the four designs, amongst which, the outward curling showed the largest decrease from 22% to 11%, therefore a 50% reduction in contamination rate. The results are promising that by combining the changes in design and aseptic trainings, it is possible to significantly lower the contamination rate.

## ACKNOWLEDGEMENTS

The authors would like to thank Blue Cross Blue Shield of Michigan Foundation for funding the project, Rollprint Packaging Products, Cardinal Health and Sencopt for their in-kind donations, as well as Lansing Community College.

## REFERENCES

[1] N.B.Johnson et al., *CDC Report*, 2014.
[2] J.P. Steinberg et al., *HERD J.*, 2013.
[3] N. Bello et al., *PLoS One*, 201

# Mechanics Based Fracture-Risk Under Gait Cycle Loading Correlates Poorly with High Mirels' Scores in Metastatic Lesions to the Proximal Femur

Palani Permeswaran, Benjamin J. Miller, Jessica E. Goetz
University of Iowa, Iowa City, IA

## INTRODUCTION

While primary cancers of the bone are relatively rare and highly variable in presentation, metastatic bone disease is an unfortunate and common complication of many more frequently encountered cancers. It has been estimated that the prevalence of metastatic disease in the United States is approximately 280,000,[1] and treatment of metastatic disease accounts for a substantial portion of the practice of most orthopaedic oncologists. Evaluation of metastatic lesions frequently involves scoring the lesion using the scoring system developed by Mirels'. In this system, a lesion is given a score of 1, 2, or 3 in the four different categories of lesion site, size of cortical involvement, lesion type, and pain. Lesions that score >9 are recommended for prophylactic stabilization to prevent pathologic fracture, and lesions scoring 7 or lower are considered unlikely to progress to fracture.[2]

Unfortunately, there are no clear recommendations for patients who score an 8, and the obvious subjectivity of the pain category can lead to challenging decisions to be made about the need to prophylactically stabilize a lesion. Unfortunately, these patients are generally very ill, and highly invasive surgical stabilization to prevent fracture is not desirable. However, fracture healing in these patients after a pathological fracture will be complicated by their overall health and cancer treatment. The goal of this work was to use patient specific computational modeling to determine if the stresses developing around a metastatic lesion correlated with the Mirels' score.

## METHODS

Under IRB approval, 6 patients with metastatic lesions to the proximal femur were retrospectively identified. All patients had a Mirels' score >8, indicating a high risk for pathological fracture. Femoral geometry was manually segmented from each patient's clinical CT scans using Osirix software. The resulting point cloud was converted into a triangulated surface model and aligned to the Bergmann coordinate system[3] using Geomagic Studio 2014. Surface models were meshed with tetrahedral elements using the open source software TetGen.[4] To ensure high mesh quality, maximum allowable radius-edge ratio was set at 1.2 and the minimum dihedral angle bound at 0 degrees. Additionally, maximum volume of each tetrahedral element was constrained at 1 cubic millimeter. Using Matlab, CT Hounsfield-based material properties were assigned to each element. To simulate stresses in and near a bony lesion during walking, a gait cycle (4 km/h) was applied to each model via a parabolic loading distributed over the femoral head using a cosine cubed distribution; human body weight was assumed to be 169 lb. Percentage body weight and the accompanying femoral rotations during gait were obtained from Bergmann et al. and discretized into 13 steps for application.[5] Abaqus Standard finite element analysis software was used to solve each model. Individual elemental Von Mises stresses were exported for analysis at each gait step. The ratio of the CT Hounsfield-based yield stress over the stress during gait was calculated on an element-by-element basis, then averaged across the model. This ratio, defined as the factor of safety (F.S), represents a model's risk of yielding; a lower average F.S. indicates a higher likelihood of failure due to fatigue. Mirels' scores were assigned by the patient's orthopaedic oncologist and correlated with each model's factor of safety at each gait step.

## RESULTS AND DISCUSSION

Each model's F.S. curve is plotted in Figure 1. Although steps 8-13 of gait show relatively significant correlations between F.S. and Mirels', earlier steps show poor correlations (Table 1).

The changes in F.S. over the full walking gait cycle were highly variable and dependent upon

progression through gait. This would be expected as the complicated and unpredictable nature of metastases to bone can cause portions of the femoral head and neck best suited for carrying load during certain times during gait to be compromised in models with lower Mirels' scores but intact in models with higher Mirels' scores.

A limitation to this work was that all of the patients studied had Mirels' scores that were high and indicative of fracture. It is possible that the inclusion of additional patients with lower risk lesions to the proximal femur may result in a better correlation between stresses and Mirels' score by expanding the range over which the correlation can be made. Additionally, utilizing each patient's weight during loading, rather than a uniform weight, may provide a more accurate representation of the stresses occurring in their specific femur during gait and improve the correlation. However, it was clear that high Mirels' scores do not directly relate to specific mechanical risks.

This work confirms recent findings by Damron, et al. that indicate that Mirels' scores are not the best predictor of fracture.[6] In-depth, patient specific mechanical analyses may be of great use in this extremely vulnerable population.

## CONCLUSIONS

Clinicians should use care when interpreting Mirels' scores, as Mirels' scores in isolation appear not to correlate with direct mechanical compromise of the affected bone.

## REFERENCES


1. Li S, et al. (2012). *Clin Epidemiol.* **4**, 87-93.
2. Mirels H. (1989). *Clin Ortho Relat Res* 256-264.
3. Bergmann, G., et al. (2001). *J Biomech,* **34**(7), 859-871.
4. http://wias-berlin.de/software/tetgen/
5. Bergmann, G., et al. (2001). *J Biomech,* **34**(7), 859-871.
6. Damron TA, et al. (2016). *Clin Orthop Relat Res.* 474: 643-651.


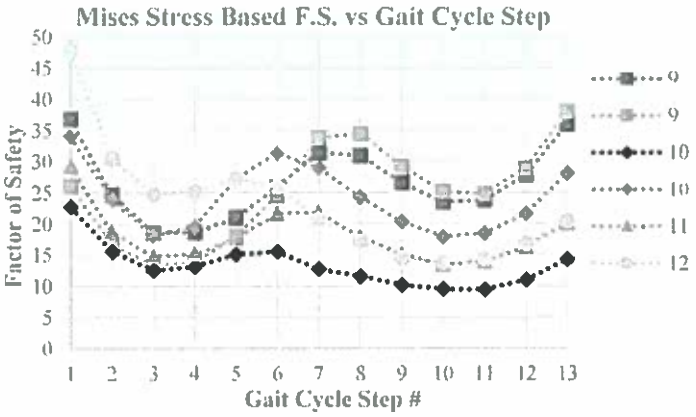


**Figure 1:** F. S. at Gait Cycle Steps

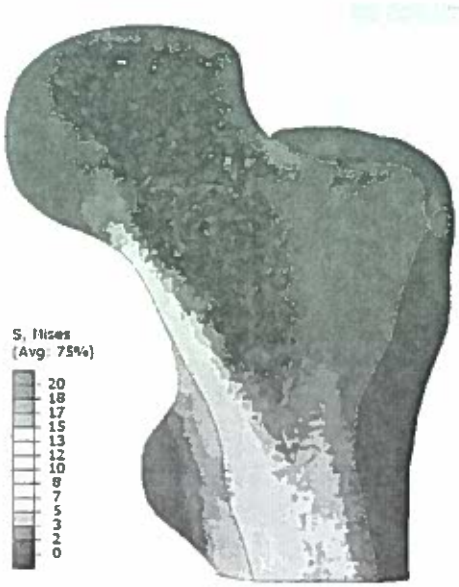


**Figure 2:** Mirels' 11 Slice Less Lesion Elements at Step 10

**Table 1:** Correlation of Mirels' Scores and F.S. at each Gait Cycle Step

| Gait Cycle Step # | 1 | 2 | 3 | 4 | 5 | 6 | 7 | 8 | 9 | 10 | 11 | 12 | 13 |
|---|---|---|---|---|---|---|---|---|---|---|---|---|---|
| $R^2$ | 0.3091 | 0.2495 | 0.3367 | 0.3429 | 0.1603 | 0.0011 | 0.3339 | 0.4834 | 0.5076 | 0.4839 | 0.4386 | 0.4382 | 0.4955 |

# VALIDATION OF A PASSIVE HYDRAULIC SIMULATOR FOR SPASTICITY REPLICATION

[1] Yinan Pei, [1] Jiahui Liang, [1]Randy H. Ewoldt, [2]Steven R. Tippett, [1]Elizabeth T. Hsiao-Wecksler

[1] University of Illinois at Urbana-Champaign, Urbana, IL, USA
[2] Bradley University, Peoria, IL, USA
email: pei2@illinois.edu, web: http://hdcl.mechanical.illinois.edu/

## INTRODUCTION

Spasticity is characterized by increased muscle tone with speed-dependency (i.e. faster passive stretch speeds lead to increased resistance) and a catch-release behavior (i.e. muscle tone spikes at a catch angle and then releases, Fig. 1). Current clinical evaluation of spasticity involves subjective assessments based on qualitative scales such as the Modified Ashworth Scale (MAS). These qualitative measures are subject to the rater's personal interpretation or experience. Clinical students (e.g., physical therapy, nursing, neurology) repetitively practice to attain reliable assessments, but the availability of practice patients can be limited and muscle tone may also change after multiple stretches (Fig. 2a).

| MAS | Qualitative Description |
|---|---|
| 0 | No increase in muscle tone |
| 1 | Slight increase in muscle tone, manifested by a catch and release or by minimal resistance at the end of the range of motion |
| 2 | Slight increase in muscle tone, manifested by a catch, followed by minimal resistance throughout the remainder (less than half) of the range of motion |
| 3 | More marked resistance in muscle tone through most of the range of motion, but affected part is easily moved |
| 4 | Considerable increase in muscle tone, passive movement difficult |
| 5 | Affected part is rigid in flexion or extension |

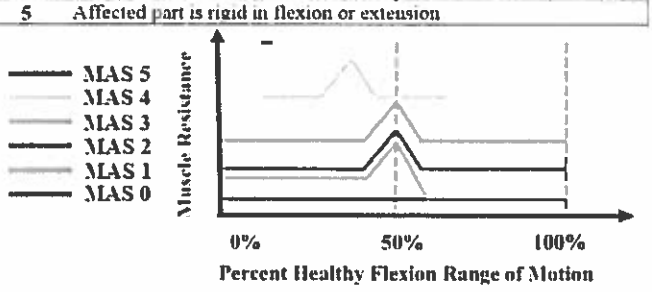


Figure 1: Qualitative descriptions [1] and conceptual interpretation of each MAS level.

A training simulator that replicated spasticity in the elbow for five MAS levels (0-4) during flexion was constructed [2] (Fig. 2b). This hydraulic simulator was entirely passive (no electro-mechanics). Muscle resistance was replicated using a piston-cylinder damper design utilizing viscous fluid and five selectable orifice sizes embedded in the piston head. Resistance values were based on published viscous resistance estimates [3]. To replicate the catch-release behavior, a cam-driven linkage was designed to maximize the moment arm at the mid-range of motion (ROM). This paper presents preliminary validation testing results.


Figure 2: Passive stretch test in clinical setting (simulated) (a) and the prototype simulator (b).

## METHODS

Validation of the design has consisted of three stages: 1) testing of the viscous damper only, 2) testing of the final prototype, and 3) system review from three experienced clinicians. In Stage 1, a material testing system (Instron 5967; High Wycombe, UK) was used to test the performance of the viscous damper. The damper was compressed up to a displacement limit under four speeds (250, 500, 750, 1000 mm/min) and average damper forces were calculated. In Stage 2, a customized measurement device that measured elbow angle & speed and force applied to the forearm by the user was deployed to evaluate the overall performance of the prototype. The resistive torque at each MAS level was examined under different input stretch speed ranges. In Stage 3, three veteran spasticity clinicians with more than 10 years of experience each were invited to evaluate the prototype. Individually, each clinician was asked to assess the degree of spasticity simulated by the prototype while blinded to the selected level on the simulator. Two trials were conducted per level, 10 trials in total for MAS 0-4, presented in randomized order across trials and levels. Agreement percentages between simulator and clinician levels were recorded and analyzed.

## RESULTS AND DISCUSSION

For Stage 1, experimental results of viscous resistance roughly fell within the range of design targets at MAS levels 0-3 (Fig. 3). Due to lack of data from [3] for level 4, no reasonable error bars could be constructed.

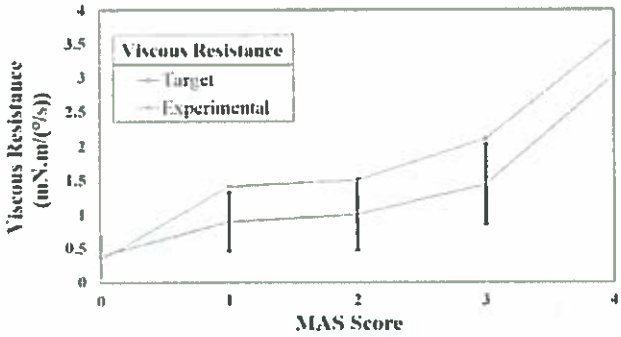


**Figure 3:** The comparison between target viscous resistance from [3] (blue) and averaged experimental viscous resistance (orange) for MAS 0-4. Error bars represent SD.

For Stage 2, the resistive torque generated by the viscous damper increased with MAS level, and within each level, the maximum torque occurred at around 40°, followed by a release for the remaining ROM (Fig. 4a). At each MAS level, the resistance also increased with faster stretch speeds to mimic the speed-dependency of spasticity (Fig. 4b).

For Stage 3, all trials were within an error margin of one MAS level (Table 1). For improvements, clinicians suggested that the simulator should (i) demonstrate a reduction in ROM for higher MAS levels; (ii) levels 0 and 1 should generate less resistance; and (iii) the catch-release behavior should be clearer since the actual catch behavior is more drastic. These post-hoc comments match their test results, and overall clinicians gave positive feedback on the prototype.

## CONCLUSIONS

Benchtop and expert tests of the prototype suggested that the design performed reasonably well relative to desired and clinically-expected performance. Future work will focus on revising the design based on suggestions to make the spasticity replication more realistic and expand the prototype's functionality to mimic spasticity in flexion and extension, followed by expert review from a larger panel of clinicians.

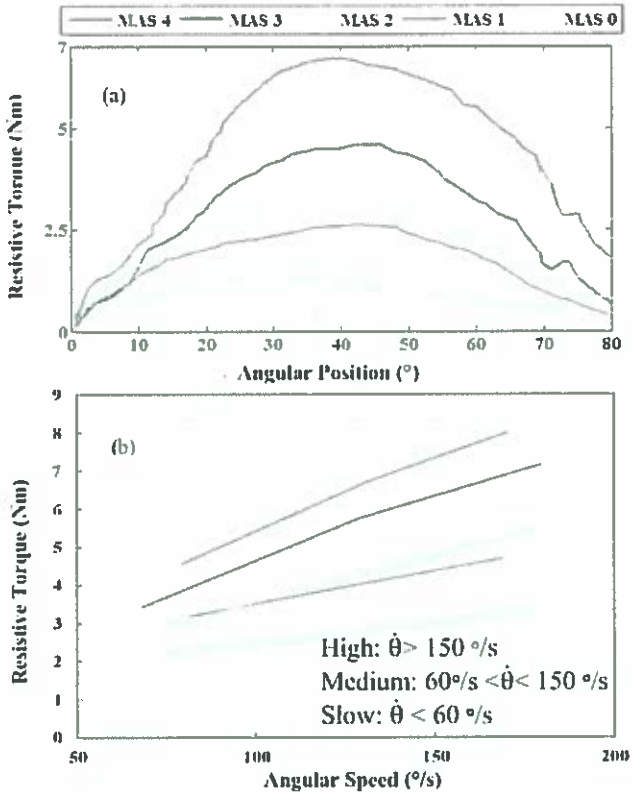


**Figure 4:** (a) Experimental resistive torque profile versus angular position for MAS 0-4 at fast stretch speed (>150°/s). (b) Average peak resistive torque at low, medium and high stretch speeds.

## REFERENCES


1. Bohannon RW, et al., Phys Ther., **67(2): 206-7**, 1987.
2. Liang J, et al., J Med Dev Trans ASME, **10(2), 020954**, 2016.
3. Lee HM, et al., J Neurol Neusosur PS. **1;72(5):621-9**, 2002.


## ACKNOWLEDGEMENTS


Funded by OSF-UIUC Jump ARCHES program. Thanks to Seung Yun (Leo) Song; David Lanier, OTR/L, ATP; Shannon Fraikes, PT; Jianxun Zhou, MD, PhD; Dyveke Pratt, MD.


**Table 1:** Blind test ratings by clinician vs. actual setting on simulator. Highlight entries indicates disagreements. All numbers are MAS levels.

| Clinician 1 | | | | Clinician 2 | | | | Clinician 3 | | | |
|---|---|---|---|---|---|---|---|---|---|---|---|
| Simulator | Rater | Simulator | Rater | Simulator | Rater | Simulator | Rater | Simulator | Rater | Simulator | Rater |
| 0 | 0 | 2 | 3 | 0 | 1 | 2 | 2 | 0 | 1 | 2 | 2 |
| 0 | 1 | 3 | 3 | 0 | 1 | 3 | 3 | 0 | 1 | 3 | 3 |
| 1 | 1 | 3 | 4 | 1 | 1 | 3 | 3 | 1 | 2 | 3 | 2 |
| 1 | 0 | 4 | 3 | 1 | 2 | 4 | 4 | 1 | 2 | 4 | 3 |
| 2 | 2 | 4 | 4 | 2 | 2 | 4 | 4 | 2 | 2 | 4 | 4 |
| Agreement (%): | | 50 | | Agreement (%): | | 70 | | Agreement (%): | | 40 | |
| w/ ± 1 error margin: | | 100 | | w/ ± 1 error margin: | | 100 | | w/ ± 1 error margin: | | 100 | |

# RELATIONSHIP BETWEEN GAZE BEHAVIOR AND FAILURE TO CROSS A STATIONARY, VISIBLE OBSTACLE

[1]Samuel M. Pontecorvo, [2]Michel J.H. Heijnen, [3,4]Brittney C. Muir, and [1]Shirley Rietdyk

[1] Department of Health and Kinesiology, Purdue University, West Lafayette, IN, USA
[2]School of Health and Applied Human Sciences, U. of North Carolina Wilmington, Wilmington, NC, USA
[3]Department of Occupational Therapy, The Sage Colleges, Troy, NY, USA
[4]Department of Physical Therapy, The Sage Colleges, Troy, NY, USA
email: srietdyk@purdue.edu

## INTRODUCTION

Successful modification of gait while navigating cluttered environments is aided by vision. Participants tasked with crossing a stationary, visible obstacle occasionally fail and contact the obstacle [1]. Examining the biomechanics of these failures has indicated that foot placement too close to the obstacle resulted in failures, due to inadequate time and space to flex the limb during crossing [2]. Failures also occur with appropriate foot placement, and most of these failures resulted from a progressive decrease in foot clearance with each subsequent trial [1]. One of the reasons for inappropriate foot placement and inadequate foot elevation may be that the participants did not look at the obstacle adequately during the approach, leading to faulty motor behavior. Participants who never contact the obstacle (successful participants) may have different gaze behaviors than those who do contact the obstacle. This study determined if gaze behaviors were different between successful and unsuccessful participants.

## METHODS

Thirty-four university aged adults (7 male, 21 ± 1.2 years of age, 1.68 ± 0.10 m) were recruited. Participants walked over a stationary obstacle that was positioned in the middle of a 6.7 m walkway for 150 trials. Obstacle height was approximately 25% of leg length.

Participants were categorized as a function of the number of obstacle contacts during the 150 trials:
· *Non-tripper*: 0 obstacle contacts in 150 trials
· *Single-tripper*: 1 obstacle contact in 150 trials
· *Repeated-tripper*: 2+ obstacle contacts in 150 trials

Gaze behavior (Mobile Eye-XG, ASL) was analyzed up to and including the participant's first contact trial, or to trial 150 if no contacts occurred. Fixation onset and offset were defined as a gaze within a 3 deg. variance with a minimum duration of 100 ms.

Nine areas of interest (AOIs) were examined (Fig. 1): the walkway was divided into 5 segments (including 60 cm in front of the obstacle where the trail foot is placed and 60 cm after the obstacle where the lead foot is placed), and the obstacle was divided into 3 segments (top, middle, bottom). The outside AOI was any area not previously designated but within the participant's field of vision. Measures included duration and frequency of fixations on each AOI, and the total duration and frequency for all AOIs combined.

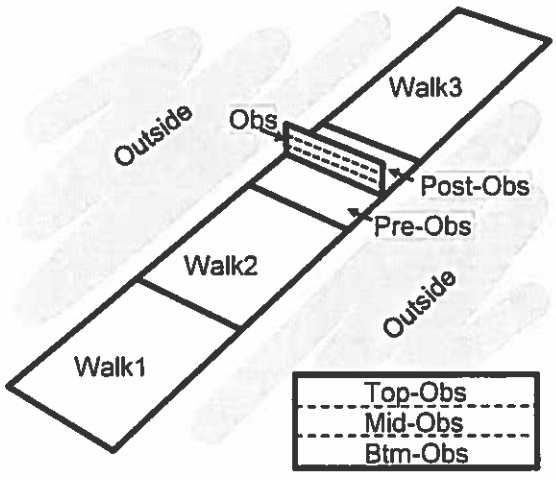


**Figure 1**: Depiction of walkway and areas of interest (AOIs). Bottom right rectangle indicates the three equal AOIs on the obstacle. Outside AOI included floor, walls, door, etc.

## RESULTS AND DISCUSSION

The participants were categorized as follows: 13 non-trippers (38%), 11 single-trippers (32%), and 10 repeated-trippers (29%).

The total number of fixations (i.e. on any AOI) in each trial was not different across the three groups (10.3, 10.3, and 10.7 for non-trippers, single-trippers, and repeated-trippers, respectively; p=0.84). The number of fixations on the obstacle AOI was different as a function of the three groups (p=0.05; Fig. 2a). Post hoc analyses revealed that compared to repeated-trippers, non-trippers fixated on the obstacle in more trials (83 vs 52%, p=0.05). Non-trippers also fixated on the obstacle for a larger proportion of the approach phase relative to repeated-trippers (13 vs 6%, p=0.05; Fig. 2b). Further, relative to repeated-trippers, non-trippers had more frequent fixations on the top of the obstacle (p=0.02), on the walkway region immediately after the obstacle (p=0.02), and had less frequent fixations on AOIs outside the walkway (p=0.01).

The higher fixation frequency on key environmental features provided more opportunity for non-trippers to obtain and process visual information, which may have enhanced obstacle crossing success. Future research will examine how the limb movements were different across the three groups, in order to identify how the gaze fixation on the obstacle optimized motor behavior. These findings warrant a randomized controlled trial to investigate the efficacy of gaze interventions for preventing falls.

## CONCLUSIONS

Higher frequency and longer duration of visual fixations on an obstacle in the environment were associated with decreased likelihood of failure. Documenting optimal gaze strategies may lead to the development of gaze interventions to prevent trips, similar to the 'quiet eye' technique that improves athletic performance (Vickers, 2009).

## REFERENCES


1. Heijnen, Muir, Rietdyk. (2012). Factors leading to obstacle contact during adaptive locomotion. Exp Brain Res, 223(2), 219-231.
2. Chou Draganich. (1998). Placing the trailing foot closer to an obstacle reduces flexion of the hip, knee, and ankle to increase the risk of tripping. J Biomech, 31(8), 685-691.
3. Vickers. (2009). Advances in coupling perception and action: the quiet eye as a bidirectional link between gaze, attention, and action. Prog Brain Res, 174, 279-288.


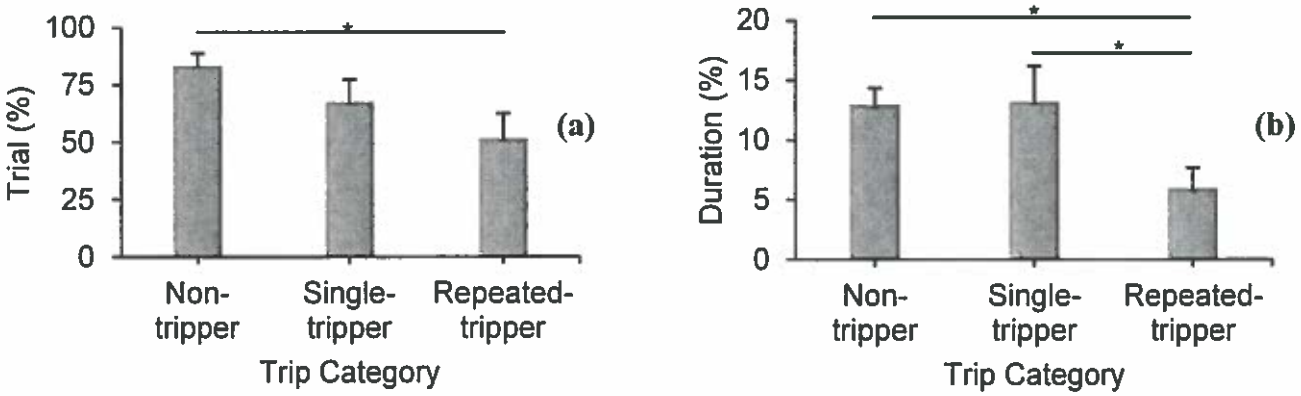


**Figure 2**: Percentage of trials with obstacle fixations as a function of trip category **(a)** and duration of the trial with a fixation on the obstacle expressed as percentage of trial duration **(b)** (calculated for each trial as total obstacle fixation duration divided by trial duration). Significant differences revealed by post hoc tests are shown with asterisks.

# MEASURING BODY SHAPE UNDER CLOTHING FOR BIOMECHANICS APPLICATIONS USING LOW-COST SENSORS

Matthew P. Reed and Byoung-Keon Daniel Park

University of Michigan, Ann Arbor, MI, USA
email: mreed@umich.edu, web: mreed.umtri.umich.edu

## INTRODUCTION

The availability of low-cost three-dimensional surface measurement systems has enabled the incorporation of body shape information into a broader range of biomechanics analyses than was previously feasible. This abstract describes ongoing work using Microsoft Kinect sensors to measure body shape, with applications to whole-body ergonomics applications and vehicle crash simulations. Statistical modeling of body shape based on measurements obtained using high-fidelity laser scanners is critical to the new methods. We demonstrate estimating body shape for children in normal clothing.

## METHODS

The first large-scale studies of human body shape in the U.S. began in the late 1990s using optical systems. A typical system records a point-cloud of over 500k points during a 12-second scan that can be processed to produce a water-tight representation of the body surface. Scans of individuals can be used to estimate biomechanical parameters such as center of mass location and segment moments of inertial.

The utility of the data is greatly enhanced by the creation of parametric statistical body shape models (SBSM) that enable the prediction of body shape as a function of input parameters such as stature and body weight. The critical processing step is fitting a homologous mesh to each scan, so that individual vertices of the mesh have consistent anatomical locations across scans. Principal component analysis is used to reduce the dimensionality of the data, and general linear models are created to predict the principal component (PC) scores as a function of overall anthropometric descriptors. Fig. XX illustrates the application of the method to modeling child body shapes. These models, which are available for interactive use at humanshape.org, generate a complete standing or seated body shape using data from 146 children approximately ages 3 to 12 as a function of stature, erect sitting height, and body weight[1,2]. The locations of anatomical landmarks on the surfaces of the scans enabled the estimation of internal joint center locations, which are then predicted along with the body shape.

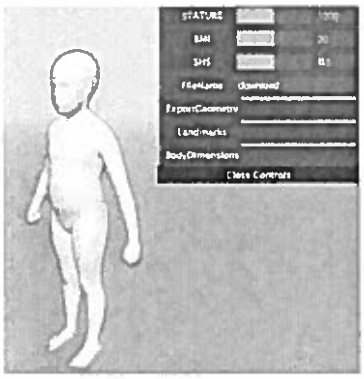


Figure 1: Illustration of interactive pediatric body shape model (see humanshape.org).

The availability of an SBSM allows low-cost sensors such as Microsoft Kinect to be applied to body shape measurement with greater fidelity than would otherwise be possible. Kinect version 2 uses a time-of-flight sensor to obtain depth data in a rectangular field of view, enabling calculation of a 3D point cloud of points on the surface of objects in the scene. Compared to laser scanners, the data are relatively noisy and coverage is sparse, unless four or more sensors are used. However, fitting the data with the SBSM helps to overcome these limitations. Specifically, an interactive process is used to find a vector of PC scores (typically 20 to 40 values) that results in a body shape that best fits the data. This

method has been applied to child body shapes using data from Kinect sensors.

The utility of this method would be enhanced if the subjects were not required to be minimally clad for the measurement. To assess the feasibility, we scanned 24 children wearing normal indoor clothing using Kinect and a high-quality laser scanner. These data were obtained using a system developed with two version-1 Kinect sensors. The data were fit using a standing child SBSM and the inscribed-fitting method that finds the largest body size obtained by a vector of PC scores that will fit fully with the scan[3]. Due to the structure of the SBSM, only realistic body shapes can be created, so clothing artifacts are effectively ignored.

## RESULTS

Fig. 2 shows the results of model fitting for one child. Note the model successfully interpolates a minimally clad body shape in spite of the noisy and incomplete data and clothing artifacts. The whole process (scanning and model fitting) requires less than 30 seconds.

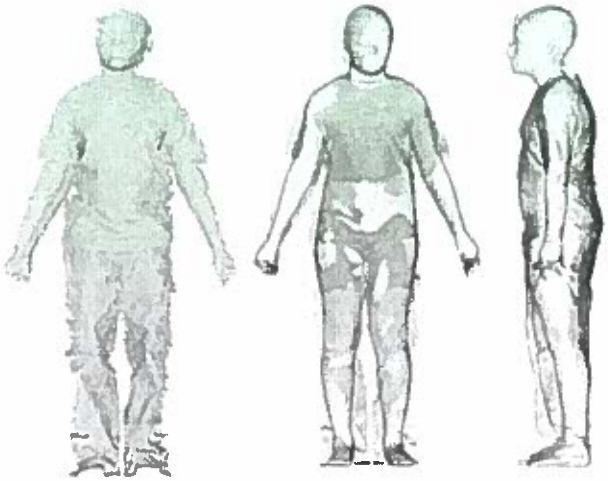

Figure 2: Kinect data (left) and fitted figures (right).

The accuracy of the method was assessed by comparing the torso contours obtained by the SBSM fitting method with laser-scan data from the same child in a minimally clad condition. Fig. 3 illustrates the error distribution for the child in Fig. 3. Mean unsigned error was 10 mm.

## RESULTS AND DISCUSSION

The proposed method is capable of providing a reasonable accurate measure of child body shape in normal light clothing. This methodology may provide a means of rapidly surveying large populations of children to determine distributions of body dimensions. By extension to parametric finite-element models, distributions of body segment parameters could also be determined. More generally, this suite of techniques will provide a low-cost means of rapidly evaluating body shape for children and adults without requiring participants to disrobe.

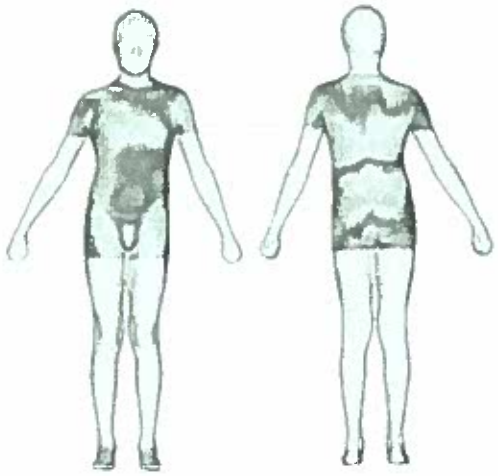

Figure 3: Illustration of fitting accuracy relative to a reference minimally clad laser scan. Yellow=25 mm, blue = 0. Mean Err: 10.0 mm, 95%tile: 22.4 mm

## REFERENCES


1. Park B-K et al. *Ergonomics*, **58**(2):301-309, 2014
2. Park B-K et al. *Ergonomics*, **58**(10):1714-1725, 2015.
3. Park B-K et al. *Proc. 4th International Digital Human Modeling Conference*. 2016


## ACKNOWLEDGEMENTS


The work reported here was supported by a range of sponsors, including the U.S. National Highway Traffic Safety Administration, the National Science Foundation, Herman Miller, Ford Motor Company, General Motors, and Toyota.

# Computational Model and Simulation of Rowing Exercise Machine

Farbod Rohani and Antonie J. van den Bogert

Cleveland State University, Cleveland, OH, USA
Email: f.rohani@csuohio.edu, web: http://hmc.csuohio.edu

## INTRODUCTION

Long-duration spaceflight missions are associated with numerus health problems including muscle atrophy and bone loss [1]. Exercise, both aerobic and resistive exercise, is important to help astronauts keep their body healthy during their stay in the space. Computational models of exercise machines are needed in order to replace the machine by a computer-controlled mechatronic system. Furthermore, models will allow simulation studies to optimize the exercise prescription.

The goal of this study is to develop a model a of a rowing exercise machine and estimate model parameters from experimental data.

## METHODS

Data were collected on a single subject using the Concept 2 rowing machine for nine trials. Three levels of air resistance were used, each with three different cadence levels. Encoders were used to measure flywheel velocity and handle velocity. The force between handle and flywheel was measured by a load cell.

The rowing machine system was modeled by a mass (m), springs (SC, PC), and a damper (D) where m represents the mass of the flywheel and PC represents the chain and ratchet mechanism. The spring SC corresponds an elastic shock cord and produces a small tension during the return while the damper D is responsible for resisting the fly wheel rotation. Fig.1 shows the schematic of the system.

The five trajectory variables of the dynamic system are flywheel position, flywheel velocity, handle position, handle velocity and handle force:

$$y = \left(x_{fw}, \dot{x}_{fw}, x_h, \dot{x}_h, F\right)^T$$

The system dynamics can be written as implicit dynamic equation:

$$f(y, \dot{y}, t, p) = 0$$

where p represent the vector of the optimized parameter of the system. A trajectory optimization approach was used to optimize the state trajectories and the hardware parameters. The objective is to minimize the tracking error between the simulation and the actual data by following the handle velocity, fly wheel velocity and the force over a rowing cycle ($T$). For simplicity, we represent all rowing cycles with their average over the period of $T$. The cost function is defined as summation of defined objectives

$$F = \frac{1}{T}\int_0^T \left[\left(\frac{\dot{x}_{fw}(t) - \dot{x}_{fw,m}(t)}{\sigma_{fw}}\right)^2 + \left(\frac{\dot{x}_h(t) - \dot{x}_{h,m}(t)}{\sigma_h}\right)^2 + \left(\frac{F(t) - F_m(t)}{\sigma_F}\right)^2\right] dt$$

where $\sigma$ represents the standard deviation of the data. To make each objective dimensionless, the difference between the simulated trajectories and the data are divided by $\sigma$. Similar to [2], the problem was transcribed into a large-scale nonlinear program (NLP) using DC, using the midpoint Euler discretization. Grid refinement showed that 50 time nodes per rowing cycle was sufficient. The resulting nonlinear program was solved by IPOPT.

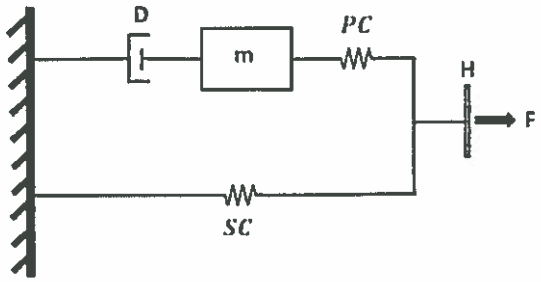


**Fig 1.** Schematic of the rowing machine system. The shock cord was modeled as a linear spring (SC) with stiffness $k_{sc}$. The pull chain was modeled as a one directional spring (PC) with stiffness $k_{pc}$. H represent the rowing handle, and F is the applied force to the handle.

## RESULTS

Table. 1 shows the optimized parameter values as well as how well the simulation fits the data for three levels of air resistance, each with three different cadence levels. The optimal parameter values are not dependent on the cadence level. Also all the parameters except the damping coefficient stay constant when the resistance level is changed. However, in trial 6, when we have medium resistance with high cadence, the simulation result cannot track the data as well as expected. This solution is a local optimum.

Fig.2 shows the results of the optimization for a typical trial for all the states. The results showed that the system could fit the data well, and that the parameter values were constant. Note that the handle position and the flywheel position are not restricted to have a specific position during a rowing cycle.

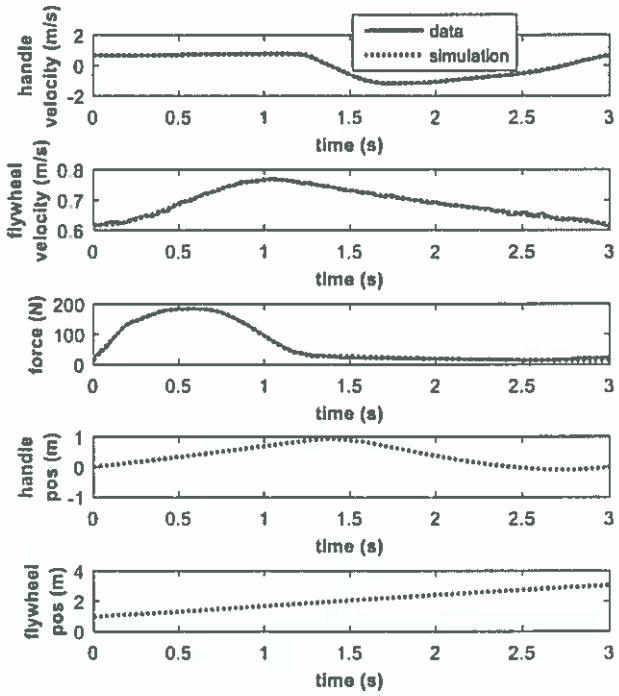


**Fig 2.** Handle velocity, flywheel velocity, force, handle position, and flywheel position for a typical simulation.

## REFERENCES

1. Baldwin KM, et al. *Med Sci Sports Exerc* **30**, 1247– 1253, 1996.
2. van den Bogert AJ, et al. *J Biomech Eng* **134**, 051007, 2012.

## ACKNOWLEDGEMENTS

Financial support was received from NSF under grants No. 1344954 and 1544702.

**Table 1.** Optimal parameter and fit values

| Resistance | High Resistance | | | Medium Resistance | | | Low Resistance | | |
|---|---|---|---|---|---|---|---|---|---|
| Cadence | Low | Medium | High | Low | Medium | High | Low | Medium | High |
| D ($Ns^2/m^2$) | 92.45 | 89.77 | 89.68 | 54.27 | 53.88 | 47.31 | 37.12 | 35.94 | 35.82 |
| m (kg) | 554.6 | 545.0 | 539.6 | 562.4 | 553.4 | 497.4 | 561.4 | 544.7 | 545.9 |
| $K_{CRH}$ (N/m) | 10646 | 27060 | 28386 | 17380 | 19345 | 50000 | 11090 | 18332 | 24734 |
| $K_{sc}$ (N/m) | 14.36 | 12.93 | 12.97 | 16.53 | 13.49 | 20.97 | 17.08 | 13.18 | 12.05 |
| Flywheel velocity fit (m/s) | 0.0044 | 0.0029 | 0.0026 | 0.0037 | 0.0029 | 0.0059 | 0.0045 | 0.0026 | 0.0022 |
| Velocity fit (m/s) | 0.0437 | 0.0676 | 0.0864 | 0.0384 | 0.0664 | 0.0892 | 0.0349 | 0.0667 | 0.0843 |
| Force fit (N) | 3.3790 | 5.257 | 7.406 | 8.039 | 7.629 | 45.20 | 5.486 | 7.252 | 7.948 |

# Soft Tissues in the Thigh and Gluteal Regions: Determining their Strain Energy Functions

[1] Zachary Sadler, [1]Josh Drost, [1]Wu Pan, [1]Tamara Reid Bush, PhD

[1] Michigan State University, East Lansing, MI, USA
email: sadlerza@msu.edu, web: www.egr.msu.edu/reidtama/

## INTRODUCTION

The different components of human tissue yield unique mechanical characteristics that when understood as a whole can aid in the modeling and analysis of soft tissue [1], [2]. Although material properties of the skin, muscle, and adipose tissue have been approximated through *in vitro* methods [3], there is little work on the properties of bulk soft tissue in the seated position. The medical, automotive, and ergonomic seating industries are especially interested in these material properties. With a better understanding of material properties, seating in all three environments can be improved to aid in comfort, support and avoiding soft tissue injuries (e.g., pressure ulcers). The purpose of this study is to characterize the strain energy function of the bulk soft tissue through the collection of force-deflection data in these areas.

## METHODS

Twenty-nine participants, consisting of both male and female of average and high BMI, were participants in the study (IRB # 15-889). Force-deflection data were gathered through a motion capture system paired with a load cell. A tissue indenter was constructed with a 5cm x 5cm contact surface and was attached to the top of a calibrated multi-axis load cell (AMTI, Watertown, MA). Due to the large tissue deflections, the interface had to be built up and smaller than the load cell so full deflection could be achieved. Reflective markers were placed along the edges of the load cell as well as on the participant to monitor the positioning of each. The femur was outlined by a marker at the greater trochanter and lateral epicondyle.

Six different locations were tested, as demonstrated in Figure 1(a). Participants were seated in a custom chair. This chair contained removable sections to easily access the tissue in the different testing areas while still supporting the participant. The test administrator applied load by hand from either behind the subject (upper and lower buttocks) or below the chair (ischial tuberosities, proximal thigh, medial thigh, and distal thigh). Load was applied until a resistance was reached, and then the indenter removed at the same rate. Force-deflection data were then analyzed using Qualysis Track Manager and MATLAB.

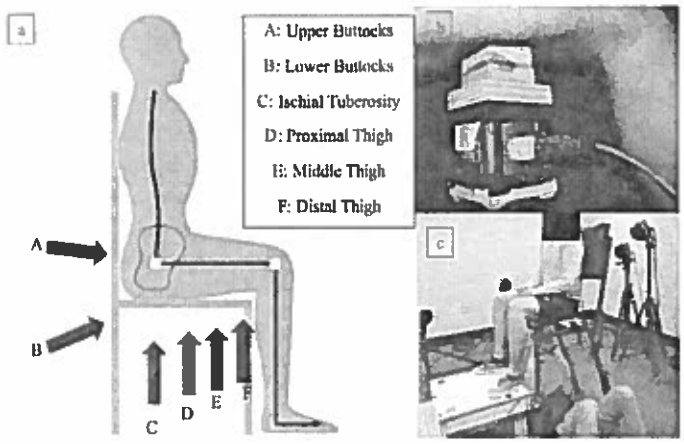


**Figure 1:** Soft Tissue Testing: (a) Testing locations (b)Tissue indenter composed of load cell, handle, reflective markers (c) Full testing setup

For the upper and lower buttocks positions, the tissue deflection was calculated as the displacement of the indenter in reference to the greater trochanter. For all other positions, the displacement of the indenter was compared to a vector created by the greater trochanter and lateral epicondyle. The original lengths of the different positions were approximated using physical measurements from testing and cadavers, as well as measurements extracted from MR images in the literature [4]. These lengths were measured from the point of contact on the soft tissue to the bony structure.

Multiple different material models were used to fit the data, including exponential, Veronda Westmann, and Mooney-Rivlin models. The strain energy function for a Mooney-Rivlin model is as follows:

$$\Psi = \frac{\mu}{2}[\alpha(I_1 - 3) + (1 - \alpha)(I_2 - 3)]$$

Where $\mu$ represents the shear modulus and $\alpha$ is a material constant. The soft tissue was assumed to be under a uniaxial compressive load with only normal stress and strain being considered. The material was also assumed to be isotropic incompressible hyperelastic.

## RESULTS AND DISCUSSION

The Mooney-Rivlin material model best represented the experiment data. Table 1 reports the model $\mu$ and $\alpha$ values. These values for each location all had $R^2$ values greater than 0.98. The upper buttocks was found to be the stiffest region while the distal thigh was the softest region. These values were then plotted with the experimental data to demonstrate the Mooney Rivlin material model fit (Fig. 2).

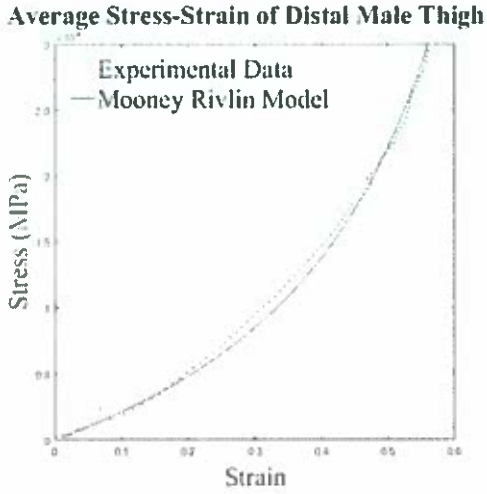


**Figure 2:** The experimental and model stress-strain data of the distal male thigh.

## CONCLUSIONS

The bulk soft tissue in the thigh and gluteal regions exhibit varying material properties with respect to position. The model and experimental data indicate that the tissues are stiffer at the upper buttocks and softer in the thighs. Understanding the material properties and being able to characterize them with a strain energy function will be extremely valuable in the development of accurate human body models and devices that interact with the body, specifically improving seats in the medical, automotive, and ergonomic industries. Further, most work that has characterized this region has used *in vitro* methods. This study was able to gather and utilize *in vivo* force-deflection in the seated position.

A potential limitation of this study is the original tissue lengths that were used for each position are average ranges compiled between measurements from the study as well as the literature. Future work will include subject-specific measurements to improve the accuracy of the modeling.

## ACKNOWLEDGEMENTS

The authors would like to thank L Nault, K Patterson, R Geary, Q Gao, and M Jakeway for their help in this study. This work is supported by NSF CBET, grant number 1603646.

## REFERENCES

[1] Setyabudhy et al., *SAE Tech. Pap. Ser.*, 1997.
[2] M. Kauer et al., *Med. Image Anal.*, 2002.
[3] T. Jee et al., *J. Biomech.*, 2014.
[4] Sonenblum et al., *J. Tissue Viability*, 2015.

**Table 1**: Average material properties of male subjects in all six locations tested.

| Optimization of Average Male Parameters | | | | | | |
|---|---|---|---|---|---|---|
| Parameter | U.Buttocks | L.Buttocks | I.T. | Proximal | Medial | Distal |
| μ (MPa) | 1.203 | 0.502 | 0.132 | 0.779 | 0.101 | 0.016 |
| α | 0.503 | 0.492 | 0.463 | 0.463 | 0.414 | 0.263 |

# Does light touch enhances manual control?

Hoda Salsabili, Joong Hyun Ryu and Jeffrey M. Haddad

Purdue University, West Lafayette, IN, USA
Email: haslsabi@purdue.edu

## INTRODUCTION

Human postural sway is reduced when individuals lightly touch a surface below a threshold that provides mechanical support [1, 2]. Lightly touching a surface provides augmented proprioceptive information that appears to be beneficial for postural control [3].

Although, lightly touching a surface reduces sway during quiet stance, there is little evidence this minimization is actually functional (i.e. stabilizes posture in a manner that allows improved control of a goal-directed task). Investigating the functionality of light touch is significant since people rarely stand for the sake of standing. Rather, in daily life, people control posture in a manner that facilitates the performance of other goal directed tasks. In the current study, we investigated if the stabilization provided by lightly touching a surface is functional. Participants performed a manual precision task with their dominant hand while lightly touching a surface with their non-dominant index finger. We hypothesized that if light touch is indeed functional, posture should be stabilized in a manner that facilitates the performance of a manual task.

## METHODS

Eighteen young college-aged participants stood comfortably on a force platform. 3D kinematics of the upper body and center of pressure (CoP) data were collected as participants performed a standing manual fitting task. Participants were instructed to pick up and then fit a block through either a small or large opening (the transport phase of the task). The block was then held in the opening for 20s (the holding phase of the task). All trials were performed while either touching (below 1.1N) or not touching a surface (Figure 1).

Figure 1: The block was (a) picked up and (b) fit into an opening. Once the block was within the opening, the participant was instructed to hold it in place for 20s.

The standard deviation (SD) of CoP and trunk position in the medial-lateral (ML) and anterior-posterior (AP) directions were assessed over the transport and holding phase of the task. The wrist straightness ratio was assessed over the transport phase of the task to examine the smoothness of the reach trajectory.

## RESULTS AND DISCUSSION

No touch by opening size interactions were observed in either the transport or holding phase of the task ($p>0.05$). However, there was a main effect of touch. CoP and trunk displacement SD in both the AP and ML directions were lower in both phases of the task when participants lightly touched the surface ($p<0.05$). We also observed a main effect of opening size. The CoP SD (Figure 2) and trunk position SD in the ML direction were smaller during both the transport and holding phase when fitting through the small opening. The wrist straightness ratio (Figure 3) was also lower when lightly touching the surface, suggesting a smoother reach trajectory ($p<0.05$).

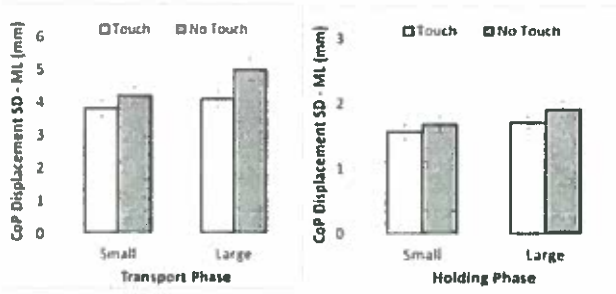


Figure 2: COP SD (ML direction) was lower during the transport and holding phase when fitting through the small opening ($p<0.05$).

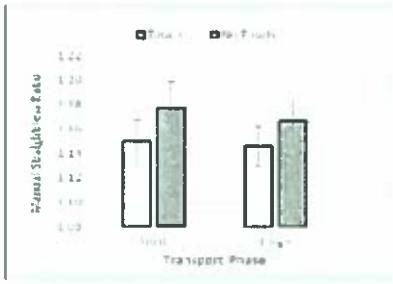

Figure 3: The straightness ratio was lower when lightly touching a surface suggesting a smoother reach trajectory ($p<0.05$).

The smoother reach trajectory and decreased trunk and arm fluctuations suggest that lightly touching a surface may indeed aid the performance of a manual task. It is however interesting to note that there was no touch by size interaction, indicating that light touch stabilization is not scaled to the task constraints. Typically, when performing a manual task, posture is controlled in a manner that facilitates performance of the task. For example, when performing a precision manual task, posture is stabilized to improve hand precision. However, when performing a non-precision demanding task, posture is not tightly constrained. Allowing sway likely improves postural flexibility [4]. Thus, the healthy postural system either allows or constrains sway based on the demands of a concurrent task [5]. Given the task-dependent nature of posture, a touch by size interaction was expected if light touch is indeed functional. In essence, overly constraining postural sway when postural sway could be beneficial may ultimately impair performance or threaten upright stance. There are many potential reasons the touch effect was not scaled to task constraints. First, it is possible that the stabilization effect emerges because light touch at the finger triggers the postural muscles in a feedforward manner [6]. If the light touch effect emerges prior to manual feedback, the touch effect may not be task dependent.

Second, one rational typically given why postural sway may, in some circumstances, be beneficial, is because it is exploratory [5]. Although constraining sway when it is not warranted could impede these exploratory processes, it is possible that the exploratory information can be generated at the finger when lightly touching a surface [7]. If the exploratory information lost by constraining sway is compensated by the finger contact, there is no cost to constraining sway.

Finally, it may be that light touch is simply an epiphenomenon of some other process and not necessarily functional. Studies with clearer performance measures may be able to better address the functionality of light touch.

## CONCLUSIONS

Our findings indicated that lightly touching a surface improves performance of a concurrent manual goal-directed task.

## REFERENCES

1. Holden, M. *J Vestib Res.* **4**, 285-301, 1994.
2. Jeka, J.J., et al. *Exp Brain Res.* **113,** 475-83, 1997.
3. Jeka, J.J. and J.R. Lackner. *Exp Brain Res.* **100,** 495-502 , 1994.
4. Haddad, J.M., et al. *Gait Posture.* **32,** 592-6, 2010.
5. Haddad, J.M., et al.. *Exerc Sport Sci Rev.* **41,** 123-32, 2013.
6. Dickstein, R., et al. *Gait & posture.* **14,** 238-247, 2001.
7. Riley, M.A., et al., *Exp Brain Res.* **117,** 165-70 , 1997.

# Using Postural Changes to Alter Loading Patterns for the Reduction of Pressure Ulcers

[1] Justin D. Scott, [1] Kelly Patterson, [1] Lindsay Hoard, [1] Michael Drost, and [1]Tamara Reid Bush

[1] Michigan State University, East Lansing, MI, USA
email: reidtama@egr.msu.edu

## INTRODUCTION

As many as 28% of individuals [1] in nursing homes suffer from some stage of pressure ulcer (PU) every year. These maladies disproportionally affect those confined to a wheelchair. Areas of high external pressure experience a diminishing of blood perfusion, contributing to PUs, malnourished tissue, and even tissue death. PUs are devastating wounds that penetrate through the tissue, some to the bone. A similar phenomenon is seen in the 282,000 people [2] who currently have a spinal cord injury (SCI) in the United States. An added complication to those with a SCI is that they may not be able to feel pressure points, resulting in loading over a long duration, and an increased risk of the formation of an ulcer. The goal of this work was to develop an articulating chair that can shift the loading from the ischial tuberosities (region at high risk of PUs) to another region of the buttocks. Developing a chair that can successfully shift loading will allow us to prescribe a postural regime that cyclically loads and unloads tissue, specifically targeting the ischial tuberosity (IT) region.

## METHODS

Prior work [3] found that typical recline angles of a seat range from 14 to 21 degrees, however the ability to articulate the spine is not currently available in wheelchairs. Thus, we designed a chair with pelvic and thoracic supports that rotate independently, allowing us to move the spine from kyphotic to lordotic positions and shift recline. The chair supports are equipped with Tekscan pressure mats and Six-Axis AMTI load cells to track overall forces on each support and areas of high pressure.

The magnitude and position of the maximum pressure was tracked statically for three individuals and dynamically for one. The participants were instructed to sit as far back in the seat as possible after each repositioning. Neutral, kyphotic, and lordotic postures were tested while the participant sat with the seat back in the vertical position and also while reclining in five degree increments through a recline angle of thirty degrees. We combined recline and articulation to determine if these could shift the loading points under the ITs. For the static tests, the participant stood up between each position and when changing the recline angle

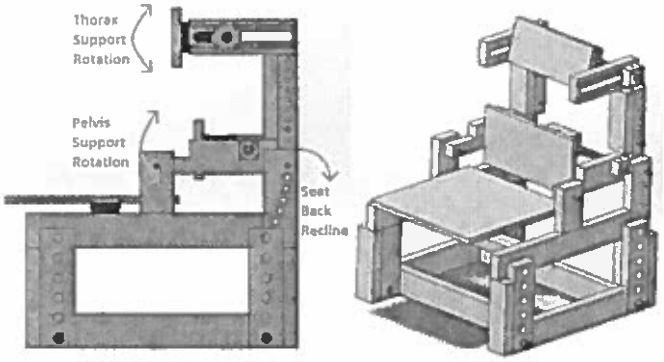


**Figure 1.** CAD design of the testing apparatus.

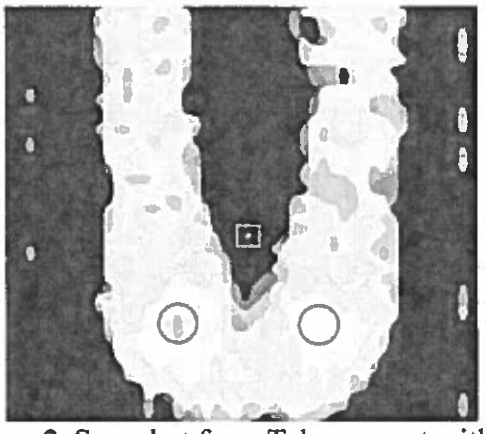

**Figure 2.** Snapshot from Tekscan mat with the center of pressure (COP) in the box and ischial tuberosities circled.

for the static tests. During the dynamic test, the participant stayed in the seat while reclining but stood to allow for thorax and pelvic support adjustment.

## RESULTS AND DISCUSSION

As is shown in Table 1, a posterior shift in the center of pressure (COP) was observed as the participant rotated through the recline angle. This was the predicted result of increasing the recline angle, but a 27.5 mm shift in the location of the COP is not enough to relieve the pressure on the tissue around the IT. The position of the COP was approximately the same for the neutral and kyphotic postures, while the lordotic posture produced a 12.7 mm anterior shift, as seen in Table 2. Currently the COP is measured from the front of the seat pan. Future considerations include measuring COP from different reference points, such as the point of contact closest to the back of the seat pan. That may account for variations in how far an individual is able to push his or her buttocks into the chair. Further measures to move the COP and location of maximum pressure are being explored, including the introduction of a pelvic cradle to facilitate pelvic rotation and the use of a footrest that actively changes the pressure points on a person's body by changing the positioning of the legs

Initial results also confirm that an increase in recline angle decreases the maximum pressure on the seat pan, as expected. The load is transferred increasingly onto the pelvic and thoracic supports as the individual reclines. While it is an effective way to relieve pressure on the buttocks and thighs, it is not feasible to have a large angle of recline for long periods of time throughout the day.

## CONCLUSIONS

The issue of pressure ulcers is prevalent for people across several populations. Anyone who is confined to a wheelchair may have encountered them; geriatric or diabetic patients often have other health problems that further complicate the wound healing process. It is necessary to prescribe a preventative procedure that will ameliorate a PU before it forms. This need is addressed through the development of an articulating chair that can shift pressures to reduce the risk of PUs and promote blood perfusion.

Our research to this point has been limited to one subject reclining and changing posture through the movement of the pelvic and thoracic supports. Future endeavors will include the exploration of the effects of a moving seat pan and foot rest on pressure points in the legs and buttocks and a larger subject population.

## REFERENCES


1. Park-Lee E, et al. *NCHS Data Brief* **14,** 2009.
2. *National Spinal Cord Injury Statistical Center*, 2016.
3. Bush TR, et al. *Proceedings of the Human Factors and Ergonomics Society* **43**, 1999.


## ACKNOWLEDGEMENTS


This work is supported by NSF CBET, grant number 1603646.


**Table 1:** Average maximum pressure for the three dynamically tested postures (slouched, neutral, lordotic) at each reline angle. Center of pressure measured from the front of the seat pan.

| Recline Angle (°) | 0 | 5 | 10 | 15 | 20 | 25 | 30 |
|---|---|---|---|---|---|---|---|
| Average Max Pressure (kPa) | 16.00±.41 | 18.51±.19 | 19.68±.07 | 18.98±.13 | 16.96±.24 | 15.64±.24 | 15.11±.23 |
| COP Position (mm) | 220.2±10.5 | 225.7±7.0 | 229.9±6.5 | 233.5±6.3 | 238.7±7.5 | 239.4±8.2 | 248.3±6.2 |

**Table 2:** Average maximum pressure of each position during the dynamic recline.

| Posture | Neutral | Kyphotic | Lordotic |
|---|---|---|---|
| Average Max Pressure (kPa) | 16.52±.26 | 17.49±.24 | 17.80±.31 |
| COP Position (mm) | 237.8±10.0 | 238.0±8.4 | 225.3±10.4 |

# WHAT ARE THE MOST EFFECTIVE EXERCISES TO PREVENT ACL INJURIES? META-ANALYTIC EVIDENCE

[1] Grace Smith, [2] Erich Petushek, and [2] Michael Stoolmiller

[1] Kalamazoo College, Kalamazoo, MI, USA
[2] Michigan State University, East Lansing, MI, USA
email: petushek@msu.edu; https://research.chm.msu.edu

## INTRODUCTION

Preventing anterior cruciate ligament (ACL) injuries has been a shared goal across many sectors and disciplines due to the prevalence, severity, and long-term consequences. Specifically, ACL injuries can lead to substantial time away from sport/work, significant financial burden, decreased function, and early onset osteoarthritis. When including the short and potential long-term issues, preventing one ACL injury would save society roughly $38.000 [1]. In soccer and basketball, the risk for ACL injury is among the highest and substantially higher (2-6 times) for females than for males [2], thus should be targeted for prevention efforts.

Well controlled neuromuscular training programs have been shown to reduce ACL injuries and are most beneficial if implemented at a young age [3,4]. Despite numerous meta-analyses conducted in this area, the most effective exercises incorporated within these prevention programs has yet to be elucidated. Therefore, the purpose of this study was to determine the exercises most frequently used within previously researched ACL injury prevention programs. In addition, a meta-analysis was performed to determine the protective/harmful effects for each of these specific exercises.

## METHODS

Studies in this synthesis and meta-analysis included ones which (1) employed a prospectively controlled design (2) included a neuromuscular training intervention and comparison/control group and (3) reported the number of ACL injuries in each group. The studies included in the analyses were consistent with the most recent meta-analyses and Physiotherapy Evidence Database (PEDro) scores for each study has been previously reported [3,4]. For each study, the specific exercises used and the number of ACL injuries in each group (control and intervention) were extracted.

The exercises from each of the studies were collated and synthesized to determine the most frequently used exercises. To investigate the protective effects of specific exercises, only the exercises that were included in at least 25% ($k>3$) of the studies were included in the analysis to reduce biases associated with largely unequal sample sizes. For example, exercises were included that were shared by at least 4 out of the 14 studies.

Random-effects models (using residual maximum likelihood estimators) were used to calculate the odds ratios and statistical parameters for each exercise. In addition to independent analysis or comparison with null effects (Odds ratio of 1), a $z$ score was calculated to assess the difference between studies including the exercise vs not including. All statistical calculations and analyses were performed using the *metafor* package with the statistical software environment R.

## RESULTS AND DISCUSSION

As can be seen in Figure 1, there was substantial heterogeneity in the exercises used in the various ACL injury prevention programs. For example, Nordic/hamstring exercises and cone jumps were the most frequently used exercises, but were only included in 7 of the 14 clinical trials synthesized. Subgroup analysis results indicated that clinical trials including lunges, scissor jumps, calf raises, vertical jumps, and Nordic/hamstring exercises demonstrated the most protective effects for ACL injury prevention (see Fig. 2). Studies that included lunges resulted in

substantially lower injury rates compared to studies that did not include lunges ($z = -2.50$; $p = 0.01$).

Results of this subgroup analysis are consistent with previous meta-analyses indicating strength exercises are important for ACL injury prevention. Specifically, the lunge exercise displayed the largest protective effects, which would align with mitigating risk factors (e.g., enhancing gluteal activity to control medial knee motion). This data also suggests that various plyometric exercises may also be important for preventing ACL injuries. Proximal control exercises have also been suggested as important to include in ACL prevention programs, however, the present data are not clear regarding this recommendation if we look only at the plank exercise [3]. Future work should consider exercise progression, intensity, and technique quality when assessing the protective effects of various exercises.

Future randomized control/comparison trials should be conducted to further examine specific exercise effects on ACL injury risk reduction. However, given the relative rarity of the injury (≈1 in 100 athletes per season), sufficiently powered randomized controlled trials will be difficult to conduct. Thus, meta-analytic evidence may be useful to create recommendations for coaches, athletes, and sports medicine practitioners.

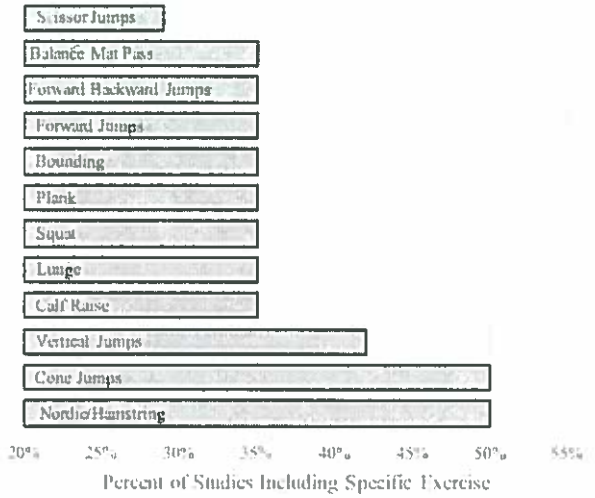


**Figure 1**: Prevalence of various exercises included in the 14 ACL injury prevention studies.

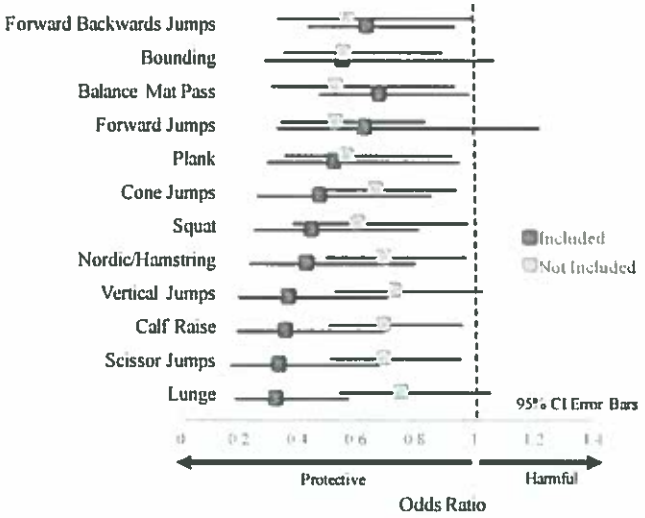


**Figure 2**: Specific exercise effects on ACL injury prevention.

## CONCLUSIONS

Understanding the most effective exercises to be included in ACL injury prevention programs will be important for dissemination and implementation of evidence-based practices. While packaged injury prevention programs exist (e.g., FIFA 11+ or PEP), coaches and sports medicine staff may want to select only the exercises that are most effective/protective. This meta-analysis suggests that lunges, scissor jumps, calf raises, vertical jumps, and Nordic/hamstring exercises are among the most beneficial exercises to include in ACL injury prevention programs.

## REFERENCES


1. Mather RC, et al., *J Bone Jt Surg-Am* **95,** 1751-1759, 2013.
2. Gornitzky, AL et al., *Am J Sports Med* **44,** 2716-2723, 2015.
3. Sugimoto D, et al., *Br J Sport Med* **49,** 282-289, 2015.
4. Sugimoto D, et al., *Br J Sport Med* **0,** 1-9, 2016.

# Aging effect on step adjustments and stability control in visually perturbed gait initiation

[1] Ruopeng Sun, [2] Chuyi Cui and [3] John B. Shea

1 University of Illinois Urbana-Champaign, Champaign, IL, USA
2 Purdue University, West Lafayette, IN, USA
3 Indiana University, Bloomington, IN, USA

## INTRODUCTION

The ability to make step adjustments in response to sudden perturbations is essential for preventing falls during locomotion. It requires the ability to inhibit original motor planning, select and execute alternative motor commands in a timely manner. The present study investigated the aging effect on step adjustments and dynamic stability control during a visually perturbed gait initiation task. A novel approach was used so that subject's anticipatory postural adjustment (APA) prior to swing foot lifting were analyzed in real time and used to trigger the stepping target perturbation.

## METHODS

Ten healthy older adults (68.0 ± 4.1 years, 6 female) and ten healthy young adults (21.5 ± 1.9 years, 4 female) participated in this study. Subjects were asked to stand upright on a force platform, initiate forward walking with their right foot, step on to a projected foot-sized virtual target located at a step length ahead of them, and continue walking on the 5 m walkway. After the initial virtual target display to trigger subjects' motor planning for gait initiation, the virtual target was randomly unchanged, or relocated laterally or medially by 10 cm. The relocation of the virtual target disrupted the preplanned step and triggered the online postural adjustments to alter foot landing position. Three trigger timing conditions (Early, Intermediate, Late) for target relocation were performed based on real time force analysis of subjects' weight distribution during APA of gait initiation cycle. Stepping accuracy, foot rotation at landing, and Margin of Dynamic Stability (MDS) at heel contact of the first three steps were analyzed and compared across timing, direction conditions and age groups using mixed model ANOVA.

## RESULTS AND DISCUSSION

Stepping accuracy decreased as a function of perturbation timing (Early – 95%, Late - 47%) as well as perturbation direction (Lateral – 87%, Medial – 64%). Older subjects exhibited significantly larger undershoot in foot placement to late lateral perturbation (Young – 84%, Old – 53%). Perturbations that occurred late in the gait initiation cycle elicited reaching-like movement (i.e. foot rotation prior to landing in order to step on the target). MDS measures revealed reduced stability in the medial-lateral and anterior-posterior direction in both young and older adults at the perturbed and the immediate subsequent step. However, young adults restored stability faster than older adults.

## CONCLUSION

The present study showed that step adjustments in perturbed gait initiation were affected by the perturbation timing and direction, with the medial stepping being more challenging to execute compare with lateral stepping. The lateral stepping task, however, yielded better separation between young and older adults in stepping accuracy. Aging effect was also observed in the number of steps needed to restore stability post perturbation. These findings could be useful for future study on screening deficits in gait adaptability and preventing falls.

## REFERENCES

1. Moraes, R., et al. (2007). "Validating determinants for an alternate foot placement selection algorithm during human locomotion in cluttered terrain." J Neurophysiol 98(4): 1928-1940.

2.Young, P. M. M. and J. B. Dingwell (2012). "Voluntarily changing step length or step width affects dynamic stability of human walking." Gait Posture **35(3): 472-477.**

3. Young, P. M. M. and J. B. Dingwell (2012). "Voluntarily changing step length or step width affects dynamic stability of human walking." Gait Posture **35(3): 472-477.**

Integrated kinematic stability relationship with standing duration between subjects with and without recurrent low back pain.

Paul Sung, Pamela Danial. Central Michigan University, Mt. Pleasant, MI 48859

## ABSTRACT

**INTRODUCTION**: Although subjects with recurrent low back pain (LBP) demonstrate altered postural control, the increased postural sway might be related to minimized trunk movement during one leg standing. The purpose of this study was to investigate the kinematic stability of the lower limbs with a core spine model in subjects with recurrent LBP during dominant and non-dominant leg standing.

**METHODS**: Sixty individuals participated in the study, including 29 subjects in the control group (18 male, 11 female) and 31 subjects with recurrent LBP (21 male, 10 female). The outcome measures included normalized kinematic stability of the lower limbs and normalized standing duration during dominant and non-dominant leg standing.

**RESULTS**: The control group demonstrated significantly longer standing duration (seconds) on the dominant ($t=-2.57$, $p=0.013$) and non-dominant ($t=-2.78$, $p=0.007$) legs than the LBP group. The kinematic stability of the core spine significantly decreased for the dominant ($t=-3.01$, $p=0.004$) and non-dominant legs during standing ($t=-3.06$, $p=0.003$) in the LBP group. For core spine stability, the LBP group demonstrated pelvis and non-dominant shank stability during dominant leg standing ($R^2=0.97$) and stability for the pelvis and dominant foot during non-dominant leg standing ($R^2=0.91$). However, pelvic stability was significantly correlated with core spine stability during standing on the dominant ($R^2=0.95$) and non-dominant ($R^2=0.97$) legs in the control group.

**DISCUSSION**: Pelvic stability for the core spine in the control group was demonstrated by longer standing duration than the LBP group. The kinematic stability of the core spine diminished as the stability of the lower limbs was significantly integrated with pelvic stability for balance performance in the LBP group. The control group took advantage of pelvic control for core spine stability to minimize lower limb movements.

**CONCLUSIONS:** Statistically significant and clinically relevant differences in core stability might prove important for enhancing pelvic stability in subjects with recurrent LBP. Clinicians need to consider motor control of core spine coordination with the lower limbs to refine postural adaptations in subjects with recurrent LBP.

References:


Aberg, A.C., Thorstensson, A., Tarassova, O., Halvorsen, K., 2011. Calculations of mechanisms for balance control during narrow and single-leg standing in fit older adults: A reliability study. Gait Posture 34, 352-357.

Hodges, P.W., Moseley, G.L., 2003. Pain and motor control of the lumbopelvic region: effect and possible mechanisms. J Electromyogr Kinesiol 13, 361-370.

Silfies, S.P., Bhattacharya, A., Biely, S., Smith, S.S., Giszter, S., 2009. Trunk control during standing reach: A dynamical system analysis of movement strategies in patients with mechanical low back pain. Gait & Posture 29, 370-376.

Sung, P.S., Leininger, P.M., 2015. A kinematic and kinetic analysis of spinal region in subjects with and without recurrent low back pain during one leg standing. Clin Biomech (Bristol, Avon) 30, 696-702.

Asymmetry of postural steadiness with lumbar spine rotation in subjects with low back pain.

Paul Sung, Alexander Gates, Sravani Kadiyala. Central Michigan University, Mt. Pleasant, MI 48859

## ABSTRACT

INTRODUCTION: This study was conducted to investigate the standing time, dynamic postural steadiness index (DPSI) as given by the force plate, and lumbo-pelvic range of motion (ROM) during one leg standing between subjects with and without low back pain (LBP).

METHODS: Sixty-two individuals participated in the study, including 30 control subjects and 32 subjects with LBP. Cross-sectional design. Each subject stood upright on his/her dominant and non-dominant legs separately in random order. The outcome measures included one leg standing time (sec), lumbo-pelvic ROM, and the DPSI, which is a composite of the medio-lateral steadiness index (MLSI), anterior-posterior steadiness index (APSI), and vertical steadiness index (VSI).

RESULTS: The control group demonstrated longer dominant ($t = 2.51$, $p = 0.01$) and non-dominant leg standing ($t = 2.67$, $p = 0.01$). The lumbo-pelvic ROM demonstrated significant interactions on region x plane ($F = 226.35$, $p = 0.001$) and side x plane x group ($F = 4.60$, $p = 0.03$). These interactions were supported by increased lumbar rotation during dominant leg standing in the LBP group ($t = -2.51$, $p = 0.01$).

DISCUSSION: The DPSI demonstrated positive correlations with MLSI and VSI; however, the LBP group did not demonstrate significant correlation with MLSI during non-dominant leg standing. The LBP group lacked medio-lateral steadiness during non-dominant leg standing in addition to increased lumbar rotation during dominant leg standing. Lumbar spine stabilization during non-dominant leg standing might enhance dynamic postural steadiness with a vertical standing alignment strategy in the LBP group.

CONCLUSIONS: The LBP group demonstrated greater lumbar spine rotation during dominant leg standing. The LBP group lacked medio-lateral steadiness during non-dominant leg standing. The asymmetry of single leg standing needs to be considered for postural steadiness and lumbar motion.

Asymmetry of limb dominance as well as trunk stability might be considered in the LBP group for postural steadiness during non-dominant leg standing.

References

Kuo YL, Huang KY, Chiang PT, Lee PY, Tsai YJ. Steadiness of Spinal Regions during Single-Leg Standing in Older Adults with and without Chronic Low Back Pain. PLoS One 2015;10:e0128318.

Sung PS, Yoon B, Lee DC. Lumbar spine stability for subjects with and without low back pain during one-leg standing test. Spine (Phila Pa 1976) 2010;35:E753-60.

Sung PS, Leininger PM. A kinematic and kinetic analysis of spinal region in subjects with and without recurrent low back pain during one leg standing. Clin Biomech (Bristol, Avon) 2015;30:696-702.

Wikstrom EA, Tillman MD, Smith AN, Borsa PA. A new force-plate technology measure of dynamic postural stability: the dynamic postural stability index. J Athl Train 2005;40:305-9.

Kinematic chain reactions on trunk and dynamic postural steadiness in subjects with recurrent low back pain. Paul Sung, Sravani Kadiyala, Alexander Gates. Central Michigan University, Mt. Pleasant, MI 48859

INTRODUCTION: Although subjects with recurrent low back pain (LBP) demonstrated altered trunk control, the kinematic and kinetic responses on spine regions were not carefully investigated for altered postural steadiness. One leg standing is required for maintaining dynamic posture and for controlling balance during daily activities.

METHODS: This study was conducted to compare the standing time, range of motion (ROM) on spine region, and dynamic postural steadiness index (DPSI) based on visual condition between subjects with and without recurrent LBP during one leg standing. Sixty-three individuals participated in the study, including 34 subjects in the control group and 29 subjects with recurrent LBP. Outcome measures included standing time, three- dimensional ROM on the spine region, and DPSI while subjects performed upright non-dominant leg standing. The DPSI was a composite of the medio-lateral (ML), anterior-posterior (AP), and vertical steadiness index (VSI) from the force plate.

RESULTS: The control group demonstrated longer standing times than the LBP group ($t = 2.96$, $p = 0.005$) in the eyes-open condition. Regarding the ROM on spine region, there was demonstrated a significant interaction with visual condition x group ($F = 7.09$, $p = 0.01$). The DPSI demonstrated a significant interaction with visual condition ($F = 10.71$, $p = 0.002$). The DPSI indicated excellent correlation coefficients with VSI in the eyes-closed condition ($r = 0.99$, $p = 0.01$) and in the eyes-open condition ($r = 0.91$, $p = 0.01$) in the control group.

DISCUSSION: The control group demonstrated a longer standing time with increased dynamic postural steadiness and motion on spine region, especially in the eyes-closed condition, when compared with the LBP group. The dynamic postural steadiness measure demonstrated an excellent correlation with the VSI to maintain dynamic balance, especially when visual input was absent in the LBP group. These kinetic

and kinematic measures indicated that DPSI and vertical steadiness might improve during one leg standing.

CONCLUSIONS: A postural correction strategy with vertical standing alignment could enhance kinematic chain reactions in subjects with recurrent LBP. The enhanced dynamic postural steadiness is highly associated with vertical steadiness. The combined kinetic and kinematic measures could help to develop a practical test.

References

Jonsson E, Seiger A, Hirschfeld H. One-leg stance in healthy young and elderly adults: a measure of postural steadiness? Clin Biomech (Bristol, Avon) 2004;19:688-94.

Ham YW, Kim DM, Baek JY, Lee DC, Sung PS. Kinematic analyses of trunk stability in one leg standing for individuals with recurrent low back pain. J Electromyogr Kinesiol 2010;20(6):1134-40.

Wikstrom EA, Tillman MD, Smith AN, Borsa PA. A new force-plate technology measure of dynamic postural stability: the dynamic postural stability index. J Athl Train 2005;40:305-9.

Sung PS, Danial P, Lee DC. Comparison of the different kinematic patterns during lateral bending between subjects with and without recurrent low back pain. Clin Biomech (Bristol, Avon) 2016;38:50-5.

# EVALUATING THE EFFECTS OF SIMULATING PATHOLOGICAL VERSUS NORMAL GAIT ON HIP JOINT MECHANICS IN DYSPLASIA PATIENTS

Holly D. Thomas, Kevin N. Dibbern, Michael C. Willey, and Jessica E. Goetz

University of Iowa, Iowa City, IA

## INTRODUCTION

Acetabular dysplasia is a form of hip deformity that changes joint mechanics, resulting in pain and hip degeneration at an abnormally young age [1]. Orthopaedic surgeons currently use 2D measurements on radiographic images to define the degree of lateral coverage deformity and acetabular version deformity [2]. One common surgical treatment of hip dysplasia is the periacetabular osteotomy (PAO), which permits multiplanar rotational correction of the acetabulum to stabilize the hip joint and reduce contact stress [3]. Radiographs are again the most common method of assessing the success of the correction, but this complex 3D deformity is difficult to capture with a single 2D image. A realistic computational model of joint mechanics in patients with hip dysplasia would assist surgeons with pre-operative PAO planning in order to improve clinical outcomes.

Previous computational models of dysplastic hips [1,4,5] have been limited by simplified modeling assumptions (e.g. spherical joint geometry) and small numbers of patients. Discrete element analysis (DEA) is a rapidly executing computational modeling technique for assessing joint mechanics by modeling the bones as rigid bodies and the articular cartilage as a bed of compressive springs [6]. This technique allows for analysis of much larger patient populations in order to establish direct relationships between changes in contact stress and patient outcomes. While the accuracy of contact mechanics determined with our custom DEA technique has been validated cadaverically, the algorithm currently utilizes an arthritic gait cycle [7] for modeling contact stresses that develop in the hip. The purpose of this study was to evaluate differences in joint mechanics resulting from the use of the existing arthritic gait compared to a gait cycle specific to hip dysplasia patients [8].

## METHODS

Under IRB approval, femoral and pelvic bone geometry from five PAO patients was segmented from pre-operative CT scans using a semi-automated program developed in MATLAB (Mathworks, Natick, MA). The cartilage surfaces were represented by a 1-mm uniform projection normal to the subchondral bone surface. The cartilage projections were smoothed toward sphericity using a custom-written algorithm. Each patient model was aligned to the coordinate system defined by Bergmann et al. for application of a walking gait cycle. First, the arthritic walking gait was simulated based on forces and rotations measured from patients that received hip implants to treat osteoarthritis [7]. Next a dysplastic gait cycle was simulated using joint reaction forces and rotations measured from hip dysplasia patients [8]. In both cases, the forces applied to each model were scaled based on the patient's body mass, and the motion was discretized into nine loading cases representing the first half of stance phase. Maximum contact stress, mean contact stress, and mean contact area were calculated for both gait cycles and compared for each loading case.

## RESULTS AND DISCUSSION

Contact stresses were highest along the superior edge of the acetabular cartilage regardless of the type of gait modeled. The use of the dysplastic gait tended to increase contact stress overall and result higher contact stress at multiple time points of the gait cycle (Figure 1). The average maximum contact stress over the entire gait cycle increased from 7.22±0.0.94 MPa with the arthritic gait to 7.77±0.78 MPa with the dysplastic gait, and mean contact stress increased from 1.44±0.13 MPa with the arthritic gait to 1.50±0.09 MPa with the dysplastic gait. There was a significant ($p<0.05$) difference in

maximum contact stress in the first step of the model (Figure 2, left) and significant ($p<0.05$) differences in the mean contact stress for steps 1, 2, 4, 5, 6, and 9 (Figure 2, middle). The use of the dysplastic gait also resulted in significant ($p<0.1$) differences in mean contact area for steps 3, 4, and 9 (Figure 2, right). Mean contact area increased significantly ($p<0.1$) from 719.03±52.39 $mm^2$ with the arthritic gait to 762.29±69.89 $mm^2$ with the dysplastic gait.

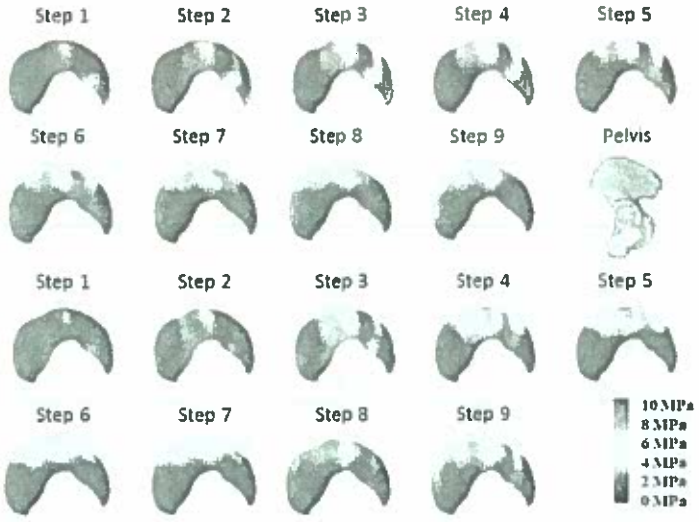


**Figure 1**: DEA analysis of acetabular contact stress developed from arthritic (first 9 steps) and dysplastic (second 9 steps) gait cycles. Scale bar in MPa.

## CONCLUSIONS

Dysplastic gait, in comparison to arthritic gait, seeks to minimize both force and rotation at the joint in order to subsequently minimize risk of dislocation. The strongest finding of this work was the tendency for increases in maximum contact stress, mean contact stress, and mean contact area with the implementation of the dysplastic gait. While there was not a key difference in maximum contact stress, there were significant differences in mean contact stress and mean contact area for numerous instances during the stance phase. These results indicate that inclusion of a dysplastic gait cycle may be extremely important to provide a realistic representation of contact mechanics in hip dysplasia patients. Further work will involve computational analysis of a large cohort of PAO patients with the improved dysplastic DEA methodology to determine if there is a useful relationship between contact mechanics and patient outcomes.

## SIGNIFICANCE

This work will assist in creating a realistic computational model of hip dysplasia in order to understand contact mechanics pre- and post-operatively. Understanding contact mechanics will enable researchers to provide quantitative assistance to surgeons in order to improve patient outcomes.

## REFERENCES


1. Hadley NA, et al. *J Orthop Res* **8**, 504-513, 1990.
2. Gala L, et al. *J Bone Joint Surg Am* **98**, 63-73, 2016.
3. Siebenrock KA, et al. *Clin Orthop Relat Res* **363**, 9-20, 1999.
4. Albers CE, et al. *Clin Orthop Relat Res* **471**, 1602-1614, 2013.
5. Armiger RS, et al. *Acta Orthop* **80**, 155-161, 2009.
6. Kern AM and Anderson DD. *J Biomech* **48**, 3427-3432, 2015.
7. Bergmann G, et al. *J Biomech* **34**, 859-871, 2001.
8. Skalshoi O, et al. *Gait & Posture* **42**, 529-533, 2015.


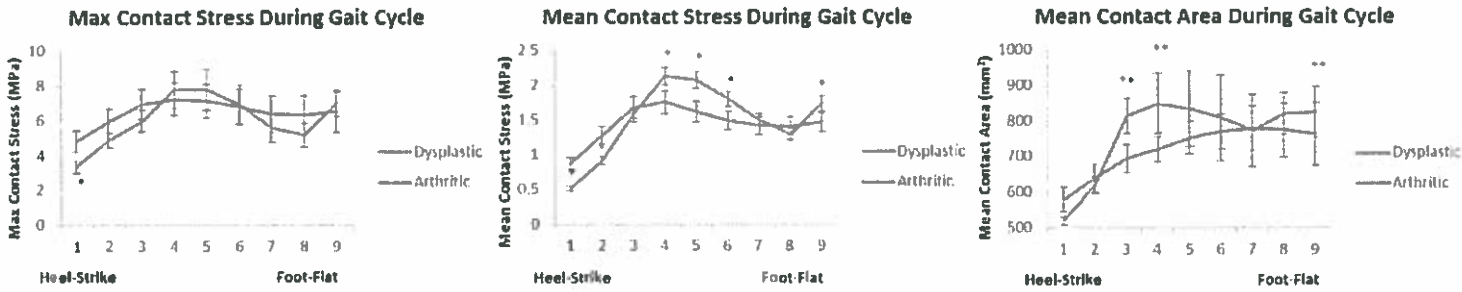


**Figure 2:** Plot of the difference in maximum acetabular contact stress (left), mean acetabular contact stress (middle), and mean acetabular contact area (right) due to the implementation of a dysplastic gait compared to an arthritic gait.

# DESIGN OF A SOFT ROBOTIC UPPER-BODY EXOSKELETON FOR REDUCING LOADS AFTER SHOULDER INJURY IN MANUAL WHEELCHAIR USERS, PRELIMINARY RESEARCH

Nicholas Thompson[1], Xiaotian Zhang[1], Girish Krishnan[2], Elizabeth T. Hsiao-Wecksler[1]

[1] Mechanical Science and Engineering
[2] Industrial and Enterprise Systems Engineering
University of Illinois at Urbana-Champaign, Urbana, IL, USA
Email: nthomps6@illinois.edu, Web: http://hdcl.mechanical.illinois.edu/

## INTRODUCTION

Between 31 and 73% of manual wheelchair users (MWUs) will experience shoulder pain due to overuse of the upper extremities for ambulation [1]. Overuse injuries are typically treated by limiting use of the affected joint [2]. In the case of MWUs, this treatment approach necessitates a loss of mobility. One possible alternate means for reducing shoulder loading during injury recovery is the use of a soft robotic upper-body exoskeleton.

The term "soft robotic" refers to a fluid-powered device that uses compliant materials for actuation. Soft robotics tend to be lighter and less bulky than traditional mechatronic "hard robotic" devices. Unlike rigid components, soft actuators have the ability to conform to different shapes, which improves comfort in a wearable device. Rigid exoskeletons must be controlled precisely to reduce risk of injury. The innate compliance of soft robotic actuators greatly reduces this risk without a need for precise control.

A common method of soft robotic actuation is pneumatic artificial muscles (PAMs), or McKibben muscles, which contract and provide tension when pressurized. A recent alternative method of actuation known as fiber-reinforced elastomeric enclosures (FREEs) have been developed by Dr. Girish Krishnan. These differ from conventional PAMs in that the fiber direction can be altered to produce not only contraction, but geometry changes, torsion, extension, and rigidity under pressure (Fig. 1). These properties make them ideal components for use in an upper-body exoskeleton.

The goal of this project is to take advantage of the compliance and unique mechanical behavior of FREEs to create an assistive exoskeleton sleeve for the upper extremities that can be worn comfortably and discreetly in daily life. This device will be designed to help with rehabilitation after shoulder injury in manual wheelchair users through reduction of peak loads during wheelchair propulsion. In this paper, we present our preliminary design approach and initial literature review findings.

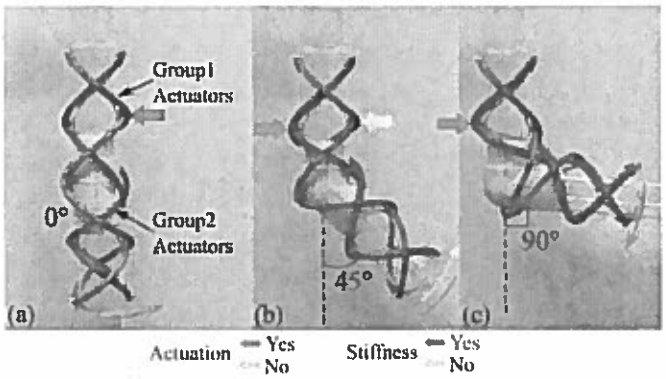


**Figure 1:** Prototype sleeve designed to actuate and stiffen the user's elbow using FREEs (from [2]).

## METHODS

Development of the exoskeleton will be structured into three phases.

Phase I of the project will focus on an assessment of upper extremity biomechanics of wheelchair users to establish *design requirements* for the assistive exoskeleton. We will determine torque and displacement requirements for typical wheelchair propulsion conditions through research and testing. This will include varying speeds and operating environments, as well as different propulsion styles. We will examine shoulder and possibly elbow biomechanics.

Phase II, will be an assessment of the FREE hardware, conducted by measuring force and displacement as functions of diameter, length, pressure, fiber angle, and architecture. We have initiated this work during the development of the FREE actuators, but testing will need to be expanded upon for our exoskeleton application [3].

Our goal will be to characterize the behavior of the hardware and establish *performance capabilities* of the FREE actuators.

Phase III will encompass prototype development and preliminary testing. Using the *design requirements* from Phase I and the *performance capabilities* of different FREEs architectures from Phase II, we will develop an upper-body exoskeleton to assist shoulder movement in wheelchair users using FREE actuators.

## RESULTS AND DISCUSSION

Preliminary literature review findings are presented here. These data will be the foundation for the exoskeleton's design requirements.

There are two phases in a manual wheelchair propulsion cycle: push and recovery, in which the hands are in and out of contact with the hand rim, respectively. There are four common propulsion patterns: semicircular, single loop-over, double loop-over, and arcing [1]. Variations in propulsion methods result in load, timing, and contact angle variations between MWUs. Peak forces and moments are experienced at the shoulder during the push phase [4]. For this reason, exoskeleton actuation can be limited to the push phase.

Dubowski et al. [5] described shoulder motion during the four propulsion patterns using two-dimensional planar contact and release angles. Contact angles were 18-55° and 81-165° in shoulders and elbows, respectively. Release shoulder angles were 27° extension to 25° flexion, and release elbow angles were 92-180°. Koontz et al. [4] described shoulder movement during wheelchair propulsion during two speeds (0.9 and 1.8 m/s) using maximum and minimum angles. Maximum sagittal extension and flexion angles were 43-64° and 6-27°, respectively. Maximum and minimum abduction angles were 42-57° and 22-27°. Maximum and minimum internal rotation angles were 52-91° and 2-55°. Multiple angles were significantly different between the two propulsion speeds tested. The exoskeleton design must be able to adapt to different displacement requirements for a single user as they alter their speed.

Koontz et al. [4] estimated resultant forces and moments on the shoulder during wheelchair propulsion at both speeds. For these two speeds, mean peak forces were 90.0 N and 108.2 N in the inferior direction, 59.9 N and 86.6 N in the anterior direction, and 34.0 and 50.4 N in the medial direction, respectively (Fig. 2). Mean peak moments were 28.6 and 36.5 Nm in sagittal flexion, 21.3 and 31.1 Nm in adduction, and 21.6 and 31.9 Nm in internal rotation for 0.9 and 1.8 m/s. In a later study, Koontz et al. [6] conducted multisite testing for shoulder kinetics during wheelchair propulsion. Mean peak forces on the shoulder were 52.9-64.9 N and 45.2-47.4 N for propulsion speeds of 0.9 and 1.8 m/s. Mean peak moments were 11.7-14.4 Nm and 17.1-18.6 Nm, respectively. These values will provide approximate maxima for required force and moment reduction provided by the exoskeleton along and about each shoulder axis. FREE actuation timing will need to be tuned to match joint kinematic/kinetics propulsion profiles (Table 1).

**Table 1:** Estimated exoskeleton operation: needed torques and ROM at shoulder during propulsion.

| | |
|---|---|
| Flexion Torque | 30 Nm |
| Adduction Torque | 20 Nm |
| Shoulder start angle (extension) | -50° |
| Shoulder stop angle (flexion) | 20° |

## REFERENCES


1. Boninger ML, et al. *Arch Phys Med Rehabil* **83**, 718-723, 2002.
2. Houglum PA, *Res Rev J Sport Rehabil*, **1**, 19–39, 1992.
3. Zhang X, et al. *Proceedings of IEEE ICAIM*, Banff, Alberta, Canada, 2016.
4. Koontz AM, et al., *J Rehabil Res Dev* **39**, 635–649, 2002.
5. Dubowski SR, et al. *J Biomech Eng*, **131**, 21015, 2009.
6. Koontz AM, et al., *J Rehabil Res Dev* **44**, 449–458, 2007.


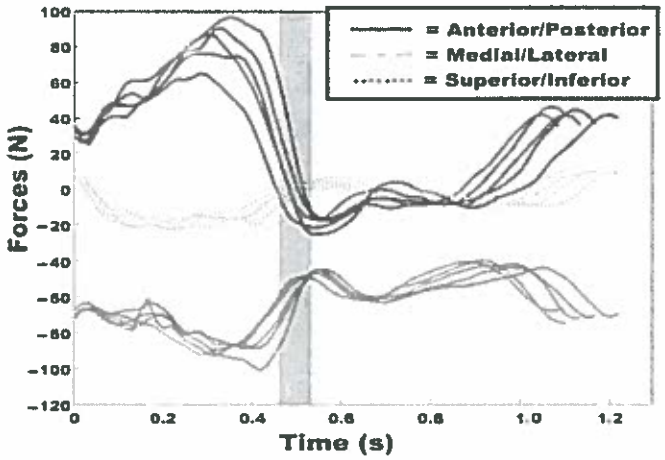


**Figure 2:** Shoulder forces during five consecutive wheelchair propulsion cycles at 0.9 m/s (from [3]).

# UNCERTAIN MOTOR PLANS LOWER STABILITY OF CURRENT PREHENSILE BEHAVIOR

Mitchell A. Tillman and Satyajit S. Ambike

Purdue University, West Lafayette, IN, USA
email: sambike@purdue.edu. web: www.purdue.edu/hhs/hk/Biomechanics-MotorBehavior/

## INTRODUCTION

Ensuring the stability of motor action is critical for executing successful movements. However, maximizing stability is not always desirable [1]. For example, a transition between motor states must be preceded by the destabilization of the prior state. *Anticipatory synergy adjustments* describe the destabilization of a motor state that begins ~300 ms before the intended change in that state is observed [2]. Similarly, when rapid movement is expected in the near future, the motor system must manage two contrasting objectives: (1) ensure the stability of the current state, and (2) achieve rapid transitions to new states, if required. We argue that the stability of the current motor state is modulated to lower values to account for uncertain task requirements and to achieve dexterous task switching.

Here, we verify if stability modulation enables the dexterous use of the fingers. Subjects performed four-finger, isometric, constant force production tasks in two conditions. In the first (stable) condition, subjects produced one constant target force and had a-priori knowledge of the target's invariance. In the other (dexterous) condition, subjects tracked a longer, unknown, randomly varying trajectory that included the constant-force target as an integral part. We hypothesize that the stability computed during the constant force-production phases in the two conditions (1) will be maximal for the stable condition, and (2) will be progressively lower as the task demands increase.

## METHODS

Twenty-five healthy subjects (6 male, 20.4±2.5 yrs) participated in the study after providing informed consent. Subjects were seated comfortably in a chair with their forearms resting on top of a table. They placed the distal phalanx of each finger of their dominant hand on one force transducer (Nano-17; ATI Automation). The transducers recorded each finger's downward vertical force at 1000 Hz. Visual feedback on the total force, $F_T$, was provided for all trials via a computer screen placed in front of the subject. $F_T$ was computed as the sum of the vertical downward forces of all fingers ($F_T=\sum F_i$; i=1 to 4).

For the stable condition (Task 1), subjects produced a constant $F_T$ value (10% of maximum voluntary contraction - MVC) for 7 s with the knowledge of the target's invariant location. This task was repeated 16 times [2]. For the dexterous condition (Tasks 2 and 3), the subjects modulated their total finger force and tracked an $F_T$ target that randomly changed its vertical position on the screen. The target $F_T$ profiles lasted for 30 s and consisted of smooth transitions between varying durations and magnitudes of constant $F_T$, including one instance of 10% MVC which lasted for at least 4 s. There were 8 distinct target $F_T$ profiles for Tasks 2 and 3 each, which were repeated once to obtain a set of 16 trials for each task type. The target moved faster for Task 3 compared to Task 2, making Task 3 harder. The trials were randomized within each task, and the tasks were block randomized across subjects.

The last 4 s of Task 1 (Fig. 1A), and the first 4 s of Tasks 2 and 3 were used for further analysis, after the data were time aligned to match the start of the 10% MVC portion (Fig. 1B). The individual finger forces ($F_i$) were filtered using a zero-lag, 4$^{th}$-order, low-pass Butterworth filter (10-Hz cut-off). At each time instant, $t$, the across-trial covariance in the finger forces was computed as the negative difference between the sum of variances in $F_i$ and the variance in $F_T$ and then normalized by the sum of the variances in $F_i$: $C_N(t)=-[\sum(\mathrm{Var}(F_i(t)))-\mathrm{Var}(F_T(t))]/\sum(\mathrm{Var}(F_i(t)))$. Note that $C_N>0$ indicates negative covariation (*synergy*) in the finger forces. This is observed during the stabilization of the total

force: If one finger force increases, others compensate by reducing their force to maintain the total force. Conversely, $C_N<0$ implies positive covariation among the fingers and that the total force is destabilized [3]. Thus, greater $C_N$ indicates a stronger synergy and greater stability. The $C_N$ values were sampled at three *Phases* (1.5 s, 2.5 s, 4 s; Fig. 1C) and subjected to a two-way, *Task* × *Phase* repeated-measures ANOVA (3 levels/factor). Bonferroni corrections were used for pair-wise comparisons.

## RESULTS AND DISCUSSION

The total force, $F_T$, in the 4 s window for Task 1 (Fig. 1A) shows fluctuations about the 10% MVC target. In contrast, $F_T$ in the 4 s window for Tasks 2 and 3 (Fig. 1B) contain an initial period when force trajectories converge to the 10% MVC target from different previous states. Consequently, $C_N$ for Task 1 displays a near-constant value, but $C_N$ for Tasks 2 and 3 show a period (up to $t$ ~0.3 s) of positive covariation ($C_N<0$) that achieves $F_T$ convergence to 10% MVC (Fig. 1C). Then, negative covariation in the finger forces gradually increases ($C_N>0$), reflecting an increasing tendency to stabilize $F_T$.

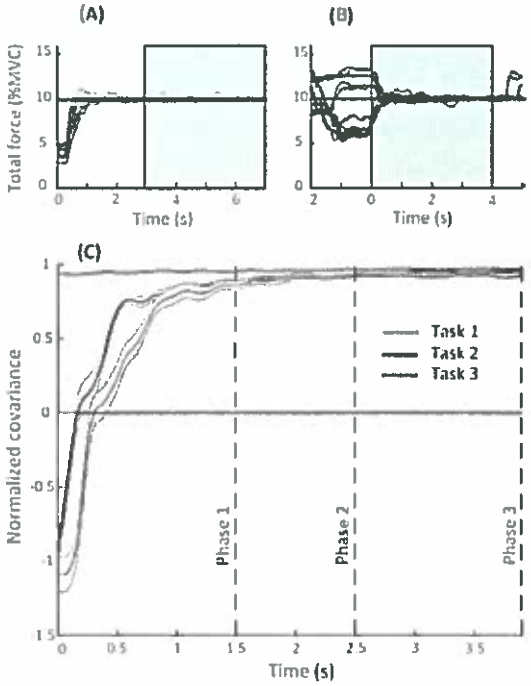


**Figure 1**: Representative data for Task 1 (A) and Task 2 (B). Data in the shaded rectangles is used for across-trial covariance analysis. Across-subject mean±SE of the normalized covariance (C).

The key observation is that $C_N$ values for Tasks 2 and 3 always remain lower than those for Task 1.

ANOVA on the $C_N$ values revealed main effects of *Task* [$F_{(1.193,28.635)}=7.909$; $p<0.01$] and *Phase* [$F_{(2,48)}=9.015$; $p<0.01$]. $C_N$ for Task 1 (0.962±0.006) > Task 2 (0.914±0.012), and Task 1 > Task 3 (0.891±0.023). There was no difference between Tasks 2 and 3. $C_N$ for Phase 1 (0.895±0.017) < Phase 2 (0.934±0.008), and Phase 1 < Phase 3 (0.938±0.013). There were no difference between Phases 2 and 3. A significant *Task* × *Phase* interaction [$F_{(2.602,62.452)}=3.414$; $p<0.05$] indicated across-task differences: $C_N$ change across *Phase* for Task 1 is minimal, $C_N$ increases from Phase 1 to Phase 2 to Phase 3 for Task 2 and continues to approach the Task 1 $C_N$ value. However, for Task 3, $C_N$ increases from Phase 1 to Phase 2, decreases from Phase 2 to Phase 3, and it is lower than the $C_N$ values for Tasks 1 and 2 at Phase 3.

Our first hypothesis was supported by the data. The stability associated with the constant $F_T$ is reduced (~7%) when subjects expect to produce force changes of unknown direction and magnitude at an unknown time in the near future. Although the drop in $C_N$ was similar for Tasks 2 and 3, it lasted longer for Task 3 (significant *Task* × *Phase* interaction). These $C_N$ changes are anticipatory synergy adjustments, but with two prominent differences: (1) they lasts over 8 times longer than the previously reported (~300 ms), and (2) we show limited destabilization that facilitates movement if and when required. In contrast, earlier work reports progressive destabilization of the current state that is necessarily followed by a state change in *self-paced actions* that do not involve uncertainty [2]. The relation between stability modulation and task performance remains to be established in our study. However, this is the first demonstration of task-specific stability modulation in hand function, and our results have implications for the understanding and the clinical assessment of manual dexterity.

## REFERENCES


1. Hasan Z. *J Mot Behav* **37**, 484-493, 2005.
2. Zhou T, et al. *Exp Brain Res* **226**, 565-573, 2013.
3. Shim JK, et al. *J Appl Physiol* **97**, 213-224, 2004.

# MINIMUM DETECTABLE CHANGE OF AN INSTRUMENTED SENIOR FITNESS TEST

Samuel Todd, Meghan Hess, Morgan Kiser, Megan Salvatore, DPT, Nathan W. Saunders, PhD

University of Mount Union, Alliance, OH, USA
email: saundenw@mountunion.edu, web: www.mountunion.edu

## INTRODUCTION

Minimum detectable change (MDC) is the minimal amount of change that is not due to error in measure or chance [1]. The APDM system, in connection with the MobilityLab software, helps assess functional movements like the 30-second chair stand, TUG, and gait [2, 3]. Currently, there are MDCs established for chair stand and other functional movements [4, 5, 6, 7], but not for the APDM system. This study will look to establish MDCs for the APDM system while also providing baseline measures for participants.

## METHODS

At least 30 elderly male and female volunteers will be included. They will be at least 65 years of age, as well as apparently healthy with no known cognitive or balance impairments. The subjects will be put through the 30-second chair stand, 8-foot timed up-and-go, and 6-minute walk test (6MWT) of Rikli and Jones's Senior Fitness Test [8].

APDM Opal sensors (triaxial accelerometers, gyroscopes, and magnetometers) will be worn on the ankles, wrists, lumbar spine, and sternum during testing. The sensors connect to MobilityLab software. Stopwatches will too be utilized for timing.

Three trials will be conducted for each functional test in the same day; a familiarization trial and two recorded trials. A cyclic format will be followed for all trial rounds, familiarization and recorded, with the 8-foot timed up-and-go coming first, the 30-second chair stand second, 6MWT third, then back to the 8-foot timed up-and-go for the next trial.

8-foot timed up-and-go will be conducted with a 17-inch tall chair. Upon indication of start by the MobilityLab software, the administrator will communicate "start" to the participant while also operating their stopwatch. The participant will rise from the chair, walk 8 feet, turn around at the marked distance, and return to the seated position where timing will stop. Time will be kept by the administrator. 2 minutes of rest will be given between the trial of 8-foot timed up-and-go and 30-second chair stand.

30-second chair stand will be administered with the same chair. Upon communication of "start," the participant will complete as many stand-to-sit cycles as they can in the time frame. They will begin in a seated position. Sit-to-stand cycles will be recorded by the administrator. 2 minutes of rest will be given between the trial of 30-second chair stand and 6MWT.

Participants will walk the marked 25 meter straight walk way course for the 6MWT. Turn-arounds will be indicated by cones. The test will start upon communication of "start." The familiarization trial for the test will be 2-minute walk test to allow participants to gain a feel for the turns and the surface they are walking on. A chair will be placed at the midpoint of the walkway for midtest rest. Upon completion, an hour rest will be given until the start of the next trial of 8-foot timed up-and-go.

The testing sequence that will be followed will aid in minimizing error. Other factors that will aid minimizing error also include maintaining testing location, surface, administrator, and rest time constant for each individual participant.

Statistical analysis will be conducted with SPSS v24. A 95% confidence interval will be used to determine MDC. The equation for MDC with 95% confidence is as follows:

$$MDC_{95} = 1.96 \times \sqrt{2} \times SEM$$

SEM represents standard error of measurement. SEM is calculated by the following equation: $SEM = SD \times \sqrt{1 - estimated\ reliability\ coefficient}$ The estimated reliability coefficient can also be seen as intraclass correlation coefficient. SD represents the standard deviation. SD is calculated by the equation:

$$SD = \sqrt{SS_{total}/(n-1)}$$

$SS_{total}$ is found by ANOVA.

## RESULTS AND DISCUSSION

The data collection and statistical analysis process will begin February 1, 2017.

## CONCLUSIONS

Again, the data collection and statistical analysis process will begin February 1, 2017.

## REFERENCES


1. Haley, Stephen M., Fragala-Pinkham, Maria A. Interpreting Change Scores and Measures Used in Physical Therapy. Journal of the American Physical Therapy Association, 2006.
2. Baston, Chiara, Mancini, Martina, Schoneburg, Bernadette, Horak, Fay, & Rocchi, Laura. Postural Strategies Assessed with Inertial Sensors in Healthy and Parkinsonian Subjects. Gait & Posture, 40(1), 70-75, 2014.
3. Mancini, M., King, L., Salarian, A., Holmstrom, L., McNames, J., & Horak, F. B. Mobility Lab to Assess Balance and Gait with Synchronized Body-worn Sensors. Journal of bioengineering & biomedical science, Suppl 1, 007.
4. Almarwani, Maha, Perera, Subashan, VanSwearingen, Jessie M., Sparto, Patrick J., & Brach, Jennifer S. The test-retest reliability and minimal detectable change of spatial and temporal gait variability during usual over-ground walking for younger and older adults. Gait & posture, 44, 94-99.
5. Hars, M., Herrmann, F. R., & Trombetti, A. Reliability and minimal detectable change of gait variables in community-dwelling and hospitalized older fallers. Gait Posture, 38(4), 1010-1014. 2013.
6. Hesseberg, Karin, Bentzen, hege, Bergland, Astrid, Hars, M., Herrmann, F. R., & Trombetti, A. Reliability of the Senior Fitness Test in Community-Dwelling Older People with Cognitive Impairment (Vol. 20; 38, pp. 37; 1010-1044; 1014). Hoboken, New Jersey: John Wiley & Sons, Inc., 2013.
7. Ries, Julie D., Echternach, John L., Nof, Leah, & Blodgett, Michelle Gagnon. Test-Retest Reliability and Minimal Detectable Change Scores for the Timed "Up & Go" Test, the Six-Minute Walk Test, and Gait Speed in People With Alzheimer Disease. Physical Therapy, 89(6), 569-579. 2009.
8. Rikli, Roberta E., Jones, C. Jessie. Functional Fitness Normative Scores for Community-Residing Older Adults, Ages 60-94. Journal of Aging and Physical Activity. Human Kinetics Publishers, Inc., 1999.